Thesis

Efficient Design of Spacecraft Electronics to Satisfy Launch Vibration Requirements

by

R. A. Amy

Supervised by

Dr. G. Aglietti

School of Engineering Science

Astronautics Research Group

University of Southampton

October 10, 2009

Contents

List of Tables

List of Figures

Acknowledgements

The author warmly thanks: Dr. G. Aglietti for his intelligent advice (even when I foolishly ignored it), continual encouragement and infinite patience; SSTL for supporting the research; Dr. Guy Richardson for his wise suggestions and broad and deep understanding of all the problems at hand; Ian Black for providing free test specimens; my friends and family for supporting me; and Laura for always being there when it mattered the most.

Nomenclature

AVF Anti Vibration Frame

BC Boundary Conditions

BGA Ball Grid Array

DIP Dual In-line Processor

DSM Design Structure Matrix

ECAD Electronic Computer Aided Design

ECSS European Cooperation on Space Standardization

ESM Environment Severity Maps

FE Finite Element

FMECA Failure Modes Effects and Criticality Analysis

FTA Fault Tree Analysis

HALT Highly Accelerated Life Testing

IEEE Institute of Electrical and Electronics Engineers

LCCC Leadless Ceramic Chip Carrier

MAC Modal Assurance Criterion

MTBF Mean Time Between Failure

MSG Method Selection Guidelines

MTTF Mean Time To Failure

MCAD Mechanical Computer-Aided Design

PCB Printed Circuit Board

PWB Printed Wiring Board

PLCC Plastic Leaded Chip Carrier

PGA Pin Grid Array

PoF Physics of Failure

PTH Plated Through Hole

PRDB Package Robustness DataBase

QFP Quad Flat Pack. also known as gull wing

REMM Reliability Enhancement Methodology and Modelling

SCA Sneak Circuit analysis

SMC Surface Mount Components

SMA Shape Memory Alloy

SMT Surface Mount Technology

SSTL Surrey Satellite Technology Ltd

SOP Small Outline Package

Note: In this text the term *component* specifically refers to any electronic device that can be soldered to a PCB, while *package* refers to any integrated circuit component (generally any SMT or DIP component). Finally *attached component* refers to any combined PCB and component system, with the intention of emphasizing the different mass and stiffness properties exhibited by *attached components*.

Chapter 1

Introduction

1.1 Introduction

During a spacecraft launch, very high intensity vibrations are transmitted through the launch vehicle and into the spacecraft structure; the severity of these vibrations can be strong enough to damage electronic equipment and cause the majority of first-day spacecraft failures. To ensure that these failures do not occur during the mission all spacecraft electronics are subjected to stringent pre-flight qualification tests, these tests are intended to make failures occur on the ground instead of during the launch. In terms of preventing mission failure, this method works very well as it allows the design to be modified before launch and ensures that vibration related mission failures virtually never occur. However, in terms of the overall design process the method is inefficient, as each failure and subsequent design iteration may take hundreds of man hours and push back deadlines by several months. Fortunately, the majority of designs pass the qualification test first time, but it is the reduction of the few occasional failures - and the consequential costly design iterations - that is the primary focus of this work. Conventionally it would be assumed that a fully detailed FEM of the electronic equipment could be made, the stresses calculated and the risk assessed. In practice, however, this is not a realistic option, because the detailed models require a lot of time and effort to create, and as the majority of designs are unlikely to fail, then this becomes a very inefficient way of finding the minority that do. This inefficiency is the main reason why such detailed models are very rarely used in industry.

To reduce the probability of these aforementioned occasional failures, this work presents an improved design process for creating spacecraft electronic equipment, this new process reduces

the chance of the equipment failing the pre-flight qualification test whilst remaining quick and simple to implement. To achieve this the design process is modified by providing three simple tools: (1) a list of different component types ordered by their ability to withstand vibration, allowing a user to choose more robust packages over weaker ones; (2) simple maps that roughly show the magnitude of the vibration response over the PCB (Printed Circuit Board), allowing the more sensitive components to be placed away from areas of intense vibration; and (3) a process to create simple yet accurate FE models of the PCB, should a design fail the qualification test these more accurate models allow more informed and efficient remedial action to be undertaken.

These tools are not intended to totally prevent failures, but to produce a higher level of improvement and quality to the design-process in the most cost effective manner. Additionally, in the unlikely event that a design should still fail, then more accurate versions of the tools are provided to help decide the most effective remedial action. These improve the efficiency of the re-design process and ensure that the chance of a subsequent design failing are very unlikely.

The principle behind this new process lies in an improved implementation of the Physics-of-Failure (PoF) method - a method to predict electronic equipment failure - with the minimum effort and complexity. The process does not attempt to provide a full implementation of the PoF method, instead it uses various simplification assumptions to allow a pseudo-optimisation that is the best compromise between accuracy and implementation time. This approach works because each of the tools are only required to make a small reduction in the failure probability for the overall failure probability to be considerably reduced, thereby making a fully detailed solution unnecessary.

It is important to note that this work does not primarily focus on proving the validity of the tools, what is more important is the background processes that are necessary to create them. The reason for this is that the proposed lists and maps will be specific to each manufacturer's processes, manufacturing quality and style of equipment, and that each manufacturer that uses them must create their own maps and lists specific to their own type of equipment; therefore, the example tools provided here are only case-studies. So it should be kept in mind that the work here focuses on defining the processes that create the tools, whilst the values given here can never be used for anything more than ball-park estimates. Likewise, the methods to calculate the accuracy of these tools are also given, but not the specific values of the accuracy as these are dependant on how the manufacturer applies them.

Thus, the primary contribution of this work is to prove the viability and accuracy of the aforementioned tools, this is achieved through a combination of experimental testing and computer simulations. For the two levels of environment prediction models (the very simple maps and the improved quality FE models used when a design is highlighted as a risk) there are three main tests as follows: First, some typical pieces of electrical equipment are modelled using FEA and the results are compared to experimental data, not only does this give the expected modelling accuracy under different conditions, but also it identifies the main factors contributing to modelling error which allows more informed and efficient creation of future models. Secondly, it is often easier during the modelling process to ignore the effects of the components added mass and stiffness on the PCB, the error contributed by this assumption is determined with greater accuracy and for a much higher number of cases than has been previously achieved. This also allows future models to be created much more effectively, for example, assuming the component mass can be ignored may introduce only a small error for models of some types of equipment but not for others, this information allows the expected accuracy of the environment maps to be calculated. Thirdly, small variations in the manufacturing and assembly cause supposedly identical pieces of equipment to behave differently; the extent of this response variation is measured for some different pieces of equipment. This highlights not only the surprising extent to which the response varies, but also the factors driving this variation and how to control these factors, this provides some simple and effective measures on how to best minimise these variations. These three sets of experiments combine to provide enough information to understand how to create the vibration response maps, and also to calculate their accuracy.

Finally, experimental tests are then carried out to create component failure rate data; this work presents an improved set of tests that measure previously unconsidered failure parameters. Additionally, these tests also highlight some very important points about the physical cause of failure. For these failure criteria, the reliability of an individual component is dependant on many factors: package type, location on PCB, lead dimensions, manufacturing technique, intensity of vibration and PCB thickness, and the relative importance of each of these factors is examined in this work.

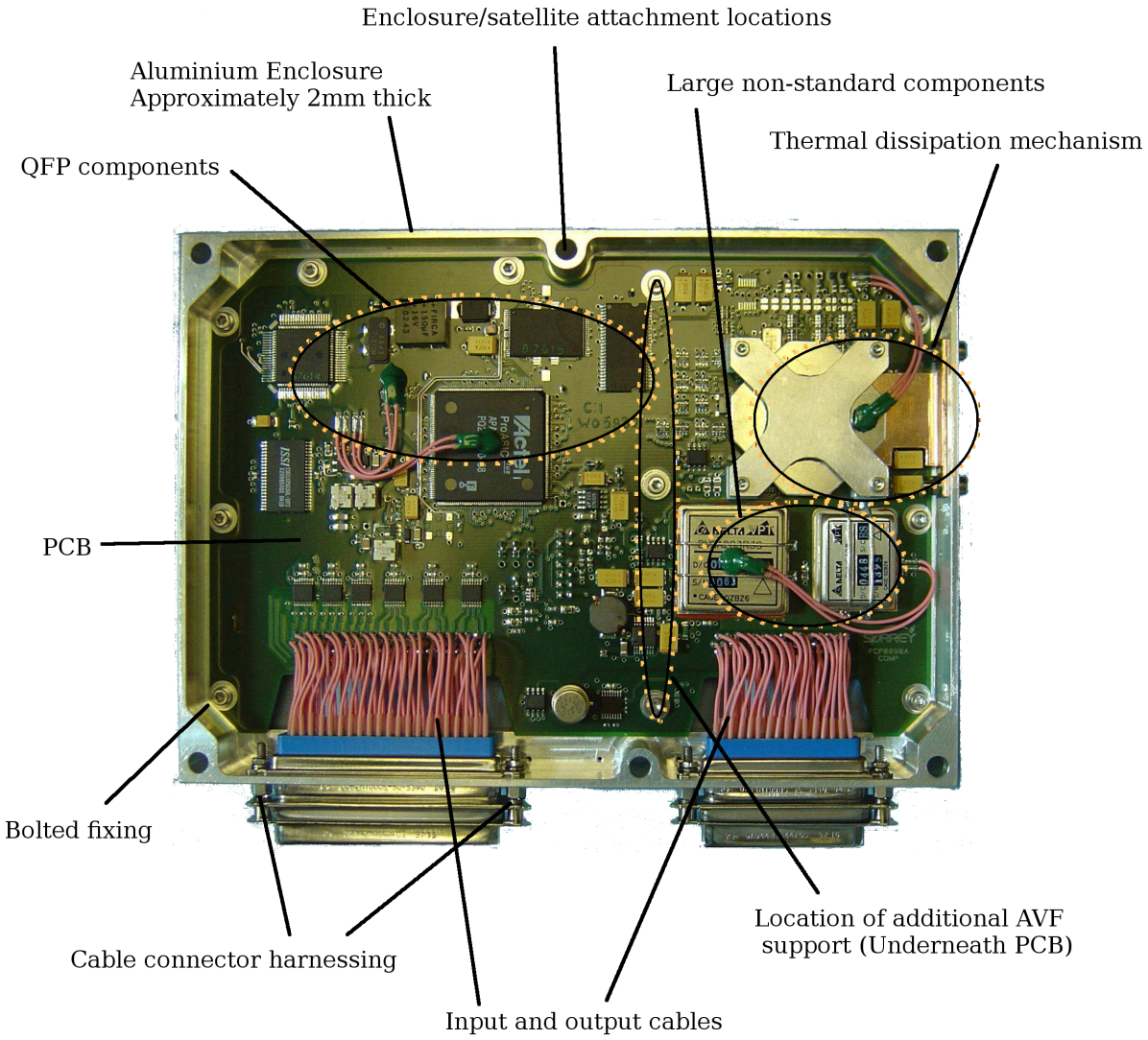

Figure 1.1: Characteristics of a typical satellite electronic enclosure, an SSTL Nanotray.

1.2 Typical Electronic Equipment of Interest

In this section the characteristics of a typical piece of electronic equipment are defined, this is to both prime the reader and also - to some extent - to define the scope.

A typical piece of electronic equipment is shown in figure 1.1 and is representative of the equipment considered in this work. Such an enclosure is normally manufactured from aluminium and is around 2mm thick to provide the best compromise between, weight, strength and radiation protection. The PCB can be attached to the enclosure by a variety of different attachment methods, but the most common is a simple bolted fitting (as shown in the

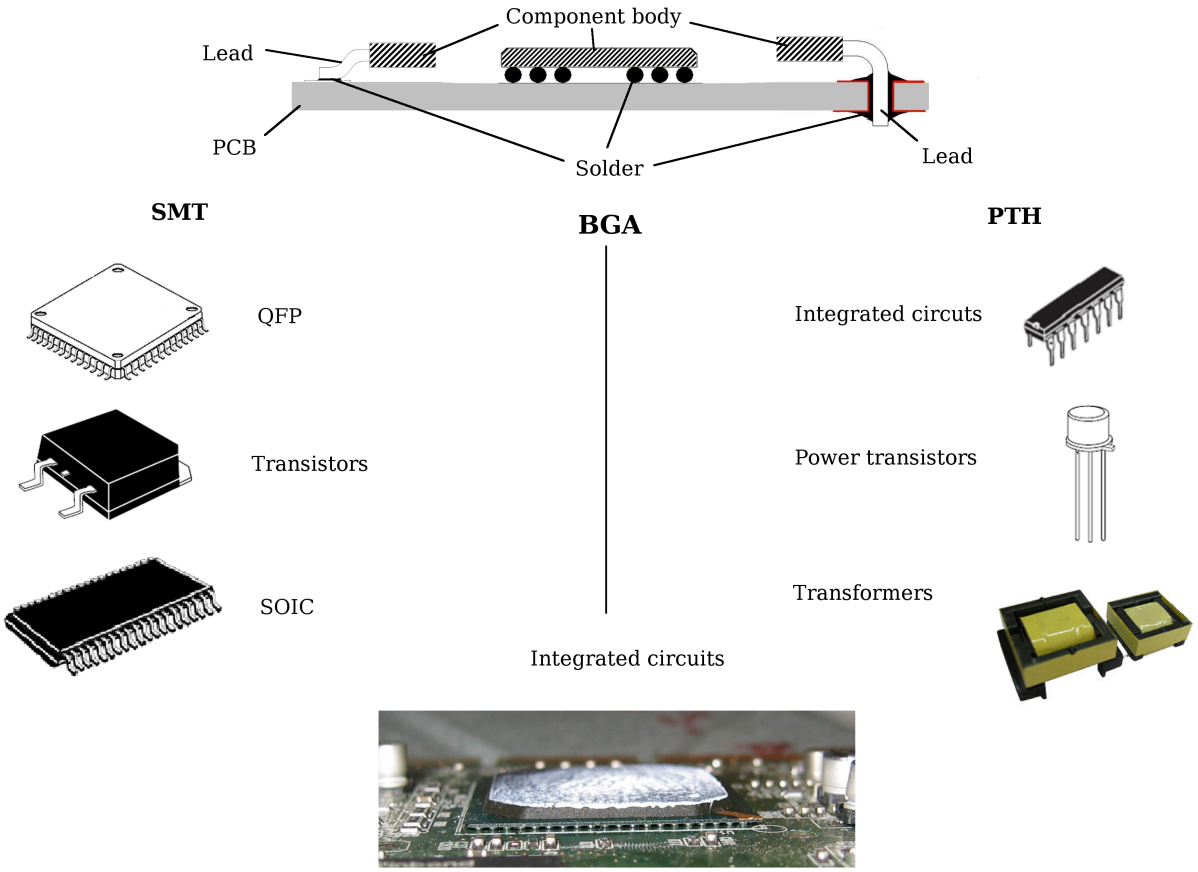

Figure 1.2: The three most commonly used package mounting technologies, SMT, BGA and PTH, with examples of common components that use each technology.

diagram). The enclosure may also provide additional support to the PCB in the form of Anti-vibration frames. The PCB is a glass-epoxy laminate, usually between 1.6 and 2mm thick, though other thicknesses may be used in specialised applications. PCBs typically have a longest edge of somewhere between 50-200mm and an aspect ratio of between one (square) and two, although other aspect ratios and sizes are used in certain applications. The enclosure must also make provisions to support the cables that connect on to the PCB; this is to restrict any cable movement that places additional stress on the PCB.

The PCBs are typically populated with Pin-through-hole (PTH) packages, Surface mount components (SMC) and Ball Grid Arrays (BGA) (see figure 1.2). PTH packages use the oldest kind of mounting technology, where the component lead is soldered into a hole that extends through the PCB. PTH components are increasingly being replaced by SMT components, these solder directly to the surface of the PCB and are generally smaller than PTH packages of

equivalent function. BGA packages further reduce the package size when compared to equivalent SMT packages; they use a small array of small solder balls that cover the underside of the package body to attach to the PCB. In addition to these standard packages there also exist bespoke packages with non-standard shapes; usually these are larger PTH components such as transformers, relays and other high-power components.
Additionally, this work specifically does not consider failures due to shock or thermal loading, the reasons for this omission are detailed in appendix sections A and B.

1.3 Main Contributions

The main contributions of this work with respect to the current state of the art (which is described in detail in chapter 2) are as follows:

- Shown that, under given conditions, the FE modelling process is sufficiently accurate enough to produce useful predictions of the PCB vibration response. This is achieved through three main investigations: (1) an analysis of the relative importance of correctly specifying various model input parameters (boundary conditions, damping, board mechanical properties, manufacturing variability and component effects), (2) a quantification of the expected error that arises when using simplified PCB models and (3) an analysis of the expected variation of the PCB vibration response that occurs as a result of small differences during the manufacturing and assembly stages.

- Illustrated an improved method of creating package failure criteria that measures previously unconsidered variables; for certain package types, these variables are shown to strongly correlate with failures. Whilst other packages are shown to be able to withstand extreme vibration levels, greatly exceeding those expected during normal spacecraft launches.

- Shown that package failures exhibit a stronger correlation with local PCB curvature than with local acceleration, this is achieved by using a test configuration that is specifically designed to investigate the relative importance of these two different measures of the PCB response.

- Provided some ball-park figures for the expected modelling accuracy and component vibration durability, which although specific to this work here, are a useful starting point

for future research and discussion.

1.4 Thesis Structure

The work that has been carried out is described in the following chapters:

Chapter one provides a basic introduction to the shortcomings of the current design process and proposed solutions and it also defines of the type of electronic enclosure that is be considered throughout this work.

Chapter two is the literature review and starts with an in-depth analysis of the kinds of failures that will be considered in this work, this leads up to a brief description the four different methods that have been used to prevent these failures, this chapter finishes with and an in-depth review of the PoF method that becomes the basis for subsequent chapters.

Chapter three looks at the application of PoF in terms of the overall design process, and by the end of the chapter the reader should: have a greater understanding of the standard electronic equipment design process, especially in terms of its shortcomings; understand the reasoning behind the design tools proposed to overcome these shortcomings; and to understand the work that is required to create these proposed tools and prove their accuracy.

Chapter four is the first of the chapters to present experimental work, it examines the accuracy to which it is possible to model a PCB in an enclosure, additionally it shows the steps that must be taken to achieve this accuracy.

Chapter five examines the accuracy of simplified PCB models that use various assumptions to avoid detailed modelling of components, the expected error from different simplification methods is measured for several different cases.

Chapter six examines how manufacturing variability can cause supposedly similar PCBs to behave differently.

Chapter seven examines different methods of creating failure data for several different component package types.

Chapter eight considers all the experimental work from chapters four to seven, discussing them in the context of the overall process described in chapter three. A case study is given of implementations of the design tools, and their effectiveness is discussed.

Chapter nine summarises the contribution made in this work and then suggests avenues for possible future research.

Chapter 2

Component Failure Prevention: Current State of the Art

2.1 Chapter Overview

The primary aim of this chapter is to introduce the reader to typical component vibration failures and the industries current state of the art at predicting when these failures may occur. To achieve this the literature review is divided into two main sections: in the first half of the literature review there is a detailed discussion of common modes of component failures, these failures are examined from the different perspectives of: location, physical cause, time to failure and operable cause. In the second half of the review the four main methods of reliability prediction (handbook, field data, test data and PoF) are briefly introduced and described, resulting in the PoF method being selected as the most appropriate for improvement. The short-comings of the PoF method are then described, this then prepares the way for the solutions proposed in the next chapter and the resulting work in the rest of the thesis[1].
Before starting the literature review it is pertinent to mention previous literature reviews on the subject: the most recent literature review on this subject is provided in IEEE (2003): however this review focuses mainly on the broad classifications of reliability models, such as Handbook, Field data, test data and Stress and damage (PoF) methods, and does not go into sufficient detail on shock and vibration failures. Foucher et al. (2002) follows a similar pattern to the IEEE review, and has a substantial emphasis on thermal failures. The previous brevity

[1]The work in this chapter is partly based on a literature review that has been already published by the same author(Amy et al., 2009a)

of analysis on PoF methods, especially with reference to shock and vibration failures merits further review into these areas. A review similar to the IEEE's is in the process of being compiled by the AIAA, but the scope of this review is currently unknown. Additionally, by far the most quoted textbook in this field is Steinberg (2000) which is the latest revision of the book that was first published in 1989 (Steinberg, 1988).

2.2 Typical Electronic Equipment Vibration Failures

Before discussing the causes of failure it is useful to consider the classic bathtub reliability curve as shown in figure 2.1 (IEEE, 2003; O'Connor, 1981). This curve shows that failures can be divided into different time-frames, namely infant mortalities, useful life and 'end of life' wear-out failures[2]. The infant mortalities are attributed to manufacturing defects within components or manufacturing processes causing failures near the start of the components operating life, the useful life is a period of a low constant failure rate, with the few failures that do occur possibly attributed to temporary events outside the expected operating conditions, the wear-out failures are caused by the accumulation of damage in components and joints until they are sufficiently damaged to fracture under the normal loading conditions.

Knowledge as to whether an equipment failure is caused by an infant mortality, constant rate failure or a wear-out failure is useful, as it suggests either poor manufacturing in the case of infant mortalities or an underestimation of the stress (or environment) in the case of premature wear-out failures.

There is also another case of failure in which the component only survives a few thousand vibration cycles before failure (within a few seconds of launch environment), this type of failure is akin to a classical over-stress failure and is distinct from manufacturing related infant mortalities as it is not directly attributable to a manufacturing defect, but poor design or a gross under-estimation of the operating environment.

This standard bathtub definition of failure rates is built upon in the discussion in the rest of the first half of this chapter. First some examples of actual failures are given, these are from

[2]This text uses the term "wear-out" as opposed to "fatigue" failures, as it is quite likely that most of the failures have some element of fatigue failure within them, however "wear-out" is intended to indicate a fatigue failure that occurs after the component has experienced some of its useful life and increases in probability with time, whereas an infant mortality failure may be fatigue related but occurs early in the component life and significantly decreases in probability with time.

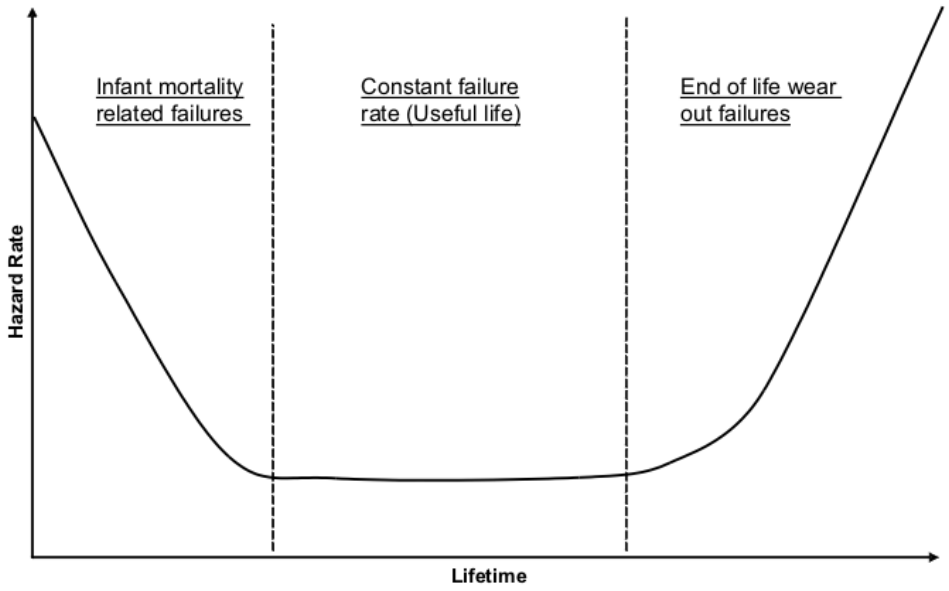

Figure 2.1: Bathtub curve of failure probability over time (IEEE, 2003; O'Connor, 1981)

previously published literature and demonstrate the most probable failure locations. After the common locations of vibration failures are identified the analysis then progresses to discuss the physical mechanisms causing these failures, this is in terms of how the stresses act on the components causing the aforementioned failures. In the third stage the bathtub definition of failures is examined in greater detail. The fourth and final stage concludes the discussion by examining the "operable causes" of failure, where this term refers to all the things that can actually be modified or controlled to reduce the probability of failures occurring (e.g. Design process or manufacturing technique).

The depth of this discussion is considered necessary to precisely determine the principal drivers of failure, and thereby allowing these factors to be specifically focused on for improvement. A secondary aim is to act as a guide to facilitate future identification of the types of failure (e.g. fatigue, over-stress, infant-mortality) from available failure data.

2.2.1 Failure Location

The discussion of failure analysis will begin with the subject of Failure location, where failure location is simply defined as the location on the component where a fracture can be seen to have physically occured.

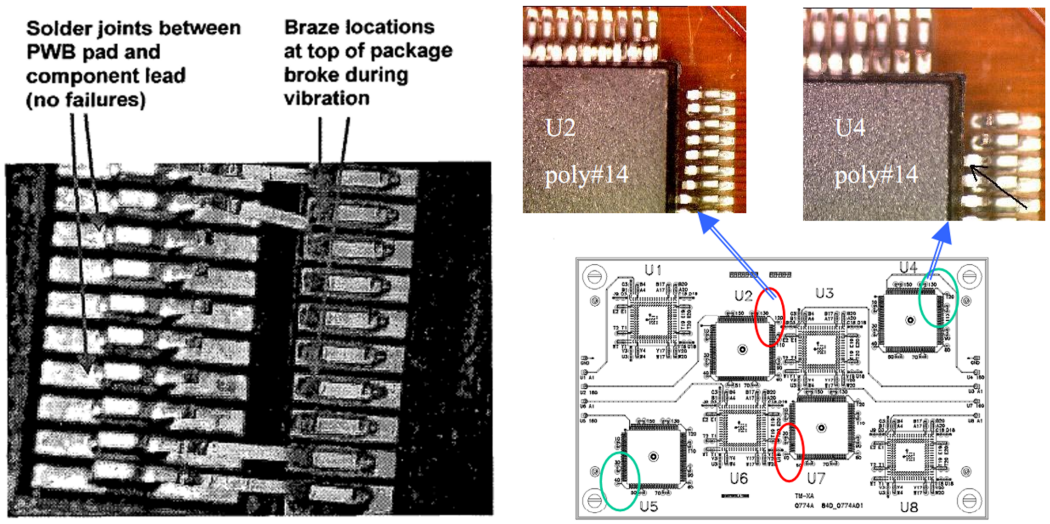

Figure 2.2: Typical QFP component lead failure. First image shows broken QFP corner leads close to component body as a result of fatigue(Estes et al., 2003). Second image shows locations of failures of QFP leads in the corner of the component(Li and Poglitsch, 2001b).

The most commonly observed failure location from mechanical stresses is in the component inter-connections, this is also the location that is subject to the most research(Barker et al., 1992; Barker and Sidharth, 1993). Furthermore, for peripherally leaded components (i.e. QFPs, SOPs, DIPs and all other components with leads around their edges) it has been shown that the maximum stresses occur at the corner leads of these components (Li, 2001; Barker and Sidharth, 1993; Sidharth and Barker, 1996; Li, 2001; Li and Poglitsch, 2001b) as shown in figure 2.2, and that these leads are the most likely to fail first.
To further narrow down the most likely failure location, failures have been shown to predominantly occur close to where the lead enters to the component body(Han and Pety, 1996) (as shown in figures 2.2); similarly, failures have also been seen to less frequently occur at the solder joint between the lead and PCB (as seen in figure 2.3).
In BGA components the most commonly observed failure location is in the solder balls that connect the component to the PCB surface. These BGA failures have recently been the focus of greater amount of research and are relatively well studied(Guo et al., 2005; Hin et al., 2003).
Second to BGA failures, the most commonly investigated failure locations is the previously

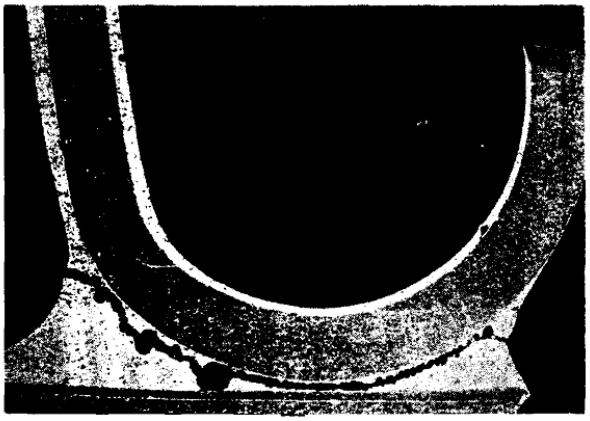

Figure 2.3: Example of the failure of an SMT J-lead PLCC component at the solder joint(Lau et al., 1988)

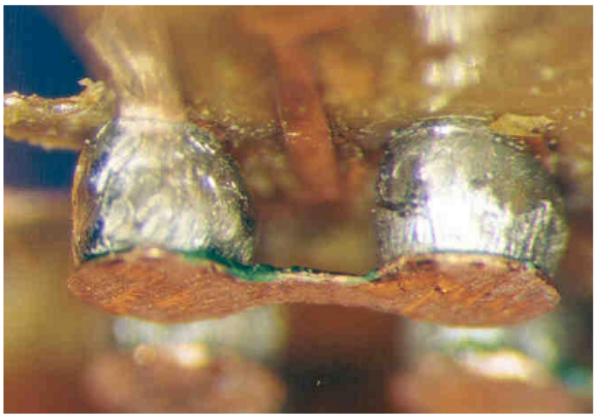

Figure 2.4: Example of a BGA failure at the solder ball(Li and Poglitsch, 2001b)

mentioned example where QFP leads fail close to the component body(Estes et al., 2003; Li and Poglitsch, 2001b; Li, 2001; Ham and Lee, 1996).

In addition to failure of the components, it is also possible for the under-lying PCB laminate to fail, this may take the form of complete structural failure of the laminate (usually de-lamination of the PCB) or failure of the copper traces that electrically connect the components (as shown in figure 2.5). Complete structural failure of the PCB requires very high forces to have occured and such failures are rarely found in the current literature, suggesting that failure of the components and inter-connections most nearly always occurs long before the PCB fails. Failure of the copper traces have, however, been documented(Li and Poglitsch, 2001b).

It is also possible for the failure to be non-identifiable, these failures usually occur somewhere

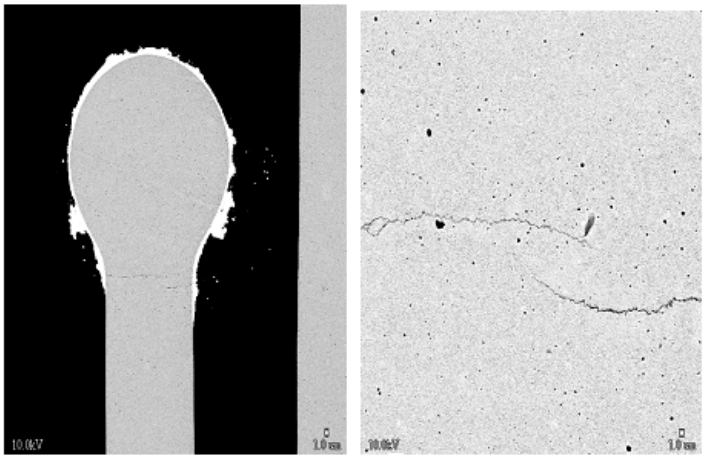

Figure 2.5: Example of a failure of a PCB copper trace from high vibration environment(Li and Poglitsch, 2001b)

within the component body and can only be identified by opening up the component and examining it with a Scanning Electron Microscope. The difficulty in identifying such failures usually means they are not located and the exact failure cause can not be determined. In the past such failures have been prevented by specifying a limit value of acceleration to which the component should not be subjected, this is commonly around 20G RMS(Steinberg, 2000); however, there are plenty of examples of components that can withstand considerably higher accelerations than this (Liguore and Followell, 1995).
In this initial discussion, the common failure locations have been identified as the failure of QFP corner leads and BGA solder balls. In next section the physical cause of these failures are considered.

2.2.2 Physical Cause

This section considers the actual forces that act on the components to cause them to fail. Ultimately, it is always stress/strain that causes any component to fail, but it is very difficult to measure these stresses within the component, so it is much more convenient to define the following variables (board curvature, acceleration and displacements caused impacts) that correlate with failure, as they are easier to measure and identify:

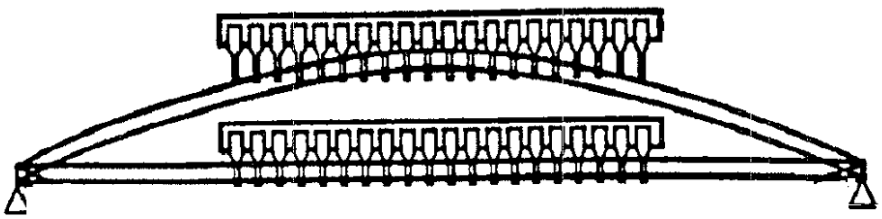

Figure 2.6: Diagram illustrating how board curvature causes the greatest strain in the leads furthest from the center of the component

High Board Curvatures

When a PCB is subjected to vibration it bends periodically, some of this bending moment is resisted by the components that are attached to the PCB. This means that there must be forces transmitted through the component leads, therefore stress must be present in the leads. Bending curvature failures occur most often at the corner or end leads of a component package, where the stresses are the greatest(Li, 2001; Barker and Sidharth, 1993; Sidharth and Barker, 1996; Li, 2001; Li and Poglitsch, 2001b) (see figure 2.6).
It has also been shown that bi-directional curvature (i.e. a PCB that is curved in both the x and y axis) causes greater damage than uni-directional curvature(Wang et al., 2004; Guo and Zhao, 2005; Han and Pety, 1996).
Bending stresses are significant failure drivers for components such as DIPs or SMCs as they cover a large area and thus for a given curvature experience greater relative displacement at their edges, heavy components are less susceptible as they are usually stiff enough to reduce the PCB curvature.

High Acceleration

During resonance, the PCB and the attached components experience very high inertia forces [3]. As a result of the component's mass large inertial forces are transmitted through the component leads. In the same way as board curvatures, these forces cause stresses in the leads. The greater the mass of the component the higher these axial forces become. Additionally, the accelerations may excite internal resonances of smaller sub-components within the packages,

[3]Steinberg defines high accelerations as $\geq 20GRMS$ (Steinberg, 1988), although accelerations of higher than $\geq 100GRMS$ are often observed in spacecraft electronics.

causing non-identifiable failures.

Large Displacements Causing Impacts

If the PCB has very large dynamic displacement and it has very small clearance with nearby objects, then it is possible that the PCB or components may impact these nearby objects. If this event occurs permanent damage is very likely; fortunately, such events are uncommon.

2.2.3 Time to Failure

Having concluded the discussion on failure locations and their physical reasons, attention is now focused on the time to failure. This is important as it provides great insight about why these failures are occurring, and is relevant when it comes to the final discussion on the operable reasons of failure. Aside from failures that fall within the wear-out failure category, there is very little literature available on this topic, this is because the all the other types of failures are seen primarily as an issue within the manufacturing design process, and are too difficult to remedy except by improving manufacturing tolerances. Practically all of the references in the previous two sections (physical cause and failure location) fall under the heading of wear-out failures.
With reference to the bathtub curve shown in figure 2.1, the different possible times to failure shall be considered(Jensen, 1995).

Infant Mortalities

This type of failure occurs within a relatively short time of the load being applied; it is attributed to manufacturing defects and material variability. Infant mortalities can be differentiated from other failures in that it is unlikely an identical board subjected to the same environment also fails in the same location. SMC are at a higher risk because of the large number of solders joints and thus represent a higher risk of manufacturing defects.
In terms of spacecraft electronics, infant mortalities are usually not a problem as they can be found during the acceptance test and then re-worked; although, this is only true if the acceptance test is severe enough to prompt them to occur.

Constant Rate Failures

This type of failure is a flat failure rate over the entire life of the equipment, these randomly distributed failures are because of inaccurate or incomplete specification of the loads imposed upon the equipment. There may be an element of fatigue in each failure, but the predominant cause is still poor specification of the loading environment.

Wear-out Failures

This type of failure increases in probability and always occurs eventually (unless the stress is below the fatigue threshold), these wear-out failures are not a problem unless the probability of one of them occurring during the mission is too high, i.e. the onset of wear-out failures should be calculated and ensured to occur after the required life.
Wear-out failures can be a difficult problem in terms of pre-flight acceptance tests for the following reason: The tests are necessary to highlight infant mortalities, but during this process some of the useful fatigue life of the component is used up. If the acceptance test is too severe it may use up too much of the fatigue life, with insufficient component life remaining to survive the launch phase. Fortunately, this can usually be avoided by considering the length of time before the failures occured in the earlier and more severe qualification tests.

Instantaneous Over-stress Failures

These type of failures are not considered in the bathtub graph in figure 2.1. They normally occur almost immediately after being place under stress, without significant fatigue damage ever occurring. Over-stress failures can be distinguished from infant mortalities by their repeatable nature, that is, similar equipments submitted to similar loads show similar over-stress failures, whereas infant mortalities show a large amount of variability. These failures generally occur from the stresses on the components being very high, because of either massively under-predicting the stress or over-predicting the component strength.
Similar to infant mortalities, over-stress failures should not cause mission failures as they would always be caught during the pre-flight qualification tests; however, it can sometimes be difficult to distinguish them from infant mortalities.

2.2.4 Operable Cause of Failure: Design

So far the discussion has explained where, why and when failures happen, but not how to prevent them. Using the ideas presented previously this section discusses how the area of design has the most potential to efficiently reduce these failures. Two other reasons that should also be discussed are "Inaccurate or Incomplete Specification of the Environment" and "Manufacturing and Assembly Process"; however, for the reasons detailed in appendix C they are outside the scope of the work here. Instead, this discussion focuses solely on poor design as the under-lying root cause of failure, thereby demonstrating that improving the design process is the most effective way to reduce the failure probability.

In terms of design related failures, either the design causes the *PCB vibration response* to be too harsh or the *components durability* to be too small. Where the *PCB vibration response* concerns everything that determines the local environment experienced by the components (i.e. physical causes of failure as defined in section 2.2.2) and the *components durability* concerns the components ability to withstand this environment. However, although the discussion has considered too harsh vibrations and too weak components, until this point it does so in vague terms without giving specific values. This is the topic of discussion in the third and final part of this section: looking at the design tools that currently exist to give a value to both the PCB response and component durability. This is arguably the most important part of this discussion on component failures, as it is this final cause that is predominantly focused on throughout the rest of this thesis.

PCB Response

The mechanical design of a given piece of electronic equipment determines its response and the greater the magnitude of this response the greater the possibility of failure occurring. To reduce the amplitude of this response either the natural frequencies or the damping can be increased, thereby reducing displacement and stress. The first of these solutions, increasing the natural frequency, can be achieved in the following ways:

Decrease mass Decreasing mass at the centre of the PCB increases the natural frequencies, this can be achieved by replacing heavy components with lighter ones, using lighter materials or removing any non-structural mass.

Increase boundary condition stiffness Altering the edge support condition so that it is

closer to a fixed edge condition increases the natural frequencies(Barker and Chen, 1993; Lim et al., 1999). Furthermore; if placed intelligently, a single point support can dramatically increase the natural frequencies(J.H.Ong and Lim, 2000; Lim et al., 1999).

Anti Vibration Frames Additional supports for the PCB increase the natural frequencies(Aglietti and Schwingshackl, 2004).

Thicker or stiffer PCB Using a PCB with a higher Young's modulus can increase the natural frequency, as does a thicker PCB.

Relocate heavy components Moving components from areas of high response to areas of low response increases the natural frequencies, although care must be taken to ensure that other modes are not significantly lowered instead.

It is also possible to reduce the response by increasing the damping, this is most often achieved through the methods introduced in appendix section E. Generally; however, modifying the damping is not used, as it fails on the compromise between weight and reliability(Steinberg, 2000).

Note: if the natural frequencies of the electronic equipment coincide with those of the supporting structure then the response of the PCB will be very high, Steinberg (2000) recommends an octave separation between the first modes of two connected structures.

Component Durability

The discussion now considers the ability of the component to withstand the local vibration environment, to which some components have a greater resilience than others. This ability of the component to withstand acceleration and bending stresses is dependant on several factors: Package type, Mounting technology, Lead dimensions, PCB thickness and package size[4], each of these factors are considered next.

Previous research has shown that different package types, either in number of leads or type used, are intrinsically more robust than others, regardless of the exact local environment (Lau et al., 1990; Li and Poglitsch, 2001a; Estes et al., 2003), this difference is even more marked in components that use different mounting technology (as mentioned earlier in section 2.2.1). No

[4]Note: Temperature can also affect the reliability of the components; Liguore and Followell (1995) states that the fatigue life is highest in the temperature range from 0°C to 65°C, with a marked reduction below −30°C and above 95°C. But it is assumed in this work that such temperatures are not experienced during launch.

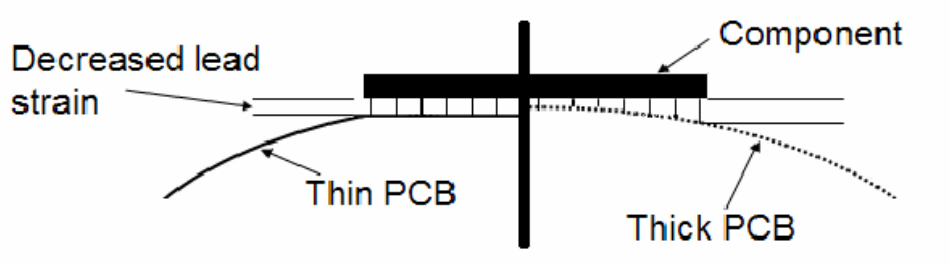

Figure 2.7: Diagram to illustrate how increasing board thickness increases the strain experienced at the component leads.

precise guidelines can be given as to which is the most robust package type or mounting technology, although Li and Poglitsch (2001a) experimentally determined BGA components to be generally more robust than equivalent QFP packages.

Previous work by other authors has shown that lead design of SMT components, significantly affects their ability withstand bending stresses(Suhir, 1988). In this work a paradoxical situation is demonstrated where packages with more compliant (flexible) leads would fail under smaller bending stresses than for packages with thicker leads, this situation is paradoxical as it was assumed that increasing the lead compliance would make the package more robust. The work showed that leads must be either very compliant or not at all. If the leads are very compliant they easily conform during board curvature without experiencing large stresses, whereas if they are stiff they locally reduce the board curvature around the component also reducing the stress on the component. However, if the leads have a compliance somewhere between these two extremes - satisfying a parameter that is defined within their work - then they fail much earlier than either rigid or flexible leads.

PCB thickness affects the amount of stress that is experienced by a component. If the PCB is very thin, then any curvature bending forces do not produce such high stresses, this is because the component locally stiffens the PCB (see figure 2.7). Whereas if the PCB is very thick the component is not be able to influence the PCB's curvature and the strain is greater.

Furthermore, work by other authors has proved that the board thickness has a definite impact on the fatigue life of a SMT components, as BGA fatigue life has shown to decrease by about $30 - 50$ times if the board thickness is increased from 0.85mm to 1.6 mm (whilst maintaining constant overall curvature) (Darveaux and Syed, 2000).

Generally the smaller components such as resistors do not contribute to poor reliability, as they are relatively robust, have well established formulas for predicting their reliability (Steinberg,

2000) and well established manufacturing processes for ensuring high reliability(ECSS, 1999). Large heavy components such as transformers and other "power" components are more susceptible to failures from high accelerations than board curvatures. The high accelerations combined with the greater mass result in large inertial forces and, subsequently, larger forces and stresses within the leads. Whilst the same large components are generally relatively stiff compared to the PCB, this generally makes board curvature less of failure driver for heavy components.

Design Reliability Parameters

So far this discussion has looked at the areas of design that can be modified to reduce the possibility of failures. However, only vague terms have been given about reducing the PCB response and increasing the components ability to survive this response. What is really required is more specific figures that can be used during the design process, i.e. a specific measure of reliability not just general rules of thumb. Unfortunately this is not currently possible because the values of acceptable PCB responses and component durability are - as shown in the previous section - very difficult to create. The main difficulty in creating such figures is that different package styles have very different durabilities, and that there are hundreds of different packages made by many different manufacturers. With this in mind it is possible to understand that with this many input variables (including board thickness and manufacturing variability as mentioned in the previous section) and package styles, a very large number of tests must be run to create useful component reliability metrics. Furthermore, blind attempts at trying to reduce the vibration response without an idea of the actual failure probability, are at best unnecessary and at worst may increase the possibility of failures. This is because the reduction may be imposed on a board that is already safe, creating unnecessary extra weight, time and cost, or - in the case of a design that might fail - the extra effort may be insufficient to make an unsafe design safe. In the very worst case, an uninformed attempt at reducing the response might actually modify the response in such a way that it causes a component to fail that would not have otherwise.

This requirement for tools that allow informed and intelligent improvement of the equipment reliability has led to the four main classes of reliability prediction methods as described in the next half of this chapter.

2.3 Evolution of Reliability Prediction Methods

The earliest reliability prediction method developed during the 1960's is now published as MIL-HDBK-217F (1995)[5]. This method uses databases of electronic equipment failures to give the expected useful life of a PCB incorporating certain components, and belongs to a class of reliability prediction methods known as "handbook methods". Despite becoming increasingly obsolete Mil-Hdbk-217F is still in use today. The limitations and inaccuracies of the Mil-Hdbk-217 have been well documented (Pecht and Kang, 1988; Luthra, 1990), which led to the development of three classes of alternative methods: Physics-of-Failure, Field data and Test data.

PoF methods predict the reliability analytically without having to resort to using historical data. All PoF methods share two characteristics of the classical method described in Steinberg (2000), of which the first stage involves finding the vibration response of a PCB for a specific vibration environment, and then - in the second stage - relating individual components failure criteria to this response. An important development in PoF method has been the development of the smeared property technique for quickly creating a mathematical model of a PCB (Pitarresi et al., 1991), this greatly reduced the complexity and time involved in accurately calculating the PCB's vibration response (see section 2.4.1). Recent developments in PoF methods have improved failure prediction for Surface Mount Technology components; however, with the exception of Barkers' method (Sidharth and Barker, 1996), these new methods are only applicable in very specific combinations of components and PCBs. There are very few methods available for large components such as transformers or large capacitors.

Field data methods improved upon the quality and implementation of the historical data used in the handbook methods. The first field data method for predicting electronic equipment reliability was documented in a paper on the HIRAP (Honeywell In-service Reliability Assessment Program) method, which was created in-house by Honeywell inc. (Gullo, 1999). The benefits of the field data method over handbook methods are significant, in fact many similar methods have recently surfaced (REMM and TRACS (Foucher et al., 2002) as well as FIDES (FIDES, 2004)). The field data method answers the handbook methods inability to satisfactorily incorporate board-layout and operating environment into the reliability estimate. This improvement is achieved by using detailed historical failure data from boards similar to

[5]Mil-Hdbk-217F is the latest and final revision of the handbook, released in 1995

the proposed design that have experienced similar operating environments. Field data methods suffer from the requirement of an extensive database of historical failure data, where each failure type must have been correctly identified, and then the cause determined. This approach is suitable for companies which produce very similar equipment, with large enough batches to have a significant number of failures to analyse.

The test data method for reliability has been used since the mid 1970's, and is usually partitioned into accelerated and non-accelerated tests. The basic approach is to create a test that exactly recreates the expected operating environment, with the intention of running the test until a failure occurs; this allows the MTBF (Mean Time Between Failure) to be predicted. If the MTBF is very high then the test duration can be reduced by using an accelerated test, this is achieved by increasing the severity of certain aspects of this test, and using existing formula to relate the failure rate in the accelerated test to the failure rate expected in service. Testing is vital for high risk components as it provides the highest confidence data; however it would be inadvisable to use it for design optimisation, because of the long iteration time.

A cursory review of the works published during the 1990's would suggest that, field data, test data and PoF methods were all competing to replace the outdated handbook methods; however, each method has its own merits and limitations, and if used appropriately provides valuable results. With this in mind, the IEEE (Institute of Electrical and Electronic Engineers) recently released a standard (IEEE, 2003), which listed all the established reliability prediction methods to date. The intention of the IEEE was to produce a guide that would ensure the engineer is well-informed of all the available methods, along with the suitability and limitations inherent with each method. Although the IEEE approach is still in its infancy it seems to have merits, because the AIAA (American Institute of Aeronautics and Astronautics) are producing a guide referred to as S-102, which is similar to the IEEE's, but also considers the relative quality of data generated by each method (Jackson et al., 2003). These guides are only intended to bring together the methods that are distributed throughout the literature on the subject.

For the reasons cited in appendix D this work does not consider any method other than PoF (these appendices also include a more in-depth description of each of these methods). The primary reason for this is because the PoF approach has the most potential for what this work is trying to achieve, with all the other methods being either too specific, complicated or inaccurate.

2.4 Physics of Failure Methods

Also referred to as Stress and Damage models, PoF models are recognised by having a two stage process to predicting reliability, the first stage involves finding the response of the PCB to the dynamic loading imposed upon it, whilst the second stage takes this calculated response to provide a reliability metric. Much of the literature to date illustrates both a response prediction method and a failure criteria process; however, as the two are best described independently this review discusses the two stages separately.

The interface between the response prediction and failure criteria stages is the response variable created in the first stage to be used in the second. The response variable has evolved from using the input acceleration at the chassis, (Li, 2001; Lau et al., 1990; Wang et al., 2004; Estes et al., 2003), through the actual acceleration experienced by the component to account for the different vibration responses of various PCB layouts (Liguore and Followell, 1995), and finally to looking at the local deflection (Steinberg, 2000) or local bending moments (Sidharth and Barker, 1996) experienced by the PCB local to the component. It has been noted that the failure is a function of component location on the PCB (Li and Poglitsch, 2001a; Guo and Zhao, 2005); therefore the models that consider the local vibration response are more likely to be accurate. The choice of whether to use the local acceleration, local deflection or bending moment depends on the case at hand. If SMT components are to be used then curvature or bending moments may be most appropriate, whilst heavy components may be more likely to fail because of local accelerations. Unfortunately no research has been provided to show which type of criteria is most appropriate in which set of conditions. When choosing a response prediction method and failure criteria it is important to choose two that provide and use agreeing response variables.

It is important to consider the validity of any PoF method used, as it would be inadvisable to use any PoF method, either analytical or FE, that has not been validated against laboratory test data. Furthermore it is important to use any model within its bounds of applicability, which unfortunately limits most current PoF models to use in very specific and limited conditions.

Good examples of general discussion of the PoF methods exist by Foucher et al. (2002); Pecht and Dasgupta (1995); IEEE (2003); Gericke et al. (2002).

2.4.1 Response Prediction

Response prediction is concerned with using the geometry and material properties of a design to calculate the required response variable. This stage is only expected to give the overall response of the underlying PCB, not the response of the individual components. There are three main types of response prediction method, Analytical, Detailed FE models and Simplified FE models described below. These methods focus on including the stiffening and mass effects of added components; However it is important not to overlook the importance of accurately modelling the rotational stiffness at the PCB edge, as this is strongly linked with model accuracy (this is discussed in section 2.4.1).

Analytical Response Prediction

Steinberg (2000) produces the only analytical method of calculating the vibration response of a PCB. Steinberg states that the transmissibility at resonance of an electronic sub-assembly is equal to two times the square root of the resonant frequency; this statement is based on unavailable data and is unverifiable. This permits the dynamic deflection at resonance to be analytically calculated, which can be subsequently used to calculate either the dynamic load from a heavy component, or the PCB curvature. This method does not directly give the local PCB response, and is only compatible with the deflection based failure criteria provided by Steinberg. The validity of the transmissibility assumption is questionable, as Pitarresi et al. (2002) measured critical damping of 2% for a computer motherboard, whilst using the given assumption would have given 3.5% (based on a natural frequency of 54Hz), which would have lead to a large underestimate of the response.

Detailed FE models

Several authors demonstrate the use of detailed FE models to calculate the PCB vibration response (Shetty et al., 2001; Shetty and Reinikainen, 2003; Li, 2001; Jih and Jung, 1998; Pitarresi et al., 2002) (Figures 2.8 to 2.11 show examples at increasing level of detail); however the use of these techniques would not be recommended for a commercial case (unless a precise prediction of the local response was absolutely vital), as the time required to build and solve such a model is excessive when simplified models produce data of appropriate accuracy much more quickly and with less effort.

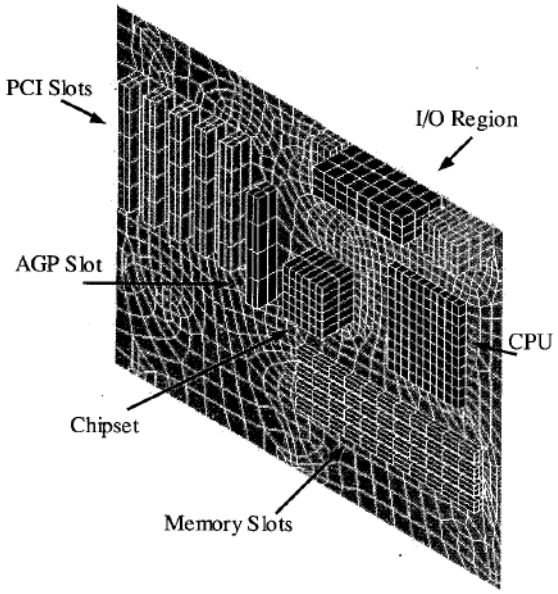

Figure 2.8: Example of a detailed FE model of a PCB (Pitarresi et al., 2002).

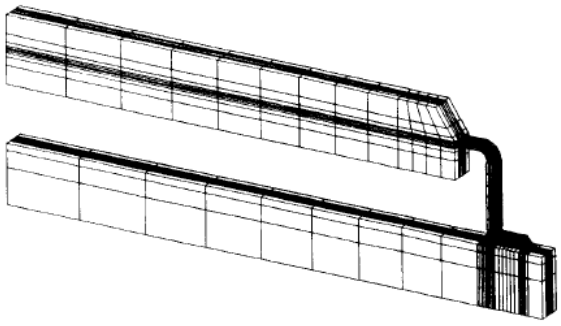

Figure 2.9: Example of a detailed model of a QFP component, this model uses symmetry to simplify the modelling process and reduce solution time (Lau et al., 1990).

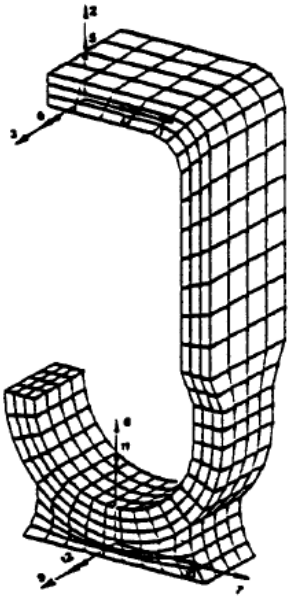

Figure 2.10: Example of a detailed FE model of a J lead (Barker et al., 1991).

The time required to build and solve a detailed FE model can be reduced by using the JEDEC[6] lead spring constants published by Kotlowitz (1989, 1990); Kotlowitz and Taylor (1991), these spring constants can be used in place of a detailed FE model of each lead [7]. It is also possible to implement the sub-structuring method (sometimes known as the super-element method) to reduce the computational time required to solve detailed models.
It should be noted that detailed FE models often blur the boundaries between response prediction and failure criteria, so the work referenced here could also fall under the failure criteria heading.

Smeared FE Models

A major difficulty with response prediction is that the PCBs vibration response is altered when a component is attached to it, as the components effectively increase the mass and stiffness of the PCB, this is particularly true when heavy or large components are present as these increase the local mass and stiffness of the PCB the most. The problem can be solved, in theory at least, by building a detailed finite element model of the PCB and components (where each

[6] Joint Electron Device Engineering Council, the semiconductor engineering standardization body of the Electronic Industries Alliance (EIA), now known as the JEDEC Solid State Technology Association.

[7] Although the primary aim of Kotlowitz's research is for calculating failure criteria metrics and not predicting PCB response.

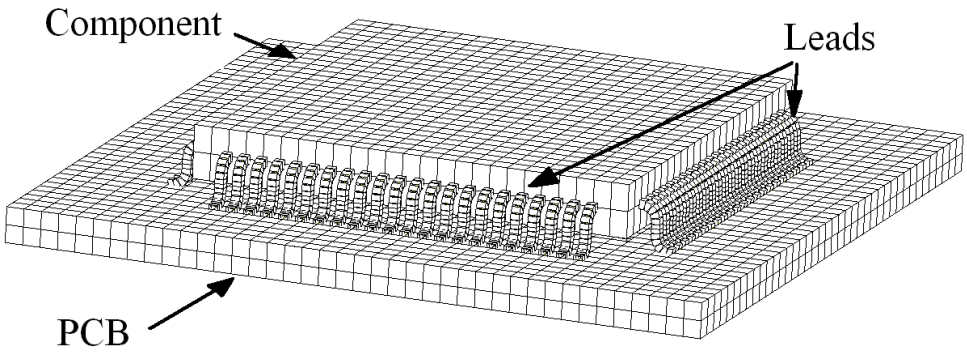

Figure 2.11: Example of a detailed FE model of an individual component, a detailed model of a PCB would incorporate several of these and other components over its surface.

component is modelled in detail as in figure 2.11); however, this approach is rarely used as it requires a long time to build and and solve the model.

Instead, the standard practice is to create simplified models where the components geometry is not modelled at all. Instead of using detailed component models to account for component effects, the components effects are now included by increasing the young's modulus and density of the PCB FE model so it effectively behaves as if components were present(see figure 2.12). Once the effective stiffness and local densities have been calculated they are applied to the elements at the location of the components (see figure 2.13). The resultant locally smeared model can be further simplified if necessary to create what is called a globally smeared model, this is achieved by averaging (smearing) the effective material properties over the whole surface of the PCB. This global smearing technique results in a FE model that does not have a patchwork set of properties to represent each component, but instead has one homogeneous property over the entire area of the model. That is, instead of including the effective component effects in specific locations the added mass and stiffness are smeared over the entire area of the PCB model. For this reason, globally smeared models are potentially useful when the final location of the components has not yet been decided. In addition to locally and globally smeared models, other levels of simplification are also possible. These other levels of simplification have been considered in previous work by other authors(Pitarresi et al., 1991; Pitarresi and Primavera, 1991) and are as follows:

Simple method Completely neglecting the effect of any components, with the FE model simply reflecting the underlying PCB. The reasoning behind these models is that ignoring

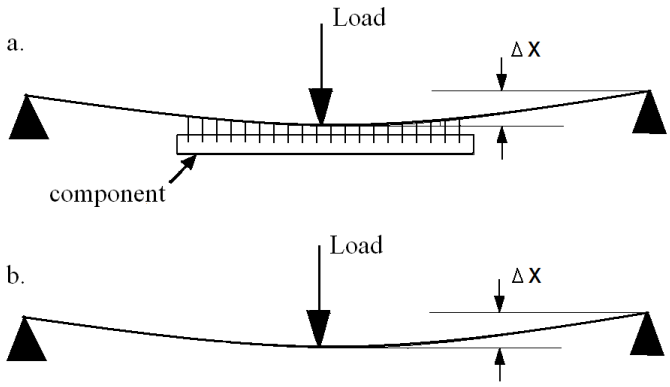

Figure 2.12: Method of creating effective stiffness. (a) An *attached component* specimen is either modelled or experimentally tested and the deflection measured, using this information a FE model of an unpopulated PCB can be given an artificially high Young's modulus (b), this new model will then exhibit the same deflection and therefore the same effective stiffness as the real specimen.

the stiffness increases the response (and lowers the natural frequency), whilst ignoring the mass decreases the response (and increases the natural frequency), thus the two compensate for each other. These models are especially useful when no data on the component density and location exist, for example, preliminary studies.

Global mass smearing The mass of the components is calculated and smeared over the entire area of the PCB, any stiffness contributions are ignored.

Global mass/stiffness smearing Both the mass and stiffness contributions are spread out over the PCB, where the stiffness is calculated by physically testing a combined component/PCB specimen.

Local Smearing Instead of smearing the mass and stiffness properties over the entire PCB, the properties are smeared over local regions of the PCB, where the local region can be defined as either areas of similar components or just the individual component region itself(as in figure 2.13).

In this previous work, the accuracy of the methods was tested by comparing the experimentally measured response of five different PCBs against FE models that used the above simplification techniques(Pitarresi et al., 1991; Pitarresi and Primavera, 1991). Each model was compared to

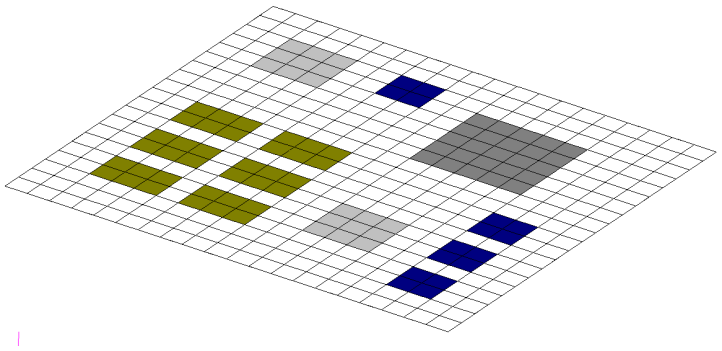

Figure 2.13: Example of a locally smeared FE model of a PCB, with shaded locations indicating areas that model the effects of components and have increased stiffness and density compared to the underlying PCB (non-shaded).

the experimentally derived results using the Modal Assurance Criterion (MAC) and also by looking at the natural frequency. The results showed that the accuracy depends on not only the smearing method used but also the characteristics of the equipment being modelled, with heavily populated PCBs requiring the stiffness and mass contributions to be included for satisfactory results, whilst very lightly populated PCBs can still be satisfactorily modelled even when the component effects are completely ignored.
The principal shortcoming of the smeared modelling method is that the accuracy of the method has not been explicitly defined. The previous work in this area considered the MAC for five boards at various levels of smearing, using un-realistic idealised free-free boundary conditions. Additionally, using a combination of numerical analysis and computer modelling Cifuentes (1994) makes the following four observations for simplified models: 1, the modes modelled must contain at least 90% of the effective mass for accurate analysis, 2, when board deflections are comparable to the thickness a non-linear analysis may be more appropriate than a linear one, 3, Small errors in the location of the components can cause large errors in measuring the response and 4, the accuracy of the response measurement is more sensitive to errors in mass than stiffness.

Boundary Condition Effects

The PCB edge rotational stiffness greatly affects the accuracy of the calculated response (Sidharth and Barker, 1996), and depending upon the specific configuration may be of much

more significance than the added component mass and stiffness. Modelling the edge rotational stiffness as zero (effectively a simply supported condition) generally gives conservative results, whilst modelling as rigidly clamped usually underestimates results, as even the stiffest PCB clamping mechanisms is unable to provide a fully clamped edge condition.
Barker and Chen (1993) validate analytical theory with experimental results to show how edge rotational stiffness affects the natural frequency of the PCB. The principal finding of this work is the strong correlation between the edge rotational stiffness and natural frequencies agreeing with theory. This also infers that large errors in modelling the edge rotational stiffness lead to large errors in predicting the response. Although this work is principally concerned with Calmark wedgelocks, the work is applicable for modelling all types of edge constraint mechanisms.
Using experimental data Lim et al. (1999) gives an example of how the edge rotational stiffness can be calculated for use in a PCB FE model; this is achieved using a method adapted from Barker and Chen (1993). This work also shows how to determine the optimum location for a single point constraint, if the maximum increase in fundamental frequencies is required.
Papers that specifically consider the effect of boundary condition modification with respect to reducing the vibration response also exist by Guo and Zhao (2005); Aglietti (2002); Aglietti and Schwingshackl (2004); Lim et al. (1999).

Predicting Shock Response

Pitarresi et al. (2002) and Pitarresi et al. (2004) use detailed FE model of PCBs to predict the response to shock and vibration, with components modelled as simple block 3D elements. These models used experimentally determined constant damping ratios to improve the prediction of response at resonance. The Shock Response Spectrum (SRS) and time-marching methods were compared for shock response prediction, with the two methods being a trade-off between accuracy and solution time.

2.4.2 Failure Criteria

The failure criteria takes a measure of the PCB response and uses this to produce a failure metric, where the failure metric may be Mean Time To Failure (MTTF), cycles to failure, probability of mission success or any other of a number of failure metrics (see IEEE (2003); Jensen (1995); O'Connor (1981) for a discussion of failure metrics). The many different

approaches to creating this data can be conveniently split up into Analytical and Empirical categories. The empirical approaches create failure criteria data by subjecting test samples of components to a measured dynamic load. Unfortunately, because of the large range of inputs (component types, PCB thicknesses and loads) that are possible, the data published is unlikely to be directly applicable as the data is only valid in very specific cases. The analytical methods do not suffer from the same disadvantages, and have much wider applicability.

Empirical Failure Criteria

As stated previously the limitation of most empirical models is that they are only valid for configurations involving similar PCB thickness, component types and input loading, which is unlikely. However the literature that is available is useful for the following reasons: they provide good examples of how to run a failure tests, they highlight the many different choices of failure metrics and they provide valuable insight into the mechanics of failure.

Li (2001) created an empirical model for predicting the reliability of 272 pin BGA and 160 pin QFP packages. The failure mode studied was fatigue in the package lead near the package body, experimental results agreed well with a damage based analysis on stresses calculated using a detailed FE model(see also Li and Poglitsch (2001b) and Li and Poglitsch (2001a)). The process gives cumulative damage for a given vibration input vibration level.

Lau et al. (1990) gave the shock and vibration reliability of specific components using Weibull statistics.

Liguore and Followell (1995) looked at the failure of LLCC and J leaded components, correlating local acceleration against the cycles to failure. The local acceleration is used as opposed to the chassis input acceleration; additionally the influence of temperature on the test results was also investigated. The paper also makes reference to the sensitivity of component reliability to PCB thickness.

Guo and Zhao (2005) compare component reliability against local torsional curvature, in contrast to previous research which used acceleration. Using a damage based fatigue approach a FE model is favourably compared with experimental results. The paper also looks at location optimisation of components to increase reliability.

Ham and Lee (1996) present a test data method for relating QFP132 lead loading to cycles to failure, based on a torsional loading input.

Estes et al. (2003) look at the failure of gull wing components because of input acceleration; this is with an added dimension of thermal cycling. The components studied are CQFP 352, 208, 196, 84 and 28, as well as FP 42 and 10. As the paper is concerned with failure of components because of in-orbit vibrations, the failure is given in terms of years in Geo-stationary or Low earth orbits. The paper notes that failure of gull wing leads is more likely at locations next to the package body than at the solder joint.
Jih and Jung (1998) look at failures because of inherent manufacturing defects in the solder joint. This was achieved by creating a very detailed FE model of a PCB and component to find the j-integral Power Spectral Density (PSD) for different manufacturing crack lengths.
It is suggested that the empirical methods by Liguore and Followell (1995) and Shetty and Reinikainen (2003) create the most accurate and useful failure data for specific *attached component* configurations, which may be of use if certain variables (board thickness, component type, range of curvature) can be assumed to be constant during the design, or if the user can afford to run such specific tests.

Analytical Failure Criteria

Various researchers have explicitly considered the failure of SMT corner leads, suggesting that this is a common mode of failure. Sidharth and Barker (1996) concludes an earlier series of papers, by providing a model to determine the strain of corner leads of SMT and outline leaded components. The model has less than 7% error when compared with a detailed FE model for six worst-case scenarios. The model is dependant on formula published earlier by Barker and Sidharth (1993), where the deflection of an *attached component* subjected to a bending moment is modelled. Suhir (1988) analytically looks at the stresses expected in package leads, because of locally applied bending moments. Barker and Sidharth (1993) build on the work by Suhir (1988) and Barker et al. (1993) by considering the effect of the lead rotational stiffness. Finally Barker et al. (1992) used detailed FE models to look at the effect of lead dimensional variability on lead fatigue life.
It is relevant to mention the work on JEDEC lead spring constants, that greatly simplifies the creation of leaded components models (Kotlowitz, 1989, 1990; Kotlowitz and Taylor, 1991). The spring constants can be used in place of a detailed model of a lead, reducing the time to build and solve a FE model or greatly simplifying the process of creating an analytical model. Using such constants in a component FE model prevents local lead stresses from being directly

calculated. Instead the overall lead strains are given which must then be related to either local lead stresses or cycle-based lead failure criteria.

Material Fatigue Data. The majority of material failure data that exists for solders and components is principally concerned with thermal failures and there is relatively little data relevant to HCF. The principal reference on this field is provided by Sandor (1991), who provides fatigue and fracture mechanics data for solders. Steinberg (2000) provides fatigue data for standard solders and kovar leads. Yamada (1989) looks at the fracture of solder samples. The failure of solder is complex because of the unusual properties of this material, the importance of this issue depends on the component to be tested, with QFP packages this is not as important as they usually fail at the lead, whilst with BGA, PGA and larger components the unusual properties can affect failure. Thus with QFP the fatigue properties of the lead is the most useful information. For BGA the life of solder joints subjected to instantaneous plastic deformation is more useful (Enke et al., 1989). For larger components Steinberg (2000) provides data on the pull-out stress of PTH solder joints.

Heavy Component Failure Models. The only failure models that exist for heavy components are provided by Steinberg (2000), who looks at the tear out strength of PTH components, and provides an example of how to calculate the maximum allowable stress that may be placed on a PTH joint.

2.4.3 Software Implementations

The Center for Advanced Life Cycle Engineering (CALCE^{TM}) at the University of Maryland provides software to calculate the vibration and shock response of populated PCBs. The software (named CalcePWA^{TM}) is a GUI interface that simplifies the process of running an FE model and automatically inputs the response calculation into a vibration model. The assumptions used in creating the FE response model are not available and the failure criteria used are taken from Steinberg (1991) (Osterman and Stadterman, 1999)(Although Barkers method(Sidharth and Barker, 1996) is also assumed to be implemented). For giving general guidelines for improving equipment reliability the software is fully recommended, especially as it simultaneously considers thermally induced stresses and requires minimal specialist knowledge; however the accuracy of the failure criteria has not been validated.

2.5 Summary

This chapter has introduced typical component failures and the current state of the art at predicting them. This was achieved by first discussing typical vibration failures, this discussion lead to the initial conclusion that - more than anything else - reliability prediction tools are the most efficient way to reduce the number of failures that occur. In the second half of the literature review the four currently existing approaches to predict reliability are compared, from this comparison the Physics of Failure approach is singled out as having the most potential for development. Finally, two shortcoming of the current PoF approach are noted: firstly, that the method of predicting the response has not been fully developed or verified. Secondly, the current component failure data is anecdotal at best and needs to be improved. The next chapter considers how to solve these problems, and more importantly how to effectively implement the PoF method within the overall design process.

Chapter 3

Proposed Solution and Design Process

3.1 Introduction

The one area of discussion absent from the previous chapter is on how the reliability prediction fits in with the overall process in a real working situation, this is something that is historically commonly overlooked and helps to explain the poor uptake of the PoF method. This chapter addresses this issue and describes how the PoF method can be improved to be more effectively implemented within the overall design process.

This chapter is structured in the following way: First, a typical design process and its shortcomings are described. Next some design tools to combat these shortcomings are proposed, where these tools improve the response prediction and component reliability stages of the traditional PoF method. Next there is a general discussion using flowcharts and other tools, this shows how the proposed tools improve the implementation of PoF within the overall design process. Finally the work required to prove the accuracy and validity of the tools is defined, conveniently this final section also conveniently lays out the structure of the work in the rest of the thesis[1].

3.2 Description of Typical Design Process

During the design process three distinct stages are involved: electrical engineering, Electronic Computer Aided Design (ECAD) and Mechanical Computer-Aided Design (MCAD), usually in

[1] This chapter is partly based upon a conference paper published by the same author(Amy et al., 2006b)

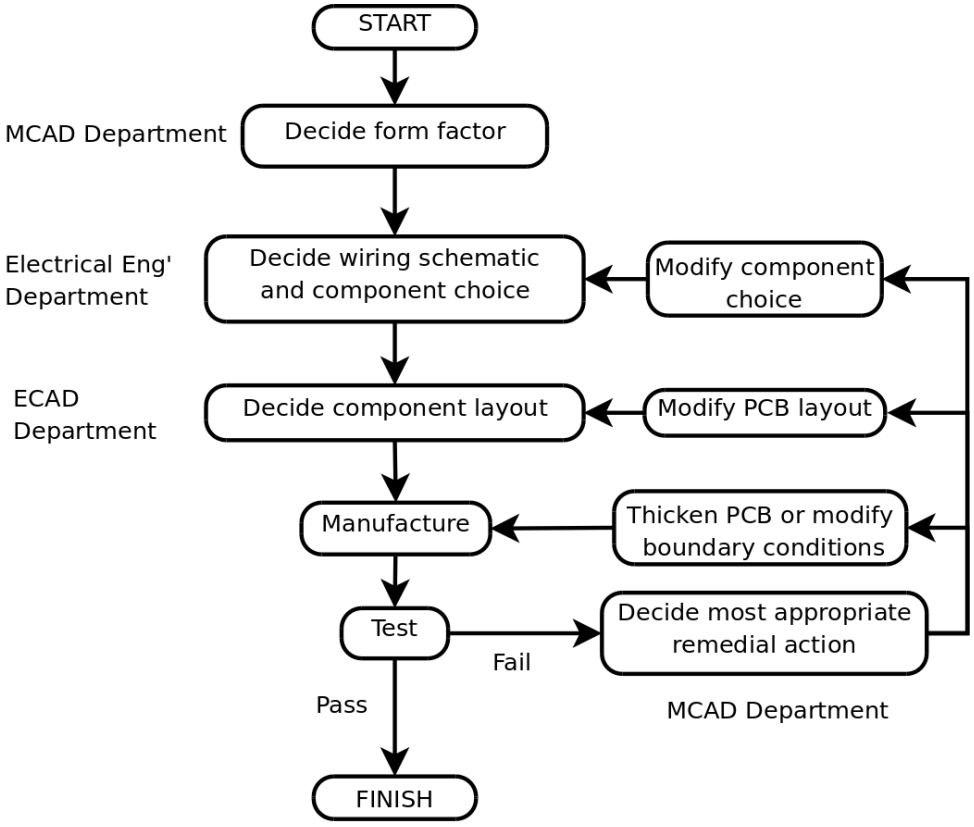

Figure 3.1: Flowchart of a typical design process for spacecraft electronic equipment.

this relative order [2]. At one extreme these stages may be carried out entirely by one individual engineer, at the other extreme they may be outsourced to completely different companies; however, what is important is that the stages must be completed in a specific order with specific information requirements. These stages are now explained and this explanation should be read with reference to the flowchart in figure 3.1:

The Electrical engineering stage decides on the components and wiring schematic, this stage is concerned with the electrical performance of the components, which components to use and creating the wiring schematic that connects them. The component's location has not yet been decided at this stage. After these decisions have been made the schematic and component list are passed to the ECAD stage.

The ECAD stage is predominantly concerned with the placement of the chosen components, this is carried out within the given form factor and is based upon the schematic decided by the Electrical engineering stage. Once the component layout is decided the equipment can be

[2] although different companies may call these stages by different names, the work must always be completed in the same order by different departments with the same basic priorities

manufactured and undergo the qualification test, if the test is successful the design process is over. The qualification test is designed to be more severe than the launch environment and it should be assumed that electronic equipment is designed to pass the qualification test and not the launch.

The MCAD department is concerned with the structural side of the equipment, this is the stage that decides the initial form factor on which the ECAD stage must place the components, they also decide the geometry of the initial enclosure. Usually, the MCAD stage is not involved with the design of every piece of equipment (only when deciding a new form factor); however, when a design fails the qualification test the MCAD stage does become involved in the design process. In this situation the MCAD stage must decide on the best course of action to modify the design to pass the test. These modifications can in some cases be as simple as increasing the PCB thickness, although sometimes more complicated and time consuming measures are required, such as modifying the layout or altering the component choice; in the event of these more complicated modification further input from the other two stages is required(Johnson and Brockman, 1996; Yeh et al., 1990).

The inefficiency in the traditional design process occurs when a design fails the qualification test, as up to three stages may have to be re-iterated in the resultant modification process. For example, if the component choice is considered to be the problem then all three stages of the design must be rerun. The resultant inter-departmental communication, re-design, manufacturing and testing stages, are time consuming and costly, this is especially true if different departments or, worse still, different companies are involved in the re-design process. Fortunately, most electronic equipment usually survives the qualification test first time, and it is only approximately $< 5\%$ of designs that fail and require a re-design or modifications, but it is decreasing this 5% that this work focuses on.

3.3 Proposed Design Process

In this section the proposed tools for each of the different design stages are described. This description is in terms of how the tools are expected to be used and the assumptions they are based upon. The work that is required to prove the validity and accuracy of the tools is discussed at the end of the chapter in a separate section.

3.3.1 Electrical Engineering Stage

A list of the robustness of the various package types is proposed, this list allows more robust packages to be chosen over less robust ones (this list shall be referred to as the Package Robustness DataBase PRDB). This tool is based on the assumption that some package types are intrinsically more susceptible to vibration than others, regardless of the exact input environment. It is expected to improve the overall process by - to a small extent - optimising the choice of components so that more robust components are used where possible. The list is only intended to be used when there is a free choice between two package types and is not intended to interfere with the electronic engineer's usual method of working. The creation of the list is a relatively straightforward process based on experimental data, an example is shown in chapter 8.

In addition to the main point mentioned above, it would also be convenient if the list could have the following characteristics: To maintain simplicity the components are split into three different categories: low, medium and high risk. The resolution of the list could be modified easily by the user, so if a simpler list was required, then the list could be altered to just low and high robustness, whereas if it was considered that higher resolution would be preferable then the package types could be split into more sections, this could also be easily achieved by common spreadsheet or database software.

3.3.2 Electronic Computer Aided Design Stage

It is proposed that maps are provided that illustrate how severe the local vibration environment is over the PCB, this is based on the assumption that the PCB's vibration response can be modelled to an appropriate accuracy even if the component layout has not been exactly specified yet. These shall be referred to as Environment Severity Maps (ESMs). The ESM database is expected to contain pre-solved maps based upon generic input parameters, namely: form factor, averaged component mass per unit area, averaged component stiffening per unit area, vibration intensity and PCB thickness, these generic maps remove the requirement to create a new map for every new design cycle.

The maps could take the form of a contour chart indicating areas of equally severe vibration environment. For the sake of argument let's say the areas are colour coded, with red being highly severe, yellow being medium severity and green being low severity. In this example, components from the bottom third of the PRDB (the most fragile components) can only go in

the green areas and not in yellow or red areas. The components from middle of the list can go in yellow or green areas, whilst the components at the top of the list (the most durable components) can go in all areas. The simplicity of this approach makes it easier to use and less likely to be applied incorrectly, all with the minimum of additional time and effort when compared to the standard approach.
Additionally, with this approach, if it is not possible to create a layout where the components are in areas that are considered safe (i.e. a weak component can only be placed in a yellow area), then pre-emptive action can be taken by passing the proposed design to the MCAD department for greater scrutiny instead of immediately manufacturing and testing the design.

3.3.3 Mechanical Computer-Aided Design Stage

The MCAD stage would be provided with a method of creating a higher accuracy FE model, this model would take into account factors such as: more accurate vibration envelope specification, component effects and the effect of modifications such as increasing PCB thickness or boundary stiffness. These models can be used to decide the most efficient way of modifying a board that fails a qualification test or is highlighted as unsafe during the design stage. Additionally, the results of any failures from qualification tests of designs could be automatically fed back into the PRDB to increase the accuracy, and also lack of failures in qualification tests can also provide very useful information.

3.4 Analysis of the Effectiveness of Proposed Process

The next two sections provide two further ideas that further strengthen the case for the proposed process.

3.4.1 Pareto Principle

The Pareto principle (Also known as the either 80-20 rule or the law of the vital few) is a convenient way to explain the philosophy behind the proposed method of improving the process. This description is included here, but it shall be referred to throughout the rest of this chapter.
The general idea behind the principle is that in many systems 80% of effects come from 20% of the causes (hence the alternative name of the 80-20 rule), and that if this 20% of the causes can

be identified and operated on then 80% of the benefit can be realised. To put this another way, 80% of the work can be achieved with only 20% of the effort, whilst the remaining 20% of the work takes the other 80% of the effort[3]. This principle is a useful and widely used analogy for analysing complex systems(Chatterjee and Sorensen, 1995).
Throughout this work the Pareto principle is used to further justify the proposed process, it is argued that by creating a simplified process that requires 20% of the effort of a fully detailed solution, 80% less of the designs will fail the qualification test. Thus the 80% reduction in the number of failed designs (as opposed to the full 100% reduction that might be realised with detailed analysis) is acceptable. The fully detailed process requires so much effort that it is usually not practical to implement in any case.

3.4.2 Design Structure Matrix

A generic process for designing electronic equipment is shown in the Design Structure Matrix (DSM) in Figure 3.2, this representation shows the inter-dependence of each of the sub-processes, with the upper quadrant showing feed-forward dependencies and the lower quadrant showing feedback. The DSM can be used to examine which sub-processes must be re-run if feedback occurs (arrows can be thought of as flow of information), i.e. if a process is required to be modified all the dependant processes must be re-run.
To explain this idea another way, the DSM can be thought of as a modified flowchart diagram (as shown in figure 3.1), with the different processes/decisons/tests found on such diagrams represented by a diagonal row of boxes. The arrows in the top right hand side show the normal forward flow of information, the arrows in the bottom left side show how the information must flow back during design re-iterations. Say a design fails the qualification test this is when the feedback arrows must be followed, which is generally a bad thing as it means more resources/time/manhours is required. Furthermore, the further the feedback arrows are from the diagonal greater the number of processes that must be re-run for that given iteration. For example, if it is found that the component choice must be altered to make a given design reliable, then it can be seen that the entire design process must be repeated(with the feedback arrow going from the last to the third process), which is a very costly undertaking. Whereas, choosing to use a thicker PCB only requires the board to be manufactured again, which is not

[3]The specific numbers of 80 and 20 are only general guidelines, and could quite easily be different, the basic idea is that the majority of effects can be controlled by a minority of the causes.

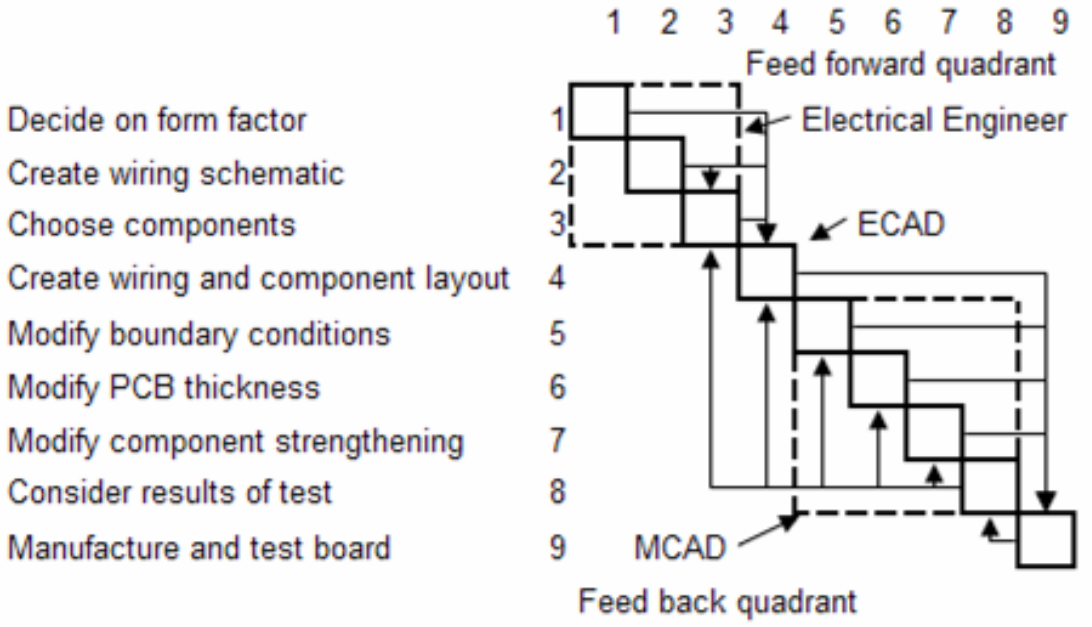

Figure 3.2: DSM representation of a generic design process for electronic equipment. Essentially, this is just a different format of the information in the standard flowchart in figure 3.1. Different processes are grouped according to their relevant stage (i.e. Electrical Engineer, ECAD or MCAD) by the dashed lines. Created through discussion with a typical spacecraft engineering company about their design process.

so costly. In the simplest terms a process can be made more efficient if the length and probability of feedback loops can be reduced, as this reduces design iterations.
This idea has been used to improve the traditional design process, the proposed process is shown in Figure 3.3, the additional sub-processes are discussed below with respect to each stage. In this diagram it can be seen that the old feedback loops that were required to optimise the choice of components, have, by various assumptions, been reduced to small feedback loops that occur during the first run of the process. That is, using the PRDB and the ESM optimises - to some extent - the component choice and location. The benefits of this optimisation are twofold, not only is the design more likely to be successful first time, but if the design does fail there is little requirement to reiterate the component choice or layout, as these have - to some extent - already been optimised, thus less inter-departmental communication is required.
In addition to the first two tools there is also the tool available to the MCAD stage should the design fail the qualification test (Process 10), the increased accuracy ESM's are used to decide the most efficient way of modifying the design to make it pass the qualification test, hopefully

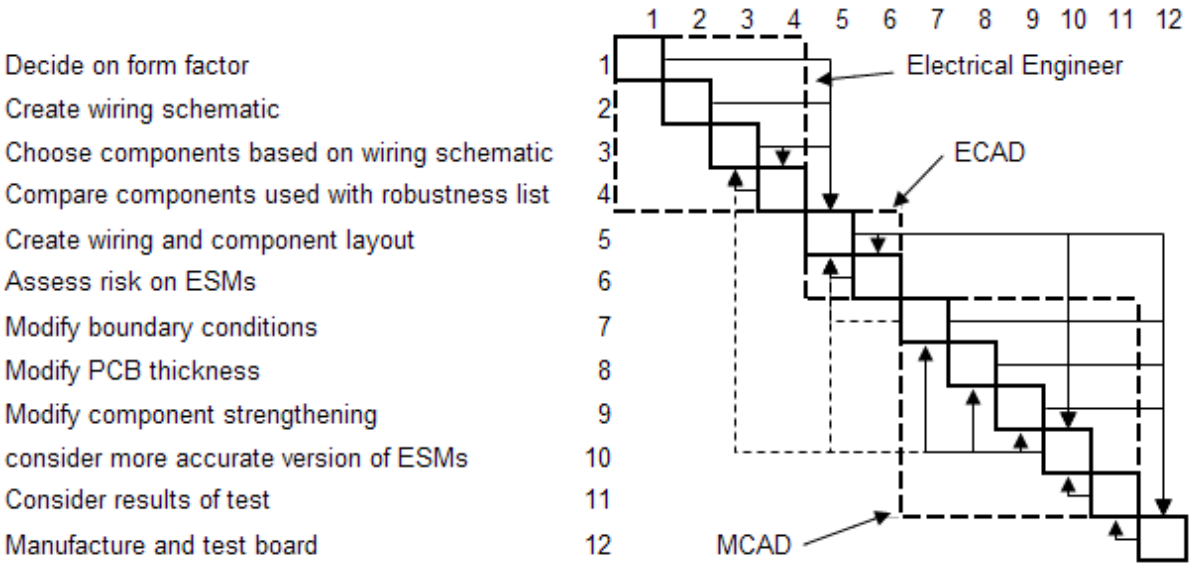

Figure 3.3: DSM for proposed process. The dotted feedback lines represent feedback loops that are much less likely to occur in the proposed process.

limiting the maximum number of iterations to two. Furthermore if a safe solution can not be found for a given schematic/component choices, then these designs are highlighted to allow the MCAD department to take pre-emptive action before manufacture, such as modifying the boundary conditions or increasing board thickness.

3.5 Work Required to Prove Tools

This chapter has, up until now, described an overall process that overcomes the shortcomings of the current state of the art, this has been achieved by proposing some relatively simple tools that can be used during the design process. What is required now is to look at the specifics of these tools. For example, what accuracy should be expected from the tools? How would a company go about creating these tools specific to their own processes and designs? What ball-park figures should be expected for component failure? In the rest of this section these type of questions are answered for the response prediction tools (ESM maps and higher accuracy MCAD versions) and then the failure criteria (PRDB) tools (this simultaneously defines the supporting work that must follow in the rest of this thesis). An important point to consider whilst reading the rest of this section is that the accuracy is different between different manufacturers and that specific values can not be given. What can be given - however - is the

process for a manufacturer to calculate these values for their own equipment (this is an important point that is continually visited throughout this work, that it is not specific values that are of interest, but the processes to calculate these values).

3.5.1 Response Prediction Tools

First, let's consider how to create the non-simplified higher accuracy models required by the MCAD department, as once these can be created it is then a relatively trivial task to create the ESM maps. These non-simplified models are only needed by the MCAD stage when a design fails, i.e. when more detailed and accurate models are required in order to fully understand the nature of the failure.

To create these models, the first task is to examine the accuracy that is possible when modelling an individual unpopulated PCB, i.e. disregarding the effect of manufacturing variability and components. At the same time as doing this, it is also convenient to investigate what factors (such as the accuracy of determining: boundary conditions, PCB properties and damping) have the greatest influence on the model accuracy, allowing future models to be made more efficiently. To achieve these two points, the modelling of two typical pieces of electronic equipment are given as case studies (this is performed in chapter 4), the models accuracy is measured and the factors that have the greatest influence on the accuracy are examined. Using the same approach it is then possible for an MCAD department to create accurate PCB FE models of an individual unpopulated PCB, and to do so more efficiently and quickly than was previously possible.

The next task is to consider what error is introduced when using smeared models of populated PCBs. This error is dependant on the specific characteristics of the case at hand, as such, one single value is not appropriate and different values must be given based on: the type of simplification applied, as different simplification assumptions give different errors; the PCB thickness, as thinner PCBs are more significantly affected by additional component effects; and the type of equipment being modelled, as ignoring large heavy components creates more modelling error than ignoring small components. To measure this error a Monte-Carlo style sensitivity analysis is performed as this permits the effect of different combinations of variability to be considered, this is shown in chapter 5. With this information, the MCAD department can find the expected maximum error with the modelling method they are using, and allow them to decide whether to use this method or to use a less simplified model.

Next, the expected variability arising from manufacturing variability is required. A process to find this variability is to measure the variation between a few different batches of identical equipment, this is shown in chapter 6. With this information the MCAD department are then able to determine the expected accuracy of not just a given PCB but also of a batch of PCBs, this can be included in the results as a safety factor.
Thus, with all these bits of information it is possible to create an accurate PCB model and - more importantly - have an idea of the expected accuracy of this model, whilst the time to create such a model is greatly reduced by removing the need to model the components in detail. The next step is to simplify this process even further so that the ESMs can be created. Two main assumptions allow the ESMs to be created, first, the choice of the components is known but not the location and, secondly, the accuracy of the ESMs does not need to be as high as is required for the MCAD FE models. These two bits of information allow the ESMs to be created before any design decisions are taken, as follows: For a given form factor several ESMs could be pre-solved with increasing levels of component mass loading (using the smearing technique), then - when the ESMs are required - it is only a matter of choosing the ESM with the correct component mass. Additionally, if a company uses more than one thickness of PCB, then the ESMs can be pre-solved for these different thicknesses; fortunately, there are only a few standard thicknesses (most often 1.6mm or 2mm) so this is not a difficult undertaking. The only real difficulty is in choosing the values to output from the solution, it is expected that either local acceleration or curvature would be the most appropriate values to take, either of which is easily achieved with modern FE packages. The creation of ESMs is relatively simple, so this discussion is accordingly short; however, a practical example of how to create the ESMs is given in chapter 8.

3.5.2 Failure Criteria Tools

Now the discussion turns to look at how a user would create component failure criteria, or more specifically a database of such criteria, this process is shown in chapter 7.
The first point to consider is that the components reliability is strongly determined by the packages used and the manufacturing techniques employed attach them, to account for this fact the same packages and manufacturer must be used during collecting the experimental data as in the real-life situations for which the experimental data is intended.
A second major point to consider is that historically the failure has been attributed to either

acceleration or local PCB curvature without the relative significance of either parameter ever being determined. To allow accurate tools to be created this ambiguity must be overcome; therefore, it is necessary to create a test that can determine this relative significance. A cantilever set-up is proposed for this purpose and shown in chapter 7, this set-up can used to determine the relative significance of acceleration and curvature for any package type in future. Furthermore, if curvature is shown to be the primary cause of failure then the direction of curvature must be determined, as the uni-axial curvature can take one of two directions across the component and also there is biaxial curvature to consider. The later work shows how to consider all these different factors and include them in to the failure database.
The final requirement to show that the tools can be created is an example of an actual failure database, what information should be included and in what format. This should be considered with respect to the ESMs and an example use be given (this is shown in chapter 8).

3.6 Conclusion

In this chapter the basics of an improved electronic equipment design process has been put forward. Starting from the traditional design process an improved process has been proposed. This new process incorporates tools that first reduce the probability of a design failing the qualification test, and secondarily help decide on the most efficient method of remedying a failure should one happen. The effectiveness of these tools has been further justified through the use of Pareto analysis and by considering the typical design workflow. Most importantly, the supporting work required to create these tools has been laid out, setting the structure for the rest of the work in this thesis. In terms of predicting response, this starts with the requirement for a process to measure expected modelling accuracy for unpopulated PCBs, thus allowing the accuracy of future PCB FE models to be assessed (this is detailed in chapter four). Next there is the requirement to examine how different types of component modelling simplification assumptions reduce the model accuracy, where this is dependant on factors such as size and number of components (chapter five). The final requirement for response prediction is to create a process that can measure the amount of manufacturing variability that is present; so that this can be included as a safety factor in future models (chapter six). In terms of the failure criteria side of the problem, the main requirement is to show a process that can create this failure data (chapter seven).

In addition to verifying the proposed processes, this work also provides some useful secondary functions, such as: how to make more accurate models with less effort, what is the most effective simplification method in different situations, how to reduce the impact of manufacturing variability and what factors principally influence component failure. Furthermore, although this work is principally focused on processes and all the values published here are only anecdotal examples for the given case studies, these values are still very useful as initial ball-park values for future work.

Chapter 4

Simplified FE Modelling of PCBs: Method and Accuracy

4.1 Chapter Overview

Using an experimental approach, this chapter examines the creation of simplified FE models of PCBs, their expected accuracy and how to most efficiently improve this accuracy. This is achieved by attempting to model two representative PCBs using the typical modelling process. Where this FE modelling process involves the following main steps (in practice many steps are omitted or assumed, especially those later in this list): create a FE mesh of the PCB; experimentally measure and include the PCBs' mechanical properties and thickness; incorporate the PCB chassis in the model; experimentally measure the boundary condition stiffness between the chassis and the PCB (or "tune" these values into the FE model); and, finally, measure the damping values of the combined chassis and PCB system (this is only a brief description, the whole process is fully described to greater detail in appendix F). This list omits the modelling of the component effects as this is considered separately in the next chapter.

To quickly recap, the primary shortcoming of this typical modelling practice is the scarcity of full frequency response comparisons between experimental and predicted responses (with only a couple of exceptions known (Aglietti, 2002; Aglietti and Schwingshackl, 2004)), as most analyses are limited to comparing natural frequencies only. The work presented in this chapter overcomes this shortcoming by using the aforementioned techniques to model two typical PCBs, allowing the accuracy of the actual board stresses to be investigated instead of just the

natural frequencies as in most previous work.
The three main contributions of this chapter - towards creating the design tools - can be summarised as follows: (1) The example process shown here can be followed to allow electronic equipment manufacturers to obtain expected accuracy values specific to their own equipment and manufacturing techniques, where these are in terms of values that much more closely correlate with failure than in previous work; (2) the observations presented here allow the modelling effort spent on future PCB models to be used much more effectively; and (3) the expected accuracies published here can be used as initial ball-park values for future work.

4.2 Properties Determination

In this section, the material and damping properties of two typical PCB set-ups are measured, and then the results from these tests are to be used to create FE models of the PCBs. Two PCB set-ups are measured as this clearly illustrates the idea that different set-ups exhibit properties and variations.
Throughout all the tests in this work, the frequency response was measured with a dynamic signal Acquisition Board (NI PCI-4472) and several small accelerometers attached to the boards (Piezotronics 0.6 or 0.2grams).
The two PCBs to be modelled are hereafter referred to as Set-up A and Set-up B, neither are populated with components, they consist of the following:
Set-up A consists of a unpopulated PCB attached to an aluminium enclosure as shown in figure 4.1. The PCB is made of FR4 laminate and is attached to the enclosure with M2.5 bolts, it measures 289mm by 316mm and weighs 359grams. The enclosure has cross-members (also known as an anti-vibration frame) to provide extra support for the centre of the PCB (as shown in figure 4.10), these have a width of 6mm and a height of 4mm. The enclosure is attached to the shaker head expander with 8 M5 bolts and using 30mm stand-offs to minimise air pumping effects. In later tests the PCB and enclosures free-free responses are measured by hanging each from elastic bands. The accelerometer's positions are shown in figure 4.1, the placement of these accelerometers was chosen to ensure that all the primary mode shapes were measured and that the response could be accurately recreated.
Set-up B consists of an unpopulated PCB directly attached to shaker head expander with 28 M3 bolts evenly spaced around the perimeter as shown in figure 4.2. The bolts gave the PCB a

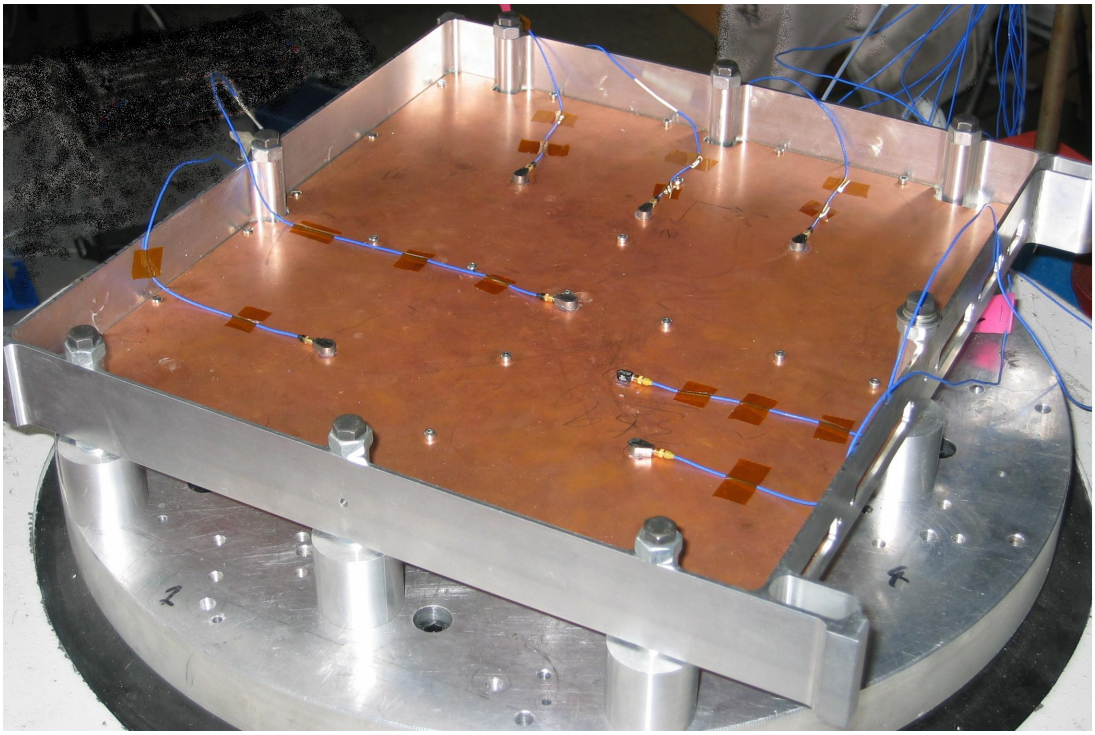

Figure 4.1: Set-up A attached to the shaker head expander.

20mm standoff (as shown in figure 4.3) to minimise air-pumping effects. Seven supposedly identical PCBs existed to allow variability tests later, all measured 250mm by 250mm and weighed within ±1g of 190.5grams. The accelerometer's positions are shown in figure 4.2, the placement of these accelerometers was chosen to ensure that all the primary mode shapes were measured and that the response could be accurately recreated.

4.2.1 Determination of PCB Properties Test

The aforementioned PCB modelling approach was first applied to Set-up A (PCB and enclosure as in Figure 4.1). The first step was to exactly determine the material properties as the values provided by the manufacturer could not be guaranteed to be correct (see Table 4.1 for a comparison of manufacturers and actual material properties). During these tests the following points were made:
The material exhibited 15% stiffness variation between the x and y axis, highlighting the significant amount of anisotropy present in the material. It was observed that during both the Young's modulus and shear tests that the FR4 had relatively high level of hysteresis, and that it was even more necessary than usual to consider both the loading and unloading cycles.

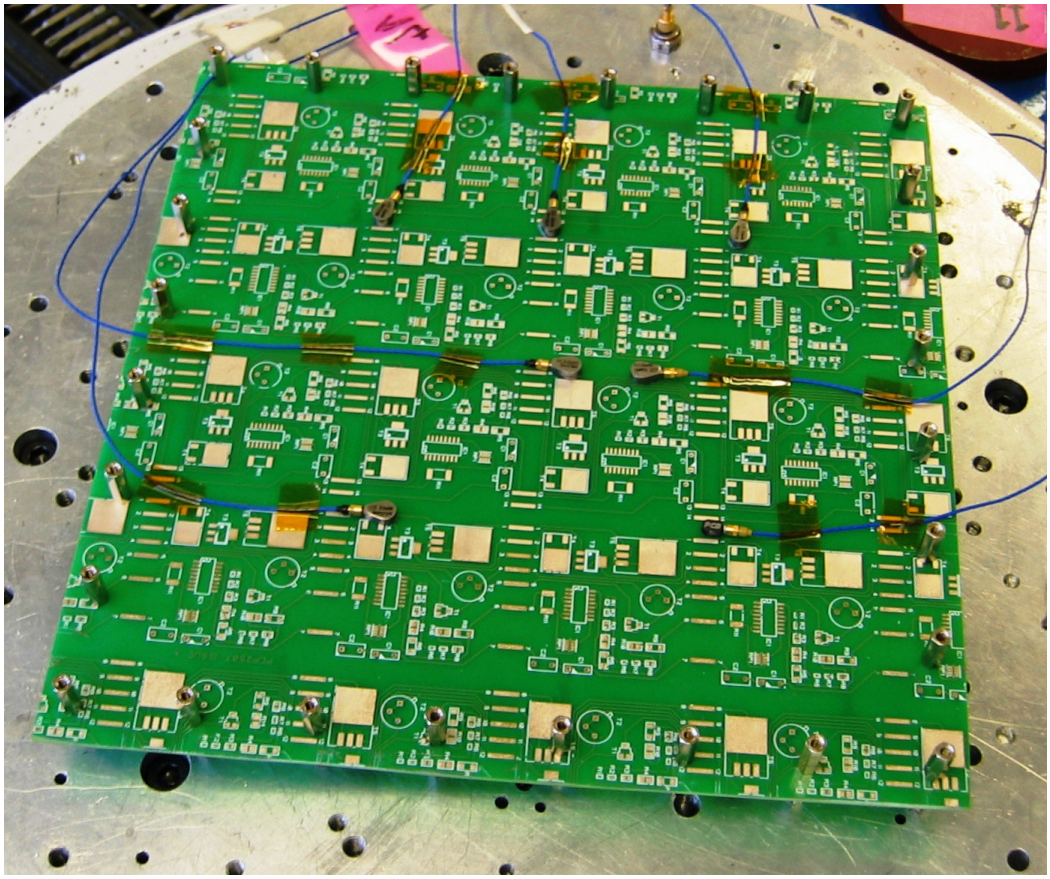

Figure 4.2: Set-up B attached to the shaker head expander.

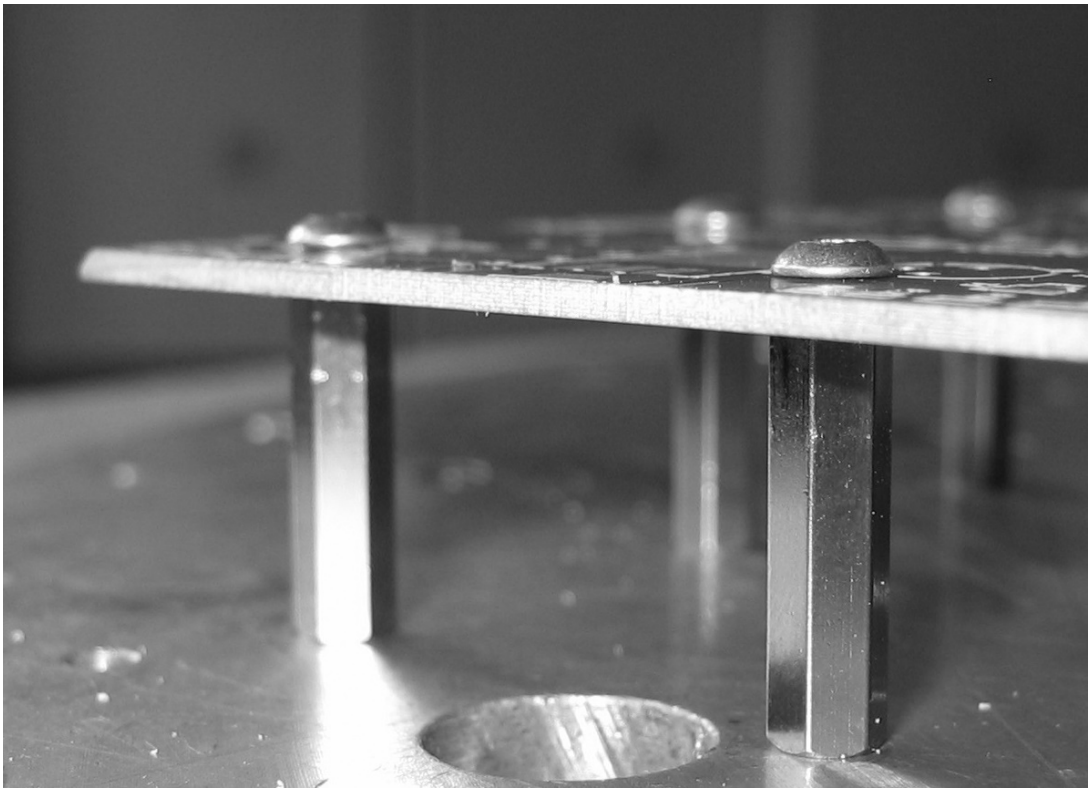

Figure 4.3: Set-up B attachment method.

The thickness of the PCB was measured at multiple points over the initial uncut specimen, where the "uncut" specimen is the original piece of FR4 from which the PCB was cut and measured $600mm$ by $300mm$; surprisingly it was found that the thickness varied over the material by 0.12mm, if this amount of variation was not considered throughout the test it would drastically affect the accuracy of the results.
The density of this particular sample measured to be 2480 kg/m^3 which was 3% higher than the value of 2400 kg/m^3 given by the manufacturers.
Overall, it was noted that the experimentally measured properties of the PCB in Set-up A were appreciably different from the manufacturers published values (see Table 4.1).
Using the damping measurement techniques introduced earlier (formulas F.4 to F.10), the damping was measured for the combined structure. To investigate whether the damping varies with PCB response the measurements were performed over a range of different input accelerations and using different vibration inputs (see figure 4.4). When using the logarithmic decrement method it was found that decay over several cycles should be used and multiple measurements taken and averaged if good results are to be obtained.

Property	Measured	Manufacturers values	Units
Young's modulus (x axis)	$4.02 * 10^{10}$	$3.50 * 10^{10}$	N/m^2
Young's modulus (y axis)	$4.56 * 10^{10}$	$3.50 * 10^{10}$	N/m^2
Density	2481	2400	kg/m^3
Shear modulus	$1.21 * 10^{10}$	not given	N/m^2
Poisson ratio	0.3	0.3	
Thickness	1.54-1.66	1.65	mm

Table 4.1: Material Properties of PCB in Set-up A, experimentally measured values and manufacturer's published specification data.

Property	Measured	Units	$\sigma(\%)$
Young's modulus (x axis)	$2.4 * 10^{10}$	N/m^2	6.4
Young's modulus (y axis)	$2.0 * 10^{10}$	N/m^2	4.0
Density	1820	kg/m^3	neg.
Shear modulus	$4.4 * 9^{10}$	N/m^2	4.35
Poisson ratio	0.3		-
Thickness	1.69	mm	0.26

Table 4.2: Average material properties of seven PCBs in Set-up B.

The whole process of properties measurement was repeated for Set-up B (set-up shown in figure 4.2, as seven identical PCBs existed it was also possible to measure the variation in the properties. Measured values are given in table 4.2 and figure 4.5). The manufacturer could not give the material properties of its boards, although it did state the boards were built according to standard IPC-4101B/21. When measuring the damping properties on this second set-up (set-up B) it was found that a much higher responses could be obtained, this allowed damping values to be given up to much higher board accelerations. The damping was assumed a function of both the board and boundary conditions.

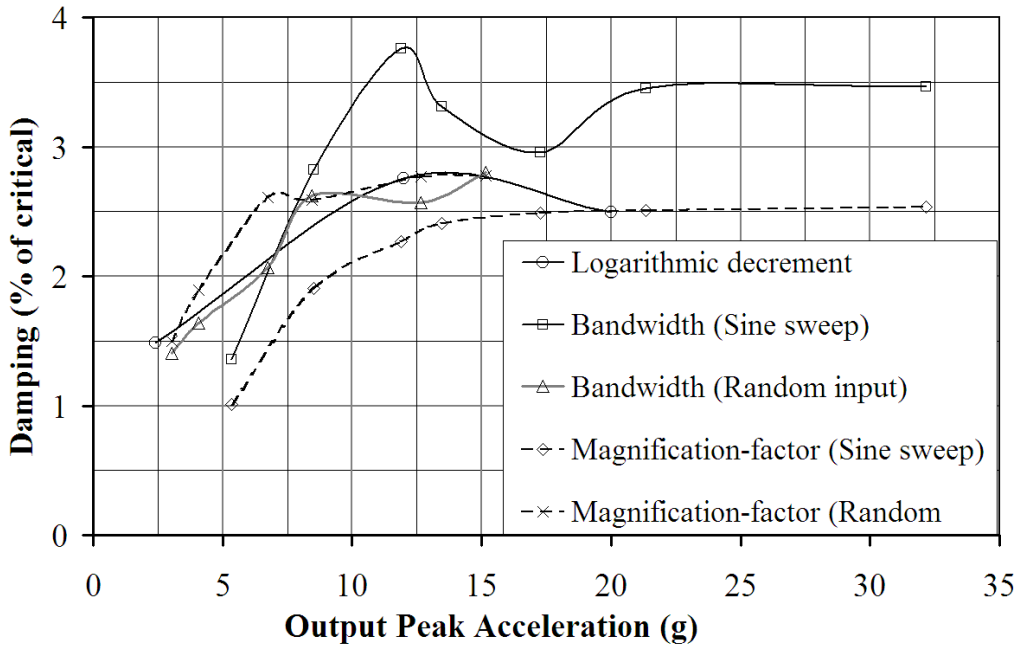

Figure 4.4: Damping of Set-up A measured using different measurement techniques, plotted against maximum acceleration of centre of PCB.

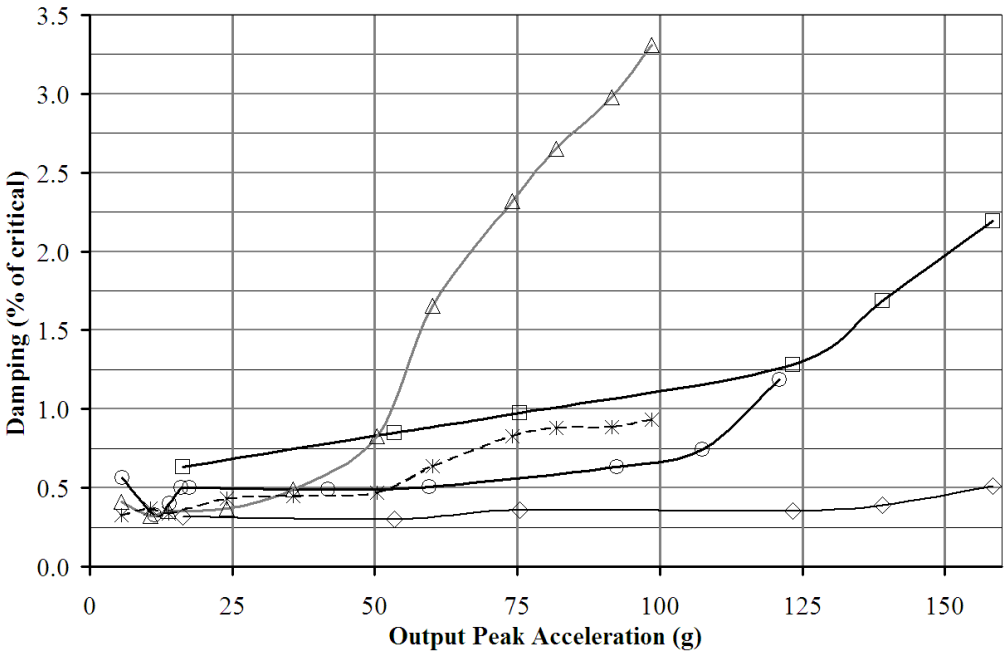

Figure 4.5: Damping of PCB in Set-up B measured using different measurement techniques, plotted against maximum acceleration of centre of PCB.(Using same legend as in figure 4.4)

Mode	f_{exp} (Hz)	f_{model}	Q_{exp}	Q_{model}
1	146.3	146.8 (-0.31%)	164.3	149.8 (8.83%)
2	547.1	534.3 (2.34%)	75.4	60.7 (19.49%)
3	564.8	572.2 (-1.31%)	47.2	64.09 (-35.8%)

Table 4.3: Comparison of experimental and predicted response of Set-up B. Figures in parentheses are percentage error values.

4.3 Finite Element Modelling

4.3.1 Set-up B

The first PCB to be modelled was Set-up B (see figure 4.2), with the intention of obtaining a plot of the predicted frequency response that could be compared against the real response. The model was built in the PATRAN modelling environment and solved using NASTRAN. The model of the PCB was simply created using QUAD4 shell elements. Material properties were created and assigned to these elements using the experimentally derived material properties, a 2D Isotropic material was used. The elements in the PCB mesh have a edge length of 6.6mm, which is determined by repeatedly reducing the element size until the solutions of the models converge, in this example this procedure generates a mesh of 37 by 37 elements.
The next step after creating the PCB model is to apply the boundary conditions. The PCB translational boundary conditions are assumed to be rigidly grounded because the PCB in the experiment is directly attached to a $30mm$ thick Aluminium plate, thus it is assumed that the response of the plate is negligible compared to that of the PCB. The PCB rotational boundary conditions are modelled by spring elements (CBUSH) attached to the mesh at each fixing location, and the rotational stiffness of these elements are increased ("tuned") until the model frequencies match the experimental frequencies (see table 4.3). The tuned model has a rotational spring constant value of $45Nm/rad$.
The final step is to apply damping to the model based on the experimentally derived values (see figure 4.5); unfortunately however, several different damping measurement techniques are possible and each gives a different value. To overcome this problem all the different experimentally measured values are tried in the model and the correlation compared to see which gives the best results. The logarithmic decrement method gives a damping of 0.5% (derived using equation F.4 and F.5) and is found to give the best results, which agrees with

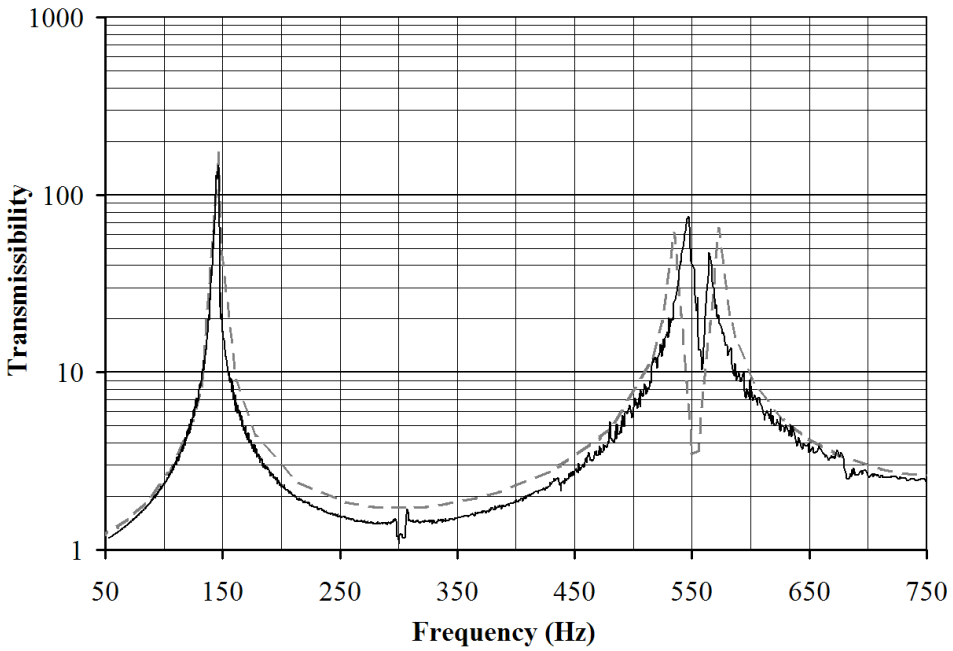

Figure 4.6: Comparison of response predicted by FE model (dotted line) and real response of Set-up B. Low base acceleration input was used. Comparison location is the centre of the PCB.

conventional theory that this damping measurement method is the most appropriate for such low values of damping(de Silva, 1999). The final predicted response correlates well with the actual response (see figure 4.6 and table 4.3).

The previous comparison is based on a very low base excitation ($0.01g^2/Hz$ flat input spectrum), permitting the assumption of negligible non-linear effects because of the very small board deflections. What would happen if the small deflection assumption could not be made? To answer this question the test is repeated at a much higher vibration level so that the deflections are significantly greater than the board thickness, ensuring that there should be some non-linear effects(Cifuentes, 1994). The FE analysis is also repeated with updated damping values based on the new acceleration input and damping values from figure 4.5. A comparison of these results (as shown in figure 4.7) shows that the non-linear effects present at the higher excitation levels significantly alter the response near resonance.

The final test on this set-up examines the effect of components on model accuracy. The board is populated with 74 grams of various different small components; these components are a mixture of different SMT and PTH components, none with an edge length greater than 10mm. This effect is then incorporated into the FE model by artificially raising the density to simulate

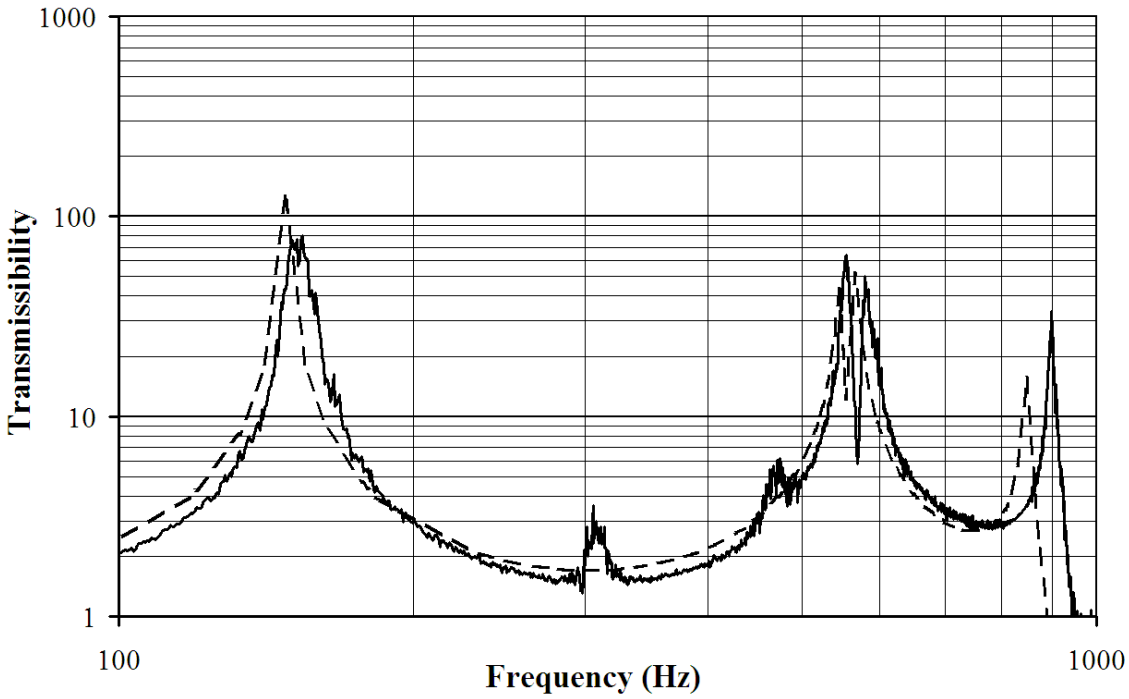

Figure 4.7: Comparison of response predicted by FE model (dotted line) and real response of Set-up B. High base acceleration input was used to investigate non-linear effects. Comparison location is the centre of the PCB.

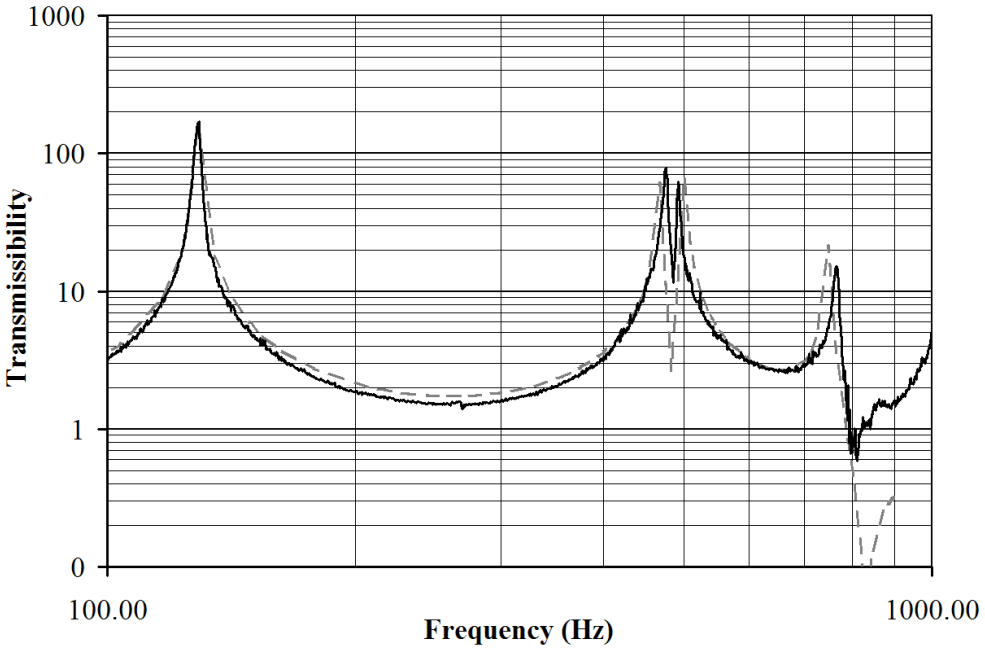

Figure 4.8: Comparison of response predicted by FE model (dotted line) and real response of Set-up B when populated with components. Low base acceleration input was used. Comparison location is the centre of the PCB.

the effect of the components. Any additional stiffening effects of the components are ignored. The effectiveness of this method can be seen in figure 4.8 and table 4.4.

4.3.2 Set-up A

The modelling of Set-up A is considered next (see figure 4.1), again with the intention of examining the difference between the predicted and experimentally measured responses. The PCB FE model is built in a similar way to the previous model (see figure 4.9), using QUAD4 elements and 2D Isotropic material. The free-free response of this PCB model is calculated and

Mode	f_{exp} (Hz)	f_{model}	Q_{exp}	Q_{model}
1	129.2	129.5 (0.21%)	170.4	171.1 (0.36%)
2	476.2	467.0 (-1.97%)	73.9	60.9 (-21.2%)
3	492.9	500.1 (1.42%)	62.5	65.0 (3.82%)

Table 4.4: Comparison of experimental and predicted response of Set-up B when populated with components. Figures in parentheses are percentage error values.

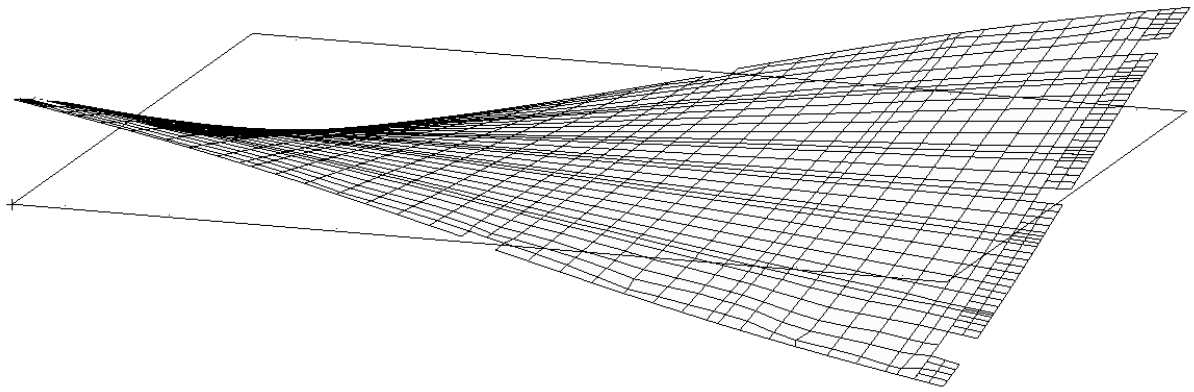

Figure 4.9: First torsional mode of finite element model of free-free PCB from Set-up A.

is shown to have good correlation with the experimentally measured free-free response (see Table 4.5 column A). Additionally, two more predictions of the free-free response are made, one prediction is made using the material properties provided by the manufacturer (Column C) and another made using the material properties measured here and the material thickness provided by the manufacturer (Column B). For this comparison a MAC Test was not performed because of the relatively few accelerometers used; instead, a qualitative comparison of mode correlation was performed to ensure mode correlation.

The chassis is modelled using a combination of QUAD4 shell elements for the chassis walls and Bar2 beam elements (see Figure 4.10). The only mode shape of any importance to the modelling of the PCB response is that of the central crossbeams, these are experimentally shown to have a natural frequency of 210.4Hz whilst the FE model of the chassis predicts frequencies of 209.8Hz, a difference of less than 0.5%.

To predict the response of the PCB in the enclosure the two models must be combined (see figure 4.11), to achieve high accuracy the PCB model is offset so that it lays exactly on top of the chassis model and anti-vibration frames. As before, the attachment is achieved using rigid translational elements and tuned rotational spring elements at the location of each fixing. Unlike the previous model, it is not possible to tune the spring elements to correlate the frequencies, as a spring constant that allowed correlation of the first natural frequency would leave other modes significantly in error ($\Delta f > 10\%$).

With some effort, it has been found that the PCB can only be modelled to a good accuracy in the following way: First, in addition to tuning the rotational stiffness it is found that modelling

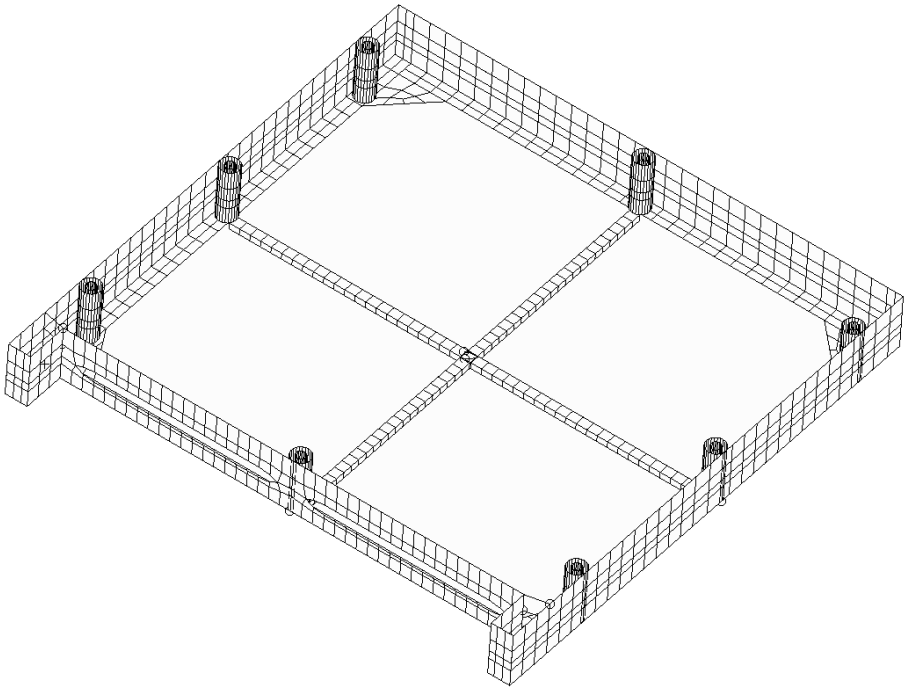

Figure 4.10: Finite element model of Set-up A enclosure without PCB attached. Notice the central cross-members that provide additional PCB support (cross-beams and internal stiffening ribs are modelled as 1D beam elements but for clarity are displayed here as representative solid elements).

the PCB fixings with a translational spring element allows good frequency correlation, these additional spring elements also required tuning. This suggests that the initial assumption of the PCB fixings being effectively rigid in translation is incorrect for this set-up. Secondly, it is found that the amplitude response prediction could be improved by specifying lower damping for higher frequency modes. This suggests that damping drops off with frequency, as the higher modes have lower displacement this would agree with the results of the earlier damping tests. The correlation of the final tuned model can be seen in table 4.6 and figure 4.12.
Finally, two additional models are included to investigate two commonly made assumptions, namely, that the PCB to chassis connection can be modelled as either clamped or completely simply supported. Figure 4.13 shows the comparison of these two models against the "tuned" model, one using rotationally rigid elements and one using elements that do not constrain rotation. A frequency variation of up to 5% can be attributed to the first mode and 10% for the second mode. Variability in the response magnitude is the same as for the tuned models (see table 4.6).

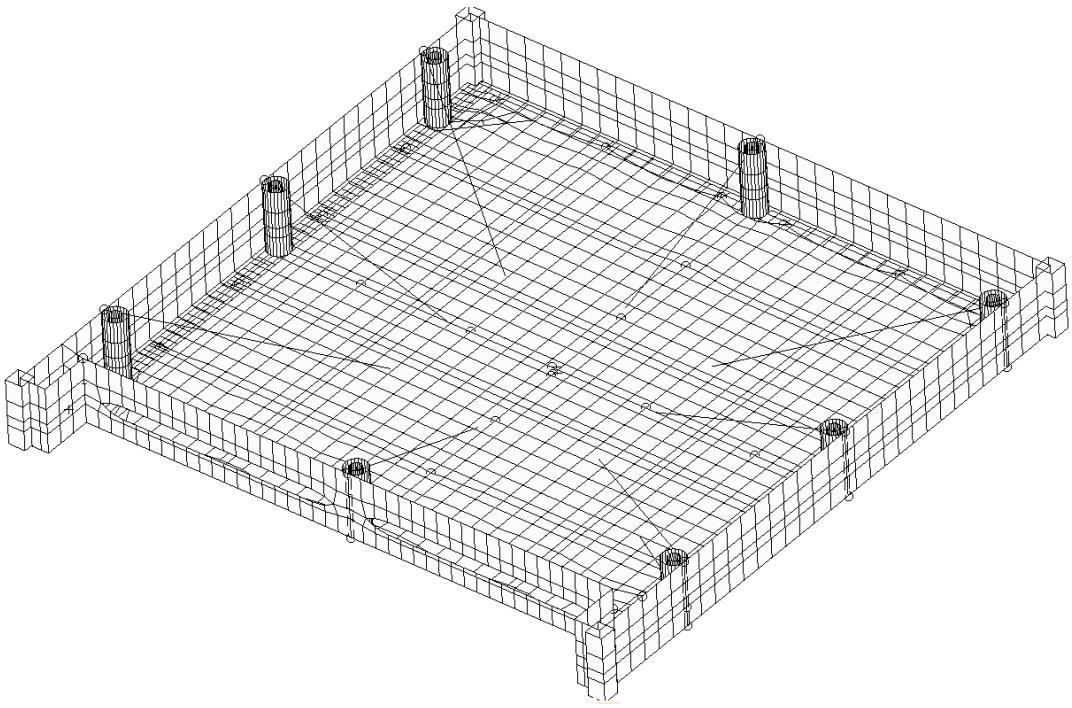

Figure 4.11: Finite element model of Set-up A enclosure with PCB attached.

4.4 Discussion

Let's consider the following question: "To what accuracy can a simplified PCB FE model predict the vibration response?" The quick answer is that if the damping, PCB material properties and boundary conditions are accurately defined then high accuracies are easily possible. In theory this is simple but what about in practice? This question is the basis of the rest of this discussion.

First, in terms of the inaccuracy that arises from poor specification PCB material properties (stiffness, density, and thickness), if the stiffness properties can be measured through bend testing, then a significant amount of this possible inaccuracy can easily be removed (assuming that density and thickness are easily measured). As it is assumed that most manufacturers confine themselves to using only a few different PCB types such bend testing would be relatively simple to achieve. The effect of not doing such bend testing and just using the values provided by the PCB manufacturer are significant (as shown in table 4.5).

The following additional points have also been noted for determining the PCB material properties: (1) The laminate material is noted to have strongly anisotropic properties and an accurate model cannot be created without using the stiffness moduli in both the x and y axis;

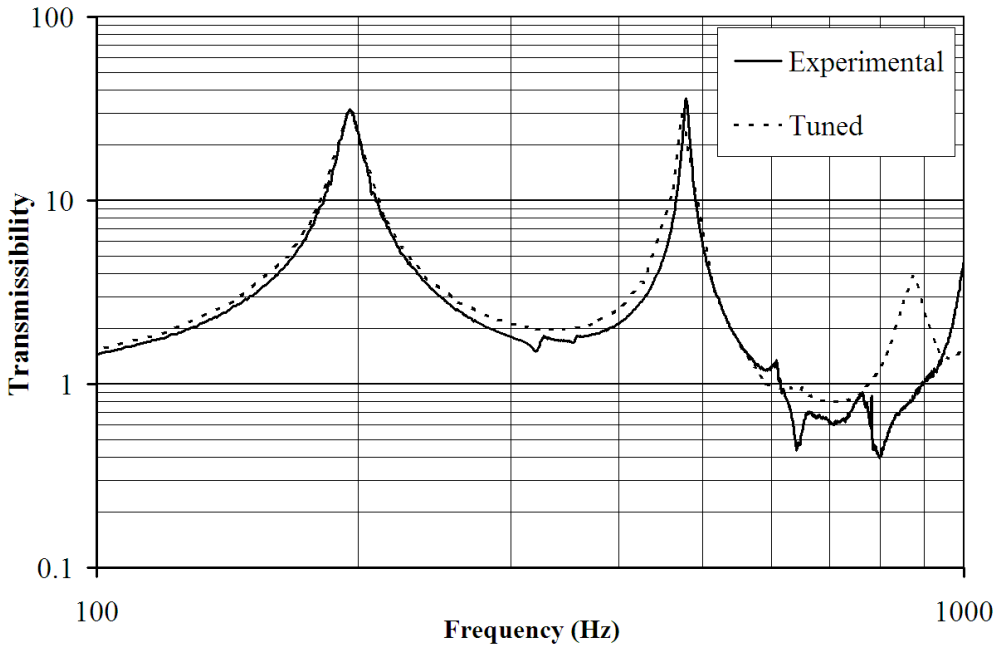

Figure 4.12: Comparison of response predicted by FE model (dotted line) and the actual response of Set-up A. Comparison location is the centre of the PCB.

Mode	Experimental	Percentage discrepancy		
	Frequency (Hz)	A	B	C
1	41.3	1.19	6.94	-15.66
2	66.6	0.15	-6.39	-31.62
3	93.3	-0.75	-13.64	-37.41
4	110	0.20	1.11	-22.36
5	119	0.79	-2.18	-26.46
6	204	-3.13	-9.05	-33.07
7	210	-0.82	-0.17	-23.67
8	243	1.12	-10.65	-15.17
9	280	-0.14	-8.48	-2.56

Table 4.5: Table showing difference in natural frequencies between experimental test on free-free unpopulated PCB and various FE models. Model A uses experimentally derived material properties and PCB thickness, Model B assumes constant PCB thickness and model C uses the material properties provided by the PCB manufacturer.

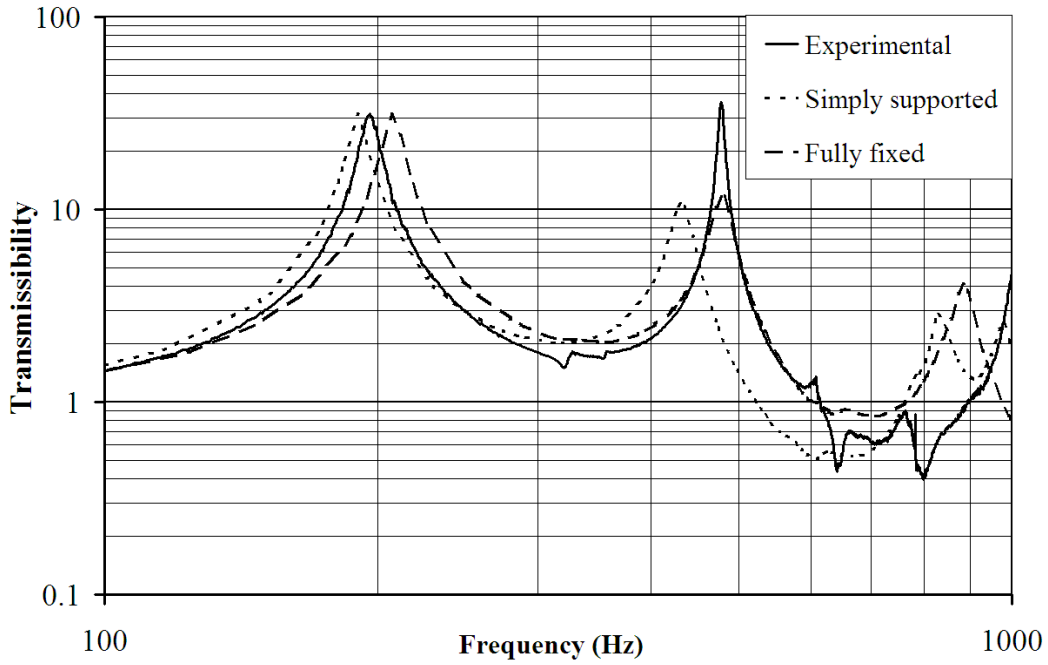

Figure 4.13: Comparison of experimental results of Set-up A with two different FE models, the "Simply supported" model assumes the PCB to chassis connection has zero rotational stiffness, whilst the "Fully fixed" model assumes a rigid rotational connection. Comparison location is the centre of the PCB.

Mode	Frequency (Hz)			
	Experiment	Tuned	SS	FF
1	196	195.6	190	207
	(*31.49*)	(*31.17*)	(*31.17*)	(*31.17*)
2	322	314	301	342
3	357	365	349	381
4	478	478	460	515
	(*35.86*)	(*34.15*)	(*11.71*)	(*11.27*)
5	637	635	618	678
6	1010	884	942	1066

Table 4.6: Comparison of experimental results and FE models using different boundary conditions. Subscripts ss, ff and tuned refer to simply supported, fully fixed and tuned edge conditions respectively. Italic values in parentheses are the peak transmissibility for that mode, where these were known.

(2) Hysteresis effects are significant in laminates making the measurement of loading and unloading cycles during bend testing more important than usual; (3) The significance of measuring and including shear stiffness in the model should not be overlooked; and (4) small thickness variations can significantly affect the accuracy of results if not considered.

Damping is another important driver of modelling error and is more difficult to measure, being complicated by the fact that it is not constant with respect to input acceleration and that it also depends on the chassis and fixing type. This is highlighted by the two modelling cases here: In set-up B the damping is easily measured and allowed accurate modelling on the first attempt. In set-up A, however, the damping is more difficult to include, as it is shown that accurate modelling could only be possible when frequency dependant damping is applied, as the difference in damping for different modes is significant.

In addition, the following points should also be considered when measuring damping: (1) Measurements should be made at different power input levels to reflect how damping varies with increased deflections; (2) The Logarithmic method is the most suitable method for measuring damping, especially when the damping is low; (3) It is highly recommended to average multiple damping readings; and (4) It is not safe to estimate damping based on Steinberg's method (see appendix F.1.5), as this predicts a damping value of 5.5% for Set-up B where the actual damping is 0.5%, although it should be noted that Steinberg's method is not specifically intended to be applied in this way.

However, what if the equipment to be modelled does not exist yet? How should the damping be found then? In this situation the only solution is to measure the damping for already existing equipment that is similar enough to the proposed design, where the similarity should extend to the approximate dimensions, fixing type and PCB thickness. It may be found that there are patterns in the damping of many different pieces of equipment for a given equipment manufacturer.

Similar to damping, the error incurred from applying boundary conditions depends on the individual case at hand, with set-up B being simpler than set-up A. Set-up B could be tuned simply using rotational stiffness only, whereas Set-up A required additional translation springs to achieve relatively good correlation.

Again, the question must be posed "What if the equipment to be modelled does not exist yet?" Just as in the damping situation the only solution is to measure the boundary rotational stiffness of some similar equipment and apply the measured values in the current FE model. In

this situation the similarity should extend to the: PCB thickness, fixing method and fixing tension.

Another point to consider is that at high levels of excitation non-linear effects may become significant and further decrease accuracy. Fortunately, the non-linear effects seem to only reduce the response, so ignoring them is a conservative assumption.

Thus, the answer to the question posed at the start of this section is not straightforward. Yes, it is possible to build very accurate FE models of PCBs if enough information is known, but how easy is it to get this information? The answer is that it depends on the specific manufacturer at hand, as well as the amount of similar equipment that the manufacturer possesses to permit the creation of rough damping and BC estimates. Therefore the process detailed in this chapter must be followed for every manufacturer to create data specific to their own equipment and modelling processes.

Finally, a test was also included to examine the accuracy of modelling populated PCBs, this showed that good accuracy can be achieved by just smearing the additional component mass over the FE model; however, this is only one anecdotal case where the components were relatively small, light and evenly distributed. A more in-depth study of the accuracy of populated models is included in the next chapter.

4.5 Summary

The work in this chapter assesses the accuracy of typical FE models used to predict the PCBs vibration response. It has been shown that if good data exists for the boundary conditions, material properties and damping, then even simple PCB FE models can deliver very accurate response prediction; however, this is rarely the case as the measurement of these properties is commonly either assumed or neglected, in this situation the work here illustrates how to measure the expected loss of accuracy that arises from these assumptions. Furthermore, the significance of each of these different factors can now be taken into account, allowing the time and effort available for future modelling attempts to be spent much more efficiently.

Chapter 5

Sensitivity Analysis of Simplified PCB FE models

5.1 Chapter Overview

As mentioned in the literature review, a major difficulty with response prediction is that the PCB's vibration response is altered when components are attached, as the components effectively increase the mass and stiffness of the PCB. This is particularly true when heavy or large components are present as these increase the PCB's mass and stiffness the most.
The problem can be solved, in theory at least, by building a detailed finite element model of the PCB and components (where each component is modelled in detail as in figure 2.11); however, this approach is rarely used as it requires a long time to build and solve the model. To save time and effort, the standard practice is to create simplified models where the components geometry is not modelled at all. In these simplified models the components geometry is ignored; instead, the component effects are included by increasing the Young's modulus and density of the PCB FE model so it effectively behaves as if components were present. The relative simplicity and speed of these simplified methods has led them to be more favourable than detailed methods.
The primary contribution of this chapter is to build upon previous work(Pitarresi et al., 1991; Pitarresi and Primavera, 1991) and show a process to calculate the additional error that is realised when using any one of the several possible simplification techniques. This is achieved using a Monte Carlo style sensitivity analysis approach, where the calculation is performed for several hundred different randomly created, hypothetical configurations to ensure that the

results are valid over a greater range of cases than previously possible. The work presented here improves on previous work by considering the response for more realistic boundary conditions (as shown in figure 5.7) and in terms of the maximum board curvature; this is because board curvature better correlates with component failure than the MAC that was used previously. This is because the MAC is only a relative measure of how similar two mode shapes are, it does not consider amplitude nor does it give useful measures of error[1].

5.2 Proposed Solution

To address the current shortcomings of the response prediction method (i.e. only considering MAC and the anecdotal nature of previous proofs), the work here examines the difference in board curvature between simplified (globally smeared) and non-simplified models (locally smeared) as shown in figure 5.1. In this work, instead of creating the locally smeared model from real experimental data, the locally smeared model is randomly created from distributions that are typical to the kind of equipment of interest (see figure 5.2). This creates a "benchmark" case to which global smearing can later be applied and the results between the two compared. Let's consider this process in more detail. First a finite element model of a hypothetical PCB is created, where small areas of the FE model have been given a higher stiffness and density value to mimic the effect of *attached components*. From this model a simplified model is created, applying global smearing (or neglecting stiffness or mass increase) as shown in table 5.5. Both of these models are then solved to find the local PCB curvature, and then the maximum percentage error between the two models can be calculated.

Unfortunately the error is not only a function of the simplification process but also other properties such as the PCB geometry and Component characteristics (e.g. Component: mass, geometry, number of leads and density), the method for choosing these variables is detailed in appendix G. To account for these different factors the process is run multiple times, with each run using different randomly created input properties, these multiple runs allow the error to be given at many different situations (i.e. simplification types, component types, component density, PCB thickness, etc.) and with a known confidence.

Finally, in addition to component effects, it is known that the PCB boundary conditions have a large influence on the vibration response (Sidharth and Barker, 1996), significantly altering

[1]The work in this chapter is based upon a paper by the same author that is currently awaiting pubication(Amy et al., 2009b)

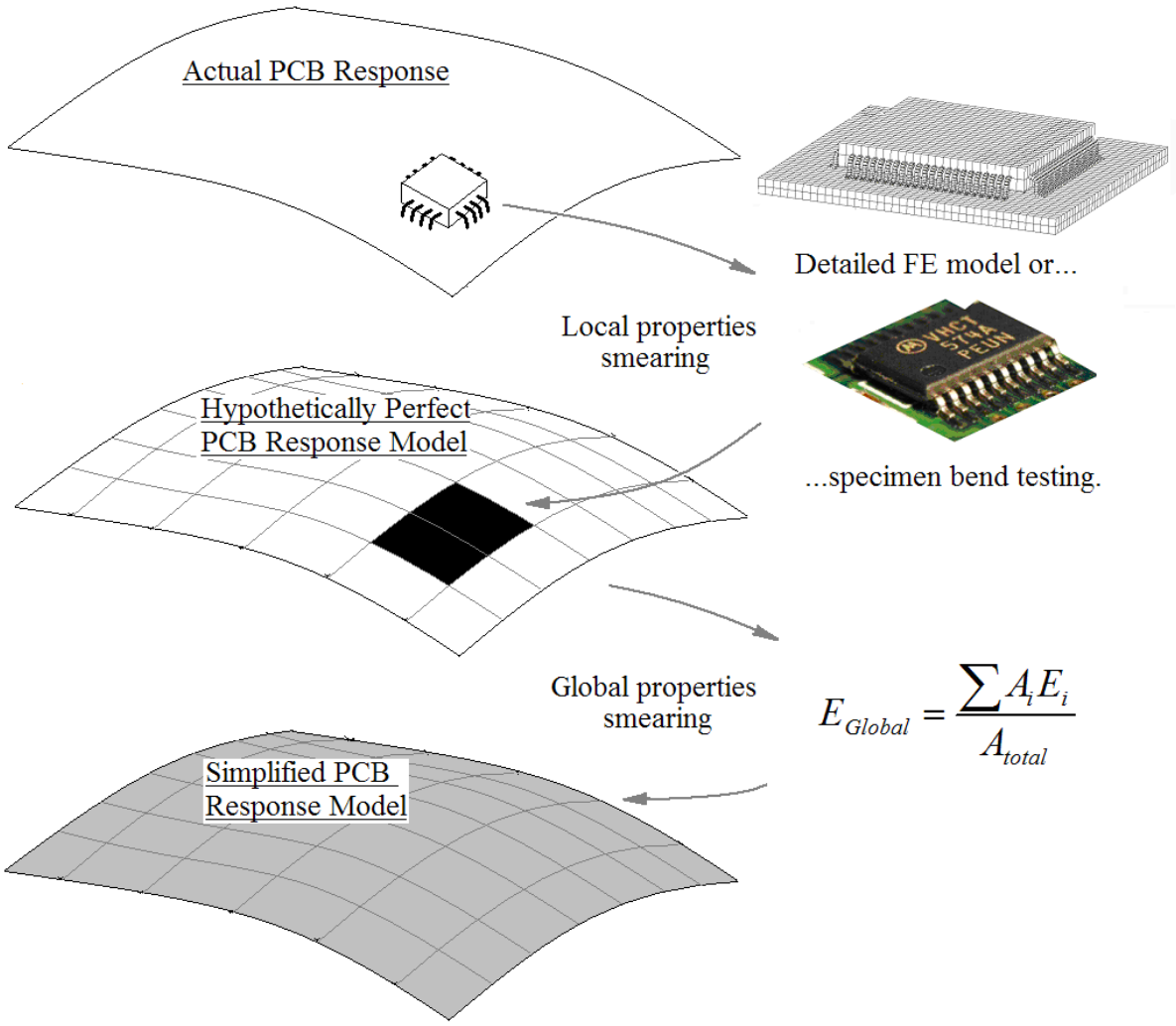

Figure 5.1: Example of two-stage PCB modelling process: local properties smearing and global properties smearing. Local properties smearing is achieved through experimental data or detailed FE models. Global properties smearing is through a numerical formula. This work randomly creates hypothetical locally smeared models to which global smearing is applied and error calculated.

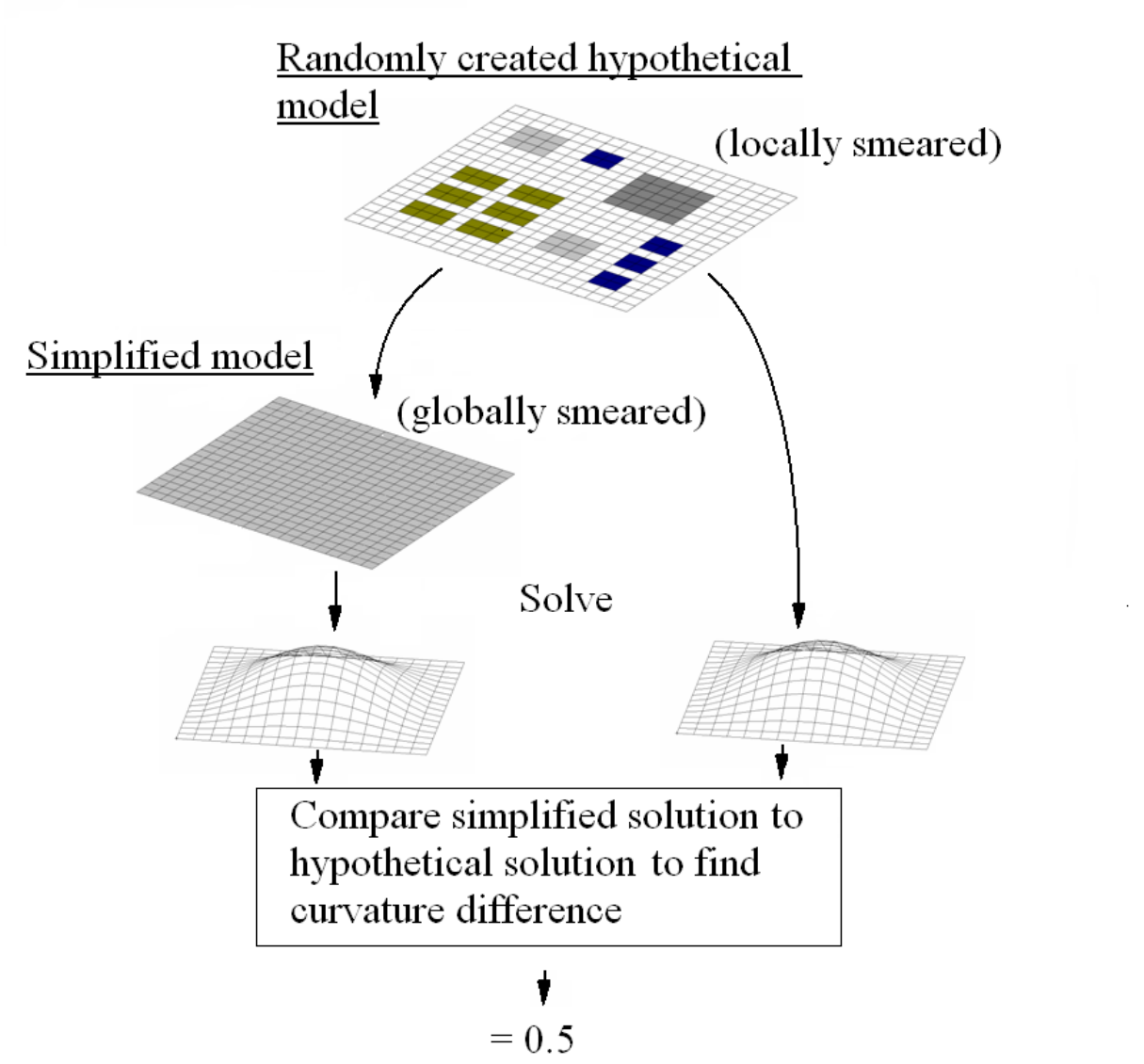

Figure 5.2: Example of sensitivity analysis process. A hypothetical model is created with random placement of components; this is solved to find the response. The model is then simplified, in this example by averaging component effect over the PCB area (global smearing), and the results are then compared to the hypothetical solution. The entire process is repeated many times with different randomly created models.

both natural frequencies and maximum deflection. The amount of boundary rotational stiffness present depends on the method of fixing the PCB to the chassis, usually bolted, with larger bolts and higher tightening torques giving greater stiffness. The previous work on validating the smearing process has only considered PCBs with free-free boundary conditions(Pitarresi et al., 1991; Pitarresi and Primavera, 1991), this avoids the uncertainty introduced by needing to measure and model the boundary conditions. However, free-free boundary conditions are rarely found in real situations, thus this work incorporates more realistic boundary conditions into the randomly created models (see figure 5.7), using values from 0% to 60% fixidity[2] randomly distributed throughout the models.

5.2.1 Proof and Applicability

It is important to realise that this work specifically only considers the error created when applying the global smearing technique (see figure 5.1); not the error from any other sources such as local properties smearing or natural variability. These other sources are divided into either sources of modelling error (other than from global smearing) or sources of manufacturing and assembly variability (considered in chapter 6):

In terms of sources of modelling error, there is the inaccuracy that arises from local properties smearing, this has already been considered in previous work Pitarresi et al. (1991); Pitarresi and Primavera (1991). This previous work compares experimental data of various different populated PCBs with their respective locally smeared models. All the models were shown to have convincingly high correlation. These previous tests avoided the need to consider other sources of error (mentioned below) by: using a free-free boundary condition to ignore BC effects, accurate bend testing measurement of the PCB mechanical properties, and making damping measurement unnecessary by only considering the MAC and frequency correlations. Fortunately, the trends highlighted later in this work suggest that ignoring this stiffness contribution is usually a conservative assumption; therefore the bend testing is unnecessary (provided that the equipment to be modelled fits within the characteristics of the case study given here).

Another factor is the inaccuracy that arises from poor measurement and specification of

[2]The percentage fixidity parameter defined by Steinberg (Steinberg, 2000). The edge stiffness may vary from 0% to 100% fixidity, with 0% reflecting a simply supported condition and 100% being fully clamped. In most cases the percentage fixidity is not greater than 60%, as higher values than this require an excessively overbuilt clamping mechanism.

damping or boundary conditions, these have already been considered in chapter 4.

5.3 Pre-process analysis

Prior to running the proposed process it is necessary to define the distribution of the input values; these distributions determine the results, and the consequent calculated errors are only relevant to equipment that falls within these distributions. For this case study, the type of equipment that is analysed has the properties shown in tables 5.1 to 5.3 which is discussed in the rest of this section. All of these properties are randomly assigned during each run of the process, unless specified they are uniformly distributed over each range. Every error distribution is calculated from the results of a hundred runs.
In this work the component types have been divided into the following three broad categories:

1. The *Light components* classification is intended to simulate small discrete components such as resistors or transistors, the size and mass of such components is small, the stiffness increase is negligible (see figure 5.3).

2. The *Surface Mount Technology components* category symbolises components such as Quad Flat Pack (QFP), Ball Grid Array (BGA) and Pin Grid Array (PGA), which are generally about 10mm to 30mm square, and have a increased density and stiffness ratios that are in proportion to the length and inversely proportional to the thickness of the PCB to which they are attached (see figure 5.4).

3. The *Heavy components* category is intended to reflect large components such as transformers, large power capacitors and resistors. The density and stiffness ratios are proportional to component length (see figure 5.5).

The SMT stiffness ratio increase was calculated using several FE models of attached SMT components of various sizes, the effective stiffness of the underlying PCB in these models was calculated and then compared to the stiffness of the same PCB without an attached component; the ratio of the results gave the stiffness ratio increase. The stiffness ratio was subsequently applied as a factor to the PCB modulus of elasticity in models. The models were created in the PATRAN modelling environment and solved using NASTRAN solvers. The main difficulty in creating the model was because of the complicated process of modelling the component leads and board attachment, this difficulty was overcome by using the published

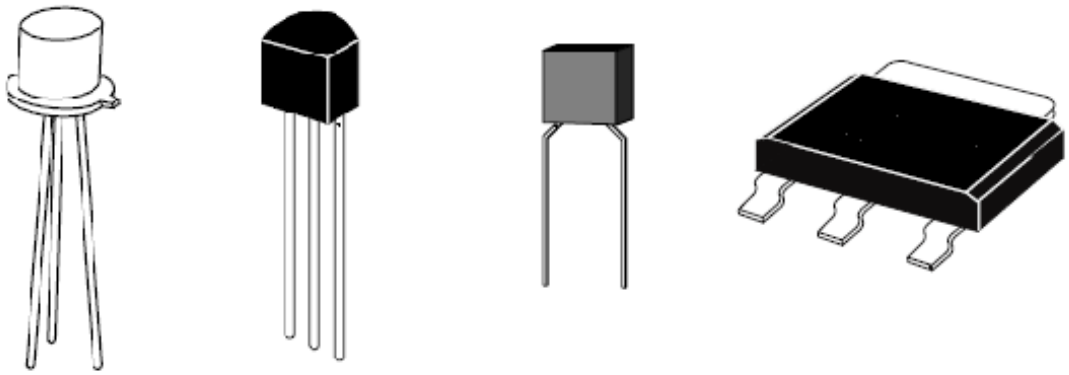

Figure 5.3: Examples of small components, from left to right, TO-39 transistor, TO-93 transistor, CK05 capacitor and SOT-223 SMT transistor. Largest dimension of all components is less than 10mm.

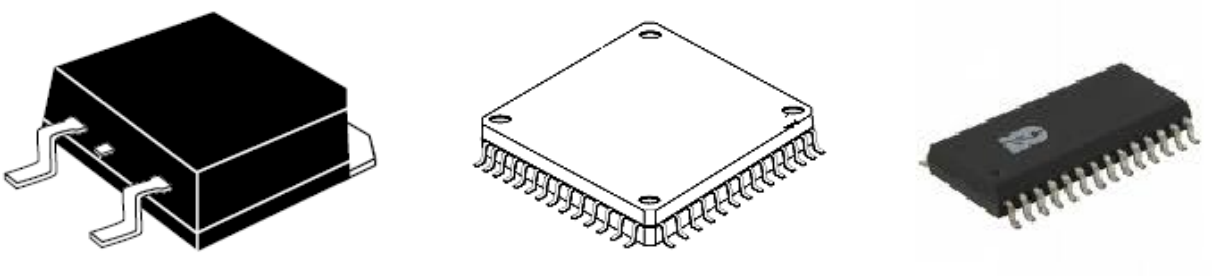

Figure 5.4: Examples of SMT components, from left to right, TO-268 transistor, QFP IC and SOIC IC. Largest dimension of all components is approximately 25mm.

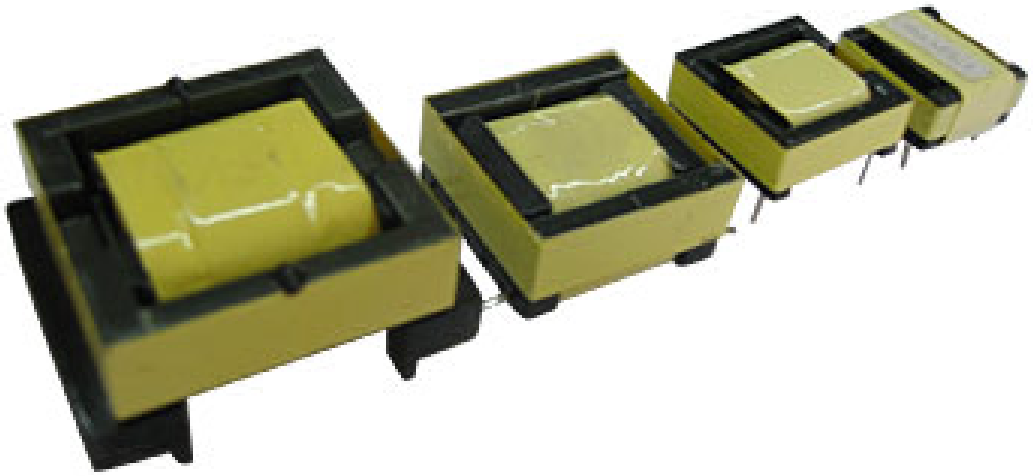

Figure 5.5: Examples of transformers for printed circuit boards, largest dimension of components range from 20 to 35mm. Other large components include large power capacitors and resistors.

lead stiffness constant formulas(Kotlowitz, 1989, 1990). These formulas remove the need to model each lead, instead each lead is replaced by a set of spring constants, where the spring elements act between the component body and solder joint location on the PCB. To fully mimic the effect of a real lead, each one was modelled by three displacement and rotational spring constants. Additionally, the component body geometry and stand-off were all based on standard package dimensions to make the model as realistic as possible (an example of one component is shown in figure 5.6).
Comparing the values calculated here with those experimentally measured in previous work(Pitarresi and Primavera, 1991) gave reasonable correlation. In fact, the previous work found the stiffness ratio for SMT components to be around 1.8-1.9 whilst the FE models calculated the ratio to vary from 1.33 to 3.5. The larger range is because the FE models examined here cover a larger range of component sizes than the previous research, if only similar size components are considered the the difference in the ratios is less than ± 0.1.

5.4 Model Input Properties

In this study the following variables were used to randomly create each run.

PCB thickness

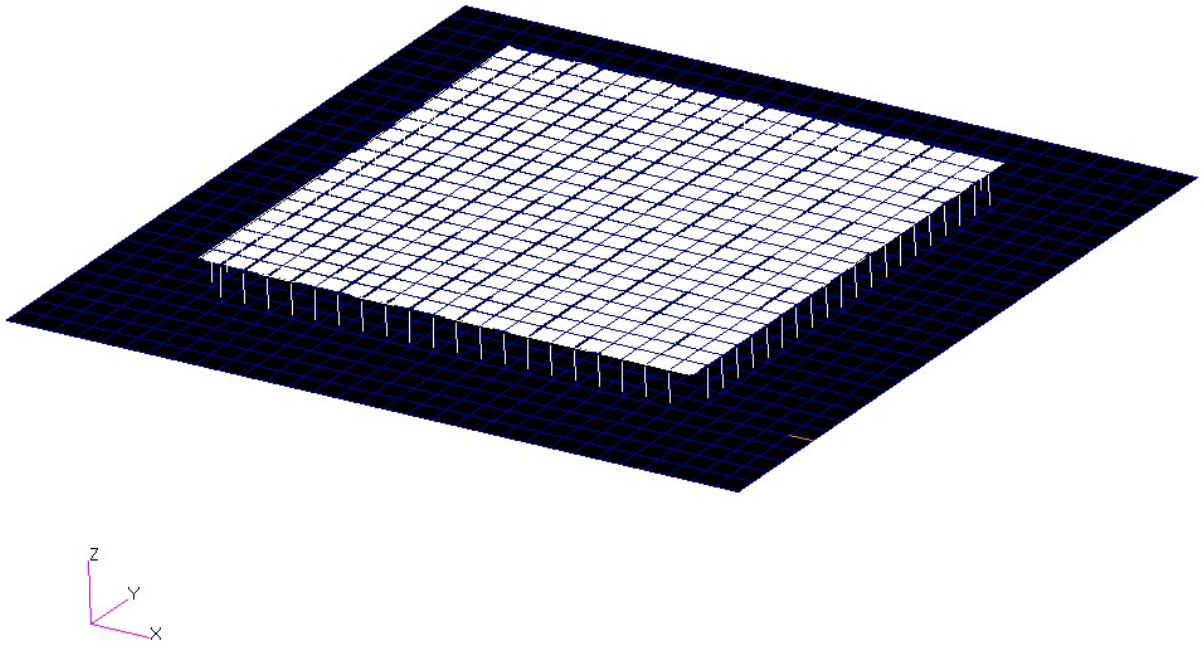

Figure 5.6: Example of a preliminary component for calculating additional stiffness. Dark section is PCB, light section is component body. The body is attached to the PCB through representative spring elements.

Variable	Range	Distribution
Thickness	1.6 or 2mm	Discrete
Edge Length	75 - 150mm	5mm intervals
Young's modulus	$25.5 * 10^9 GPa$	Single value
Density	$1900 kg/m^3$	Single value
Edge ratio	1.0 - 0.7	Continuous
Component areal density	0.1 - 0.5	Continuous

Table 5.1: Table of PCB properties. Component areal density refers to the area of the PCB that is populated with components.

Edge Degree of Freedom	Condition
Translational displacement	Fixed
Rotations perpendicular to specific edge	Fixed
Rotation parallel to specific edge	0% - 60% fixidity

Table 5.2: Boundary condition limit of applicability

Component classification	Edge length (mm)	Smeared property ratio		
		Stiffness	Torsional stiffness	Density
Light	5 - 10	1.3 - 1.6	1.6 - 2	1.5 - 2
SMT	10 - 30	1.33 - 3.5	1.6 - 7	1.5 - 6
Heavy	20 - 35	3 - 4	5 - 6.5	6 - 56

Table 5.3: Component properties (all values are from continuous distributions, apart from length which is in $5mm$ intervals)

To reflect standardised industry thicknesses, the PCB thickness was given the possibility of two discrete depths of $1.6mm$ and $2mm$. It would be possible to specify a continuous distribution or a larger range of intervals if necessary.

PCB edge length and ratio

The PCBs longest edge was given from a distribution of edge lengths from $75mm$ and $150mm$. The ratio of the edge lengths was from a distribution of 0.7 and 1 which was used to calculate the length of the shortest edge.

Component type

There are three different types of component: Light, SMT and Heavy. These have been discussed previously.

PCB type

In this study it was relevant to create four different categories of PCB to reflect the different types of equipment that are modelled, each different category to reflect the predominant type of components used in that model(see table 5.4).

1. **Power** Using only heavy components.

2. **Power and Processing** Using equal area of heavy and SMT components.

		Component Types		
no.	Equipment Type	Light	SMT	Heavy
1	Power			1
2	Power & Processing		0.5	0.5
3	Processing		1	
4	Light Processing	0.5	0.5	

Table 5.4: Table of relative component distribution for different PCB classifications. For example, a hypothetical model that is intended to simulate a PCB of the type "Light Processing", has 50% SMT components and 50% light components.

3. **Processing** Using only SMT components.

4. **Light Processing** Using equal area of SMT and light components.

More categories could be identified or even a continuous (as opposed to discrete) range could be used if required.

Boundary rotational stiffness

The boundary rotational stiffness was given a value between 0% and 60%, based on Steinberg's percentage fixidity parameter(Steinberg, 2000). These values were chosen because a percentage fixidity above 60% is very difficult to achieve in practice (see figure 5.7 for an example of PCB boundary conditions).

Areal component density

The areal component density were given a uniform distribution between 0.1 and 0.5, with 0.5 reflecting a board with 50% of its area covered by components. These values were relevant to this individual case study and the types of board expected to be modelled.

Component location

In addition to the other variables, the position of each component on each model is randomly chosen, removing any dependence on relative component location and ensuring the results are applicable to a large range of PCB layouts (see figure 5.8 for an example).

5.5 FE Model Creation and Solution

Once the models geometry and layout have been defined it is possible to create the FE model. The FE model is a very simple 2D mesh of shell elements, with component locations

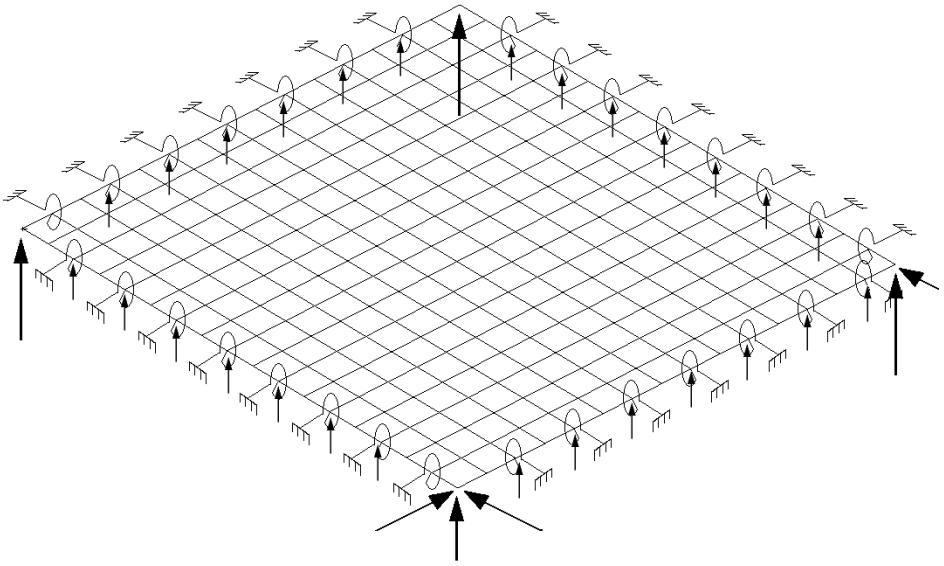

Figure 5.7: Example of boundary conditions. Edge displacement is constrained in the out of plane direction and edge rotation is limited by spring elements.

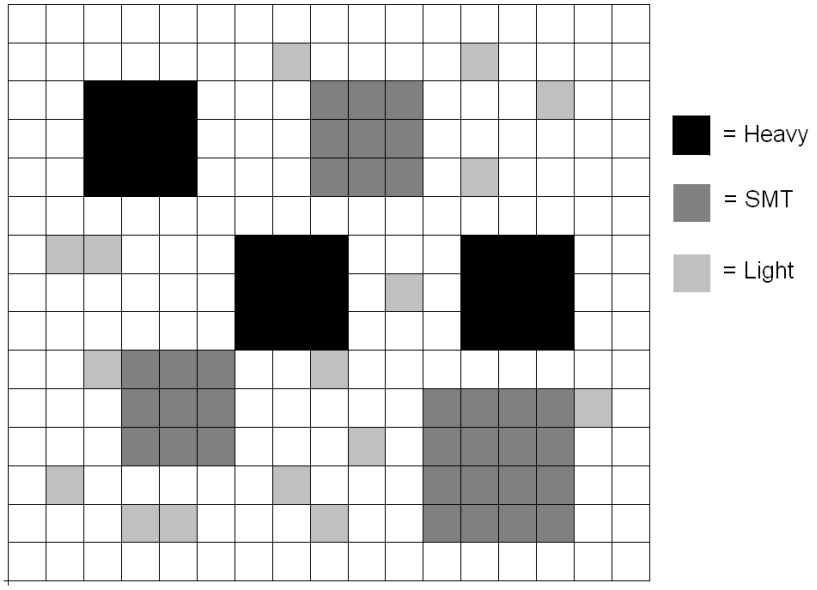

Figure 5.8: Example of random component placement.

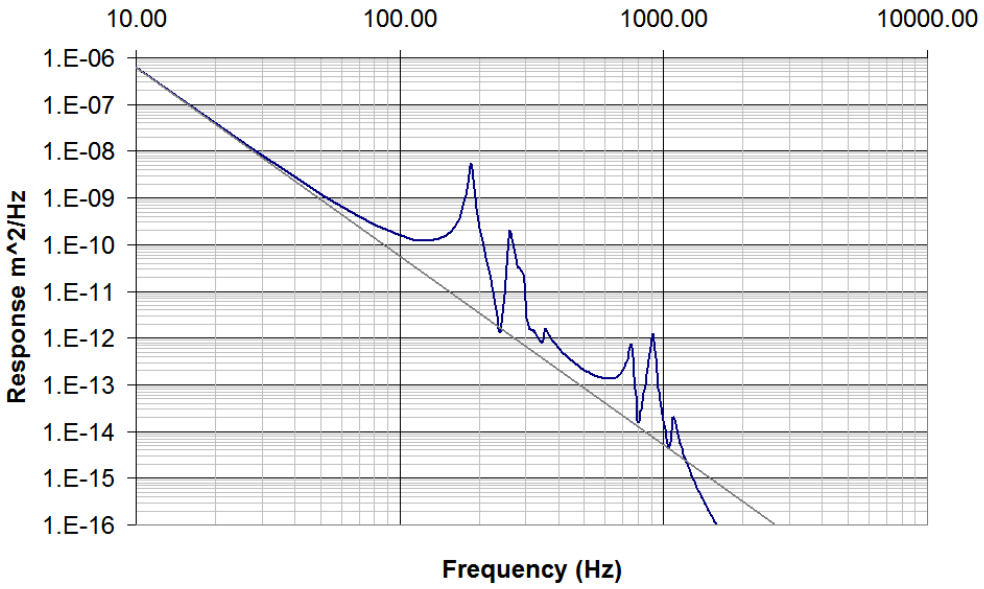

Figure 5.9: Displacement spectral density of an example PCB. Showing the displacement response of the centre point of a PCB relative to the input displacement.

represented by areas of higher stiffness and mass (i.e. local smearing). The model was created in the MATLAB environment, using the OpenFEM element library and solutions. The nodes of the mesh were at $5mm$ intervals, as this was shown to give good convergence of results in both MATLAB and NASTRAN.

In terms of boundary conditions, the edge displacements of the model were fixed while the two rotational degrees of freedom were free. The last rotational DOF was constrained by CELAS elements with rotational spring constants, where the constant was calculated from the board percentage fixidity and formula published by Barker (Barker and Chen, 1993).

The out-of-plane RMS displacement for a flat acceleration input ($0.1g^2/Hz$) was calculated up to 1000 Hz, because the value of 1000Hz was found to adequately account for the majority of displacement for the cases considered. Figure 5.9 shows the displacement of a typical PCB, this illustrates how the displacement spectral density rapidly drops off as the frequency increases.

5.5.1 Levels of Simplification

The mass and stiffness distributions over the board were the main variables to be simplified during this study, although useful observation were also gained by examining edge rotational stiffness simplification. Each simplified model was created and solved automatically by altering

Simplification id.	Density	Stiffness	Torsional Stiffness
1	Exact	Exact	Exact
2	Averaged	Exact	Exact
3	Exact	Averaged	Averaged
4	Averaged	Averaged	Averaged
5	Exact	Averaged	Neglected
6	Exact	Neglected	Neglected
7	Averaged	Neglected	Neglected
8	Neglected	Neglected	Neglected

Table 5.5: Simplified properties of the different simplification combinations

the properties of the "benchmark" case in MATLAB. As a result of the three different combination of properties that can be averaged: mass, stiffness and torsional stiffness, and the two different types of simplification: averaging and neglected, there are multiple different possible simplification combinations possible. Table 5.5 shows the different combinations of simplification types chosen for this study.

The smearing process is weighted to include the components area, so that the larger the components area the greater the influence its stiffness has on the overall smearing. The same is true for the density, such that the overall mass of the benchmark case and the globally smeared cases is always the same. However, when using the "neglected" simplification technique the effect of components are simply completely ignored. These particular combinations were chosen as they could reasonably be imagined to be utilised in a real working environment; for example, it is very unlikely that the exact stiffness properties are known but not the densities, thus this combination is not considered.

Additionally it was possible to simplify the edge rotational stiffness, reducing the edge fixidity to zero and giving a simply supported edge condition. The simply supported edge condition was chosen as it is a commonly used assumption during modelling.

5.5.2 Calculation of Error Distributions

Using the calculated deformations it is possible to compare the "benchmark" and simplified cases. This was achieved on a per node basis, where the curvature in both the x and y directions was calculated, this was simply performed by measuring the angle between the nodes as in

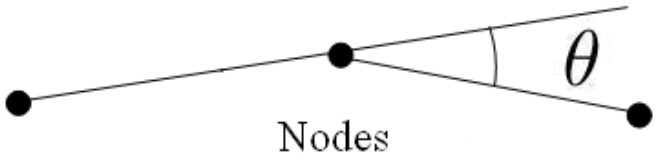

Figure 5.10:

figure 5.10. The ratio of the curvatures between the two cases could then be calculated at each node. The resulting set of ratios ($\delta\theta$), could then be examined to find the maximum curvature underestimate for each level of simplification. Other measures of variation, as opposed to the maximum curvature that was considered here, could also be used depending on the users preference; for example, 3σ or 75th percentile. The method is best explained through the use of an example: If a hundred hypothetical "benchmark" models of PCBs are created, and each of these models is then simplified by, say, ignoring all the components. The response is calculated for both the simplified and "benchmark" cases and then compared. The comparison is achieved by first calculating the curvature at each node for each model and then finding the error ratio of these two values between the simplified and "benchmark" cases. This comparison is carried out twice for each node of the model as the curvature is measured in both the x and y axis, so for each simplified model there are twice as many error ratios calculated as their are nodes. Once the percentage error in the curvature at each node is known, the maximum of these values is taken, i.e. the node with the highest under-estimate of the curvature was found and that under-estimate was chosen as the value for that individual PCB. This value was then found for all the other one hundred simplified models, and the maximum value of all these one hundred models was then found. Thus, it can be seen that the under-estimate calculated is the maximum out of all the nodes of a hundred models, and each model usually had at least 400 nodes. The large number of nodes (at least 40,000) tested means that the test is relatively strict, i.e. out of well over 40,000 nodes this is the greatest under-estimate of the response. These percentage error values can later be similar to any subsequent models that can be considered to be within the bounds of the hypothetical models that were tested. Also it should be kept in mind that in this work the whole process was repeated for several different simplification types and four different distributions of components.

This method is an improvement over the previous attempts of determining response accuracy using the MAC, as the MAC only considers the general shape of the PCB, whereas not only is

the curvature directly related to failure but also that its error is being directly measured.

5.6 Results

The results for a 1.6mm and 2mm thick PCB are shown in tables 5.6 and 5.7 respectively. The tables are decomposed into equipment type and simplification type. In the cases where no underestimate was seen the expected error was considered to be unity. As an example, a 1.6mm thick PCB for a "power" application (equipment type 1), modelled by neglecting components (simplification id. 8), has an expected maximum error of 0.408.

It can be seen immediately that thinner PCBs generally have greater modelling error than the thicker PCBs; this is because the components have a greater influence on the response of thin PCBs than on thicker PCBs. In terms of equipment type and the type of components used, it can be seen that the PCBs with the heavier components (lower "Equipment type" numbers) generally have greater modelling error than those that use smaller lighter components (higher "Equipment type" numbers). This is justified by the fact that the larger components have a greater effect on the response; therefore, the effect of neglecting them is greater than for small components. Finally, the reason that simplification types 5 and 6 are all unity is that these two methods consistently overestimate the results.

The most important observation that can be made from the results concerns the effect of the neglecting the mass or the stiffness. In the cases where only the additional component mass was omitted it was observed that an underestimate of the response was likely, whereas overestimates occurred where only the additional stiffness was omitted. As such it is inferred that omitting the stiffness is a conservative and fairly safe assumption, whilst omitting the mass leads to non-conservative predictions. The same can be seen to be true for the effect of averaging (as opposed to neglecting) the additional component mass or stiffness, but to a lesser extent.

It is possible to give an idea of how conservative the results are by comparing the errors given previously against safety factors based on the average under-estimate of the response (as opposed to the maximum under-estimate of the response). Based on the average over-prediction of the curvature, simplification types 3 and 7 over-predict the real response by up to 10%, types 2 and 4 by up to 20% whilst simplification type 8 can over-predict the response by up to 60%.

Simpl'n id.	Simplified properties			Equipment type			
	Mass	Stiffness	Torsional stiffness	1	2	3	4
1	E	E	E	*1*	*1*	*1*	*1*
2	A	E	E	*0.775*	*0.806*	*0.943*	*0.926*
3	E	A	A	*0.909*	*0.935*	*0.952*	*0.952*
4	A	A	A	*0.787*	*0.80*	*0.926*	*0.806*
5	E	A	N	*1*	*1*	*1*	*1*
6	E	N	N	*1*	*1*	*1*	*1*
7	A	N	N	*0.877*	*0.885*	*1*	*0.990*
8	N	N	N	*0.408*	*0.352*	*0.833*	*0.826*

Table 5.6: Modelling error (in italics) for a 1.6mm thick PCB, divided into different equipment types and simplification methods. The first four columns define the simplification method used (as defined in table 5.5) by which properties have been simplified, where E, A and N denote Exact, Averaged and Neglected respectively. The results are then further sub-divided into different equipment types (as defined in table 5.4).

Simpl'n id.	Simplified properties			Equipment type		
	Mass	Stiffness	Torsional stiffness	1	2	3
1	E	E	E	*1*	*1*	*1*
2	A	E	E	*0.794*	*0.820*	*0.952*
3	E	A	A	*0.952*	*0.962*	*0.971*
4	A	A	A	*0.806*	*0.820*	*0.952*
5	E	A	N	*1*	*1*	*1*
6	E	N	N	*1*	*1*	*1*
7	A	N	N	*0.855*	*0.870*	*0.990*
8	N	N	N	*0.318*	*0.388*	*0.855*

Table 5.7: Modelling error (in italics) for a 2mm thick PCB, using the same formatting as table 5.6. For example, a 2mm thick PCB for a "processing" application (equipment type 3), modelled by averaging the effective component mass and stiffness contributions over PCB area (simplification id. 4), underestimates response by a factor of 0.952.

5.7 Summary

A process has been illustrated that calculates the expected error for FE models of electronic equipment, using a Monte Carlo style sensitivity analysis approach to ensure that many possible configurations are considered. The resulting errors can be used on a wide range of equipment (as defined in the limits of applicability) and can be decomposed into different variables (in this case thickness, simplification type and equipment type) to increase relevancy. The process that is described here is an improvement on the current state of the art for the following reasons: Firstly, the very large number of configurations that can be tested ensure that the results are accurate in many different cases. Secondarily, as the error is calculated for the variable that is directly linked to component failure (curvature), the results are much more useful than previous analyses that only considered the MAC. Furthermore, the error in the curvature variable is measured for a very large number of nodes, further increasing the confidence in the results.

In addition to the process that is described here some additional observations have been made during the analysis, notably the significance of accurately modelling the mass if accurate results are required.

Chapter 6

Determining Manufacturing and Assembly Variability

6.1 Introduction

Say the response of an individual piece of electronic equipment is known, to what extent should the responses of other pieces of equipment be expected to be the same? This is the question that is answered in this chapter. To achieve this, a series of tests are presented that measure the expected response variability as a result of: assembly variations, manufacturing variation and damage, where each of these effects has a different contribution to the overall variation. Thus, the primary objective of the work presented in this chapter is to present a process to obtain statistics of variation for some typical PCBs, where the different experiments are carefully controlled so that only one source of variation is considered during each experiment. At the end of the chapter there is a discussion on how these different effects combine to affect overall accuracy.

In addition to the main contribution of measuring the expected variation, two additional contributions are also provided in this chapter: First, the main drivers of this variation are highlighted, this allows future attempts at minimising response variation to be taken much more efficiently; and, secondly, the work provides initial ball-park values for amount of expected variation as a starting point for future work.

6.2 Experimental Set-up

Throughout all the tests in this work, the frequency response was measured with a dynamic signal Acquisition Board (NI PCI-4472) and several small accelerometers attached to the boards (Piezotronics 0.6 or 0.2grams). Where multiple tests were performed on identical boards the accelerometers exact position was ensured to be identical between each test.
The four PCBs to be tested are hereafter referred to as Set-up A to D, they consist of the following:

Set-up A is an unpopulated PCB attached to an aluminium enclosure as shown in figure 4.1, the enclosure has cross-supports to provide extra rigidity to the centre of the PCB (see section 4.2 chapter 4 for more detail).

Set-up B consists of an unpopulated PCB directly attached to shaker head expander with 28 M3 bolts evenly spaced around the perimeter as shown in figure 4.2(see section 4.2 chapter 4 for more detail).

Set-up C consists of an MS-6323 Micro-ATX motherboard attached to shaker head expander by six M4 machine screws as shown in figure 6.1. In this test the board only had a 6mm stand-off as this is how the board is usually mounted. Seven of these boards existed to allow the difference between each to be measured, each measures 244mm by 205mm and a mass within ± 1 of 465grams. In some tests the motherboards free-free responses were measured, this was achieved by hanging each board from elastic bands.

Set-up D consists of a graphics card (Vanta TNT2M64) suspended by elastic bands to measure free-free response (shown in figure 6.2), ten cards were tested this way, each has a mass within ± 0.5 of 69grams and measures 150mm by 83mm and are 1.6mm thick

6.3 Variability Experiments

6.3.1 Assembly Variability Test

This first test illustrates the sensitivity of a PCBs response to small changes in boundary conditions. This involved removing and re-installing the same Set-up C (as shown in figure 6.1) several times and testing the vibration response after each installation. Any slight variations in the boundary conditions between tests would be apparent as the vibration response would also change between tests (see figure 6.3 and table 6.1). The boards were subjected to a 0.5g vibration input swept from 20 to 400Hz at two Octaves per minute; this frequency was chosen

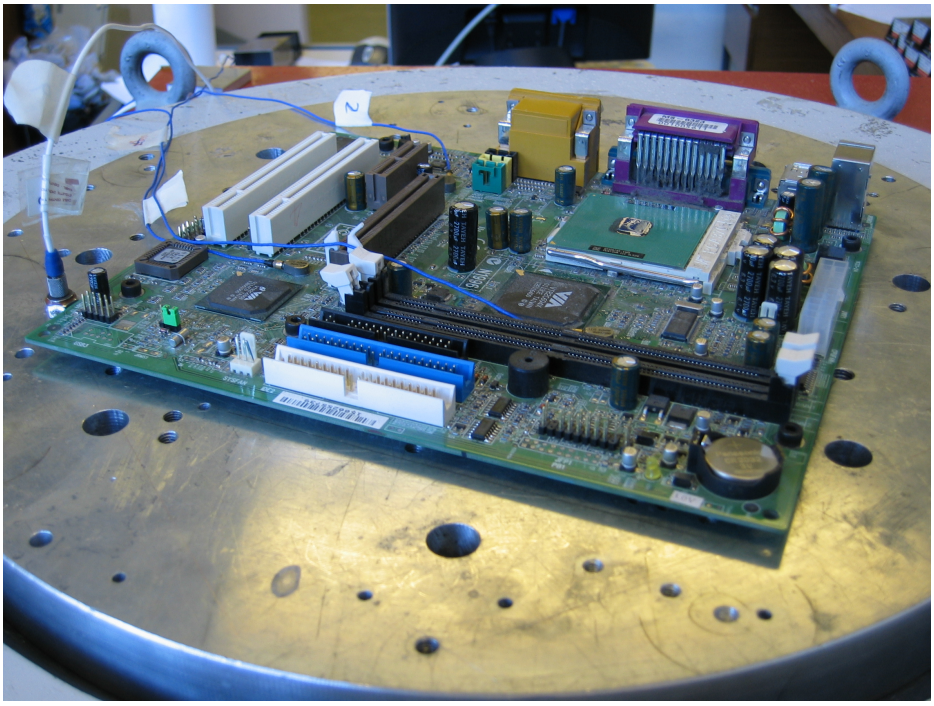

Figure 6.1: Set-up C attached to the shaker head expander.

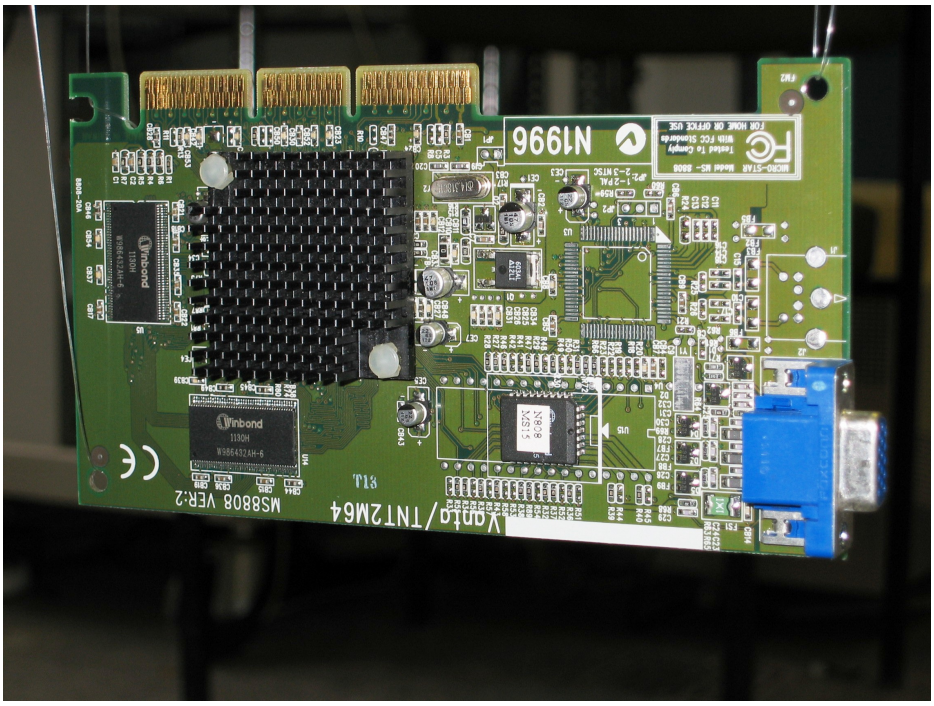

Figure 6.2: Set-up D for measuring free-free response of graphic cards.

Attempt	Mode 1		Mode 2	
	f (Hz)	Q	f (Hz)	Q
1	92.6	9.20	128.8	15.25
2	93.4	7.92	131.6	18.84
3	97.4	8.4	130.0	10.20
4	97.6	8.40	130.0	16.0
5	98.0	8.72	131.0	16.25
6	97.8	9.60	131.0	18.0

Table 6.1: Frequencies and peak transmissibilities of first two modes for Set-up C, between each attempt the PCB was removed and then re-installed with bolts re-tightened to the same torque. The first three attempts used a random bolt tightening pattern; the last three attempts used exactly the same bolt tightening pattern.

as it contained the most significant modes, whilst the value of 0.5g vibration input was a compromise between a good signal to noise ratio and possible damage to the boards. The first test involved removing and re-installing Set-up C three times, the bolts were tightened to the same torque each time. The second set of tests was the same except that not only was the torque identical but also the tightening pattern. Consequently it was found that only by tightening the screws in exactly the same order and to exactly the same torque (1.5N/m) could any repeatability be achieved (see table 6.1), thus all subsequent experiments used exactly the same tightening pattern and torque.
It was suspected that different test set-ups might be more sensitive to slight changes in boundary conditions than others might. To investigate this assumption the tests were repeated for two set-ups A and B (the statistics of variation are shown in table 6.2). Preliminary testing showed the sensitivity to bolt tightening pattern was found to be insignificant in both these tests, so this part of the original test was not repeated.

6.3.2 Manufacturing Variability Test

The second set of tests involved testing and comparing the response of seven supposedly identical motherboards as in Set-up C, these were tested in a mounted condition similar to the previous tests. It was immediately apparent that identical manufacture did not mean identical response (see figure 6.4 and statistics of variation in table 6.3). Additionally, some correlation

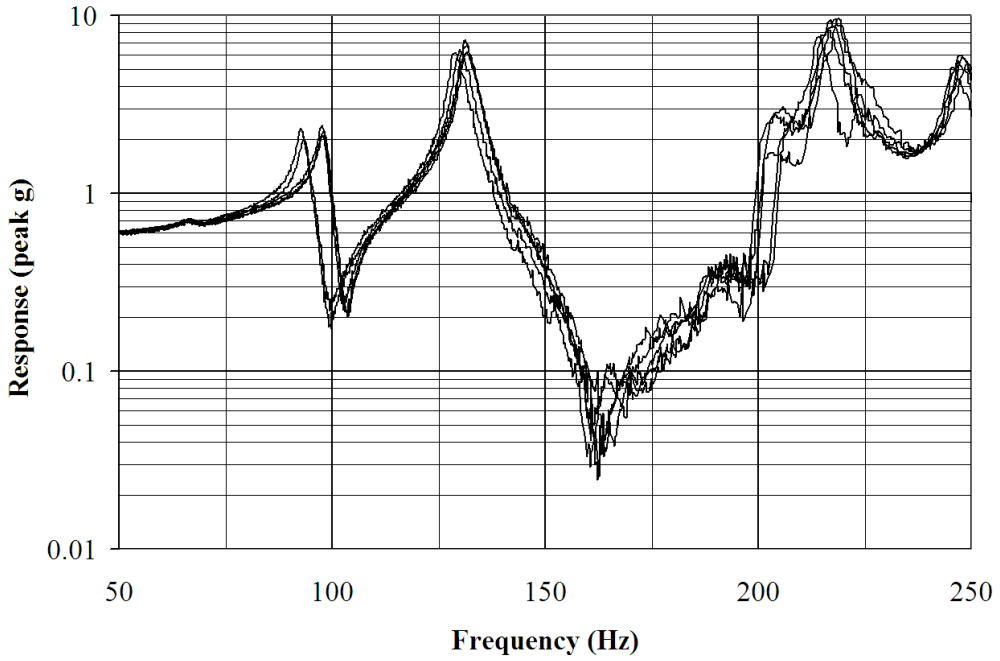

Figure 6.3: Frequency response of Set-up C over successive removal and re-installation attempts, to show sensitivity of board to small variations in boundary conditions (see table 6.1).

	mode	$\bar{f}$ (Hz)	σ_f	$\sigma_f(\%)$	$\bar{Q}$	σ_Q	$\sigma_Q(\%)$
Set-up C	1	94.5	2.57	2.72	8.50	0.64	7.90
(random pattern)	2	130.3	1.40	1.08	14.76	4.34	29.40
Set-up C	1	97.8	0.20	0.20	8.91	0.62	6.98
	2	130.7	0.58	0.44	16.75	1.09	6.51
Set-up A	1	194.4	1.35	0.70	21.14	0.70	3.30
	2	333.0	1.17	0.35	4.80	0.15	3.16
	3	361.9	0.65	0.18	3.67	0.26	7.06
	4	483.5	1.28	0.26	48.14	2.25	4.68
Set-up B	1	145.3	1.72	1.19	147.3	6.67	4.53
	2	543.5	6.20	1.14	69.78	9.19	13.18

Table 6.2: Statistical parameters of the vibration response of different set-ups after three successive re-installation attempts. The symbol "σ" denotes standard deviation.

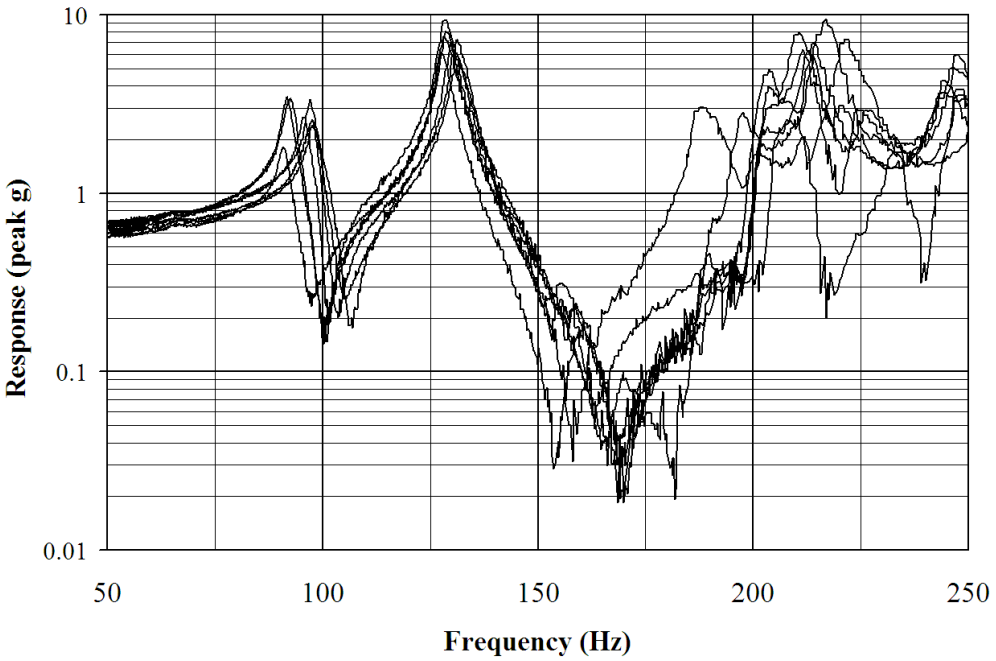

Figure 6.4: Frequency response of seven supposedly identical motherboards (Set-up C), each board was installed in exactly the same manner, with identical torques and bolt tightening pattern (see Table 6.3 table for specific information).

was noted between the motherboard thickness and first natural frequency (see figure 6.5), leading to the conclusion that small differences in motherboard thickness were partly responsible for the variation in the response.

The tests were repeated on set-ups B and D to investigate whether this level of variation was typical (set-ups shown in figure 6.1 and 6.2 but free-free). To remove any possible boundary condition effects this second set of tests was performed using free-free conditions (results are shown in table 6.4).

mode	$\bar{f}$ (Hz)	σ_f	$\sigma_f(\%)$	$\bar{Q}$	σ_Q	$\sigma_Q(\%)$
1	94.74	2.94	3.10	11.34	2.54	22.42
2	129.31	1.45	1.12	14.80	0.82	5.56

Table 6.3: Statistics of mechanical properties variation for seven identical Micro-ATX motherboards in Set-up C, each with identical installation procedures.

Set-up	Mode	$\bar{f}$ (Hz)	σ_f	$\sigma_f(\%)$
Set-up C	1	53.51	1.50	2.80
	2	76.00	0.86	1.13
	3	103.10	1.57	1.52
	4	134.03	1.68	1.25
	5	157.1	4.06	2.58
Set-up B	1	23.5	0.54	2.31
	2	48.0	1.41	2.94
	3	62.1	0.62	1.00
	4	72.0	1.33	1.84
	5	75.2	0.75	1.00
	6	133.0	0.79	0.59
	7	149.2	0.82	0.55
	8	157.5	0.70	0.49
	9	179.1	0.89	0.50
	10	230	1.57	0.68
Set-up D	1	202.4	3.22	0.79
	2	262.1	3.74	0.71

Table 6.4: Statistics of modes of several identical PCBs for free-free conditions. Seven boards were tested in Set-up B and C, and ten were tested in Set-up D.

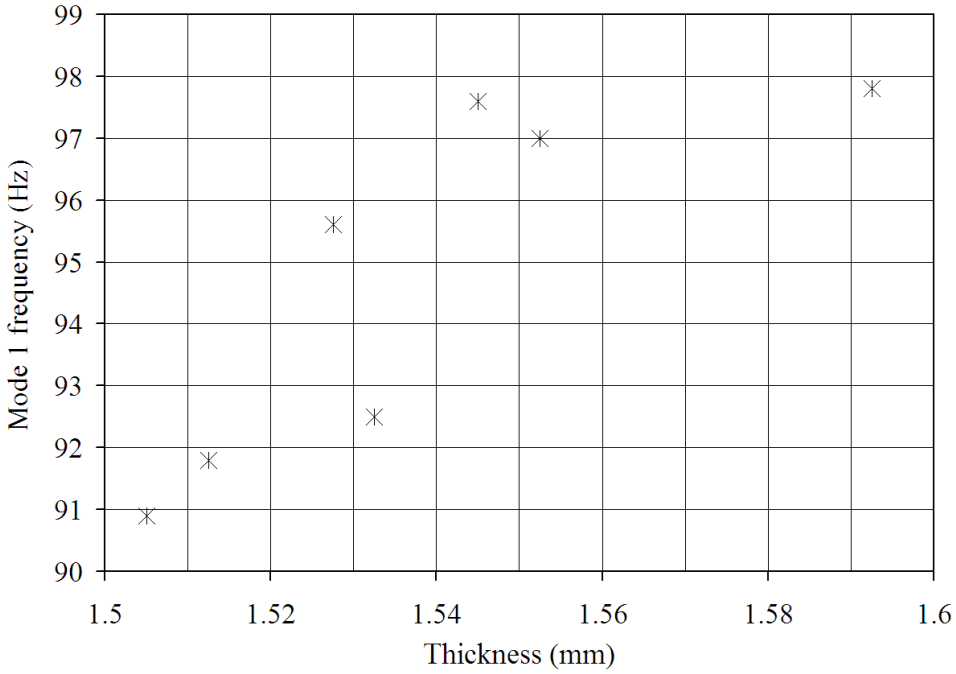

Figure 6.5: Thickness against first natural frequency for identical MicroATX PCBs as in Set-up C.

6.3.3 Variations in Response after High Acceleration

A test was carried out to show how the response of a PCB might be irreversibly altered because of damage from high vibration loading, where this damage is most likely to be a result of local yielding around the bolted fixing. In this test Set-up B was attached to a shaker head expander and excited at several levels of vibration from 0.2 to 40g sinusoidal input, the vibration input was a sinusoidal input at just below the first resonant frequency of the board, each level lasted ten minutes. A visual inspection of the PCB after each test did not show any signs of obvious damage. The response of the board was then measured between each stress test using a low-level sine sweep at 0.2g. It was apparent that the response of the PCB was affected when more intense vibrations were applied (see figure 6.6), as the first resonant frequency of the PCB fell 3.2% and the acceleration response fell 11%. This first test used a set-up that incorporated nylon washers that were suspected of being susceptible to yielding, so the test was repeated with another set-up that had no washers. Over this second test the frequency dropped by only 1.5% while the response dropped by a significant 18.6%. It was observed that the majority of the reduction for the second test occurred when the board centre

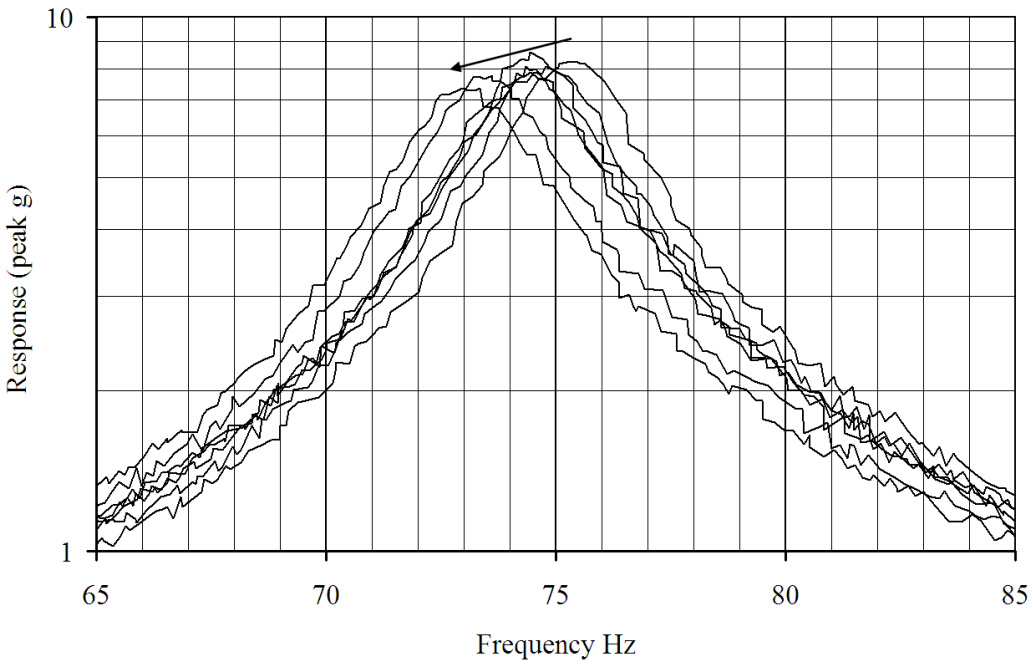

Figure 6.6: Graph to show decrease in first resonant frequency of a Set-up B because of damage from extreme vibrations. Arrow points in the direction of increasing levels of vibration.

response reached over 160g peak acceleration, whilst for the first test the reduction - and therefore damage - occurred evenly throughout the test.

In summary, the response was irreversibly altered because of high accelerations even though no visible damage occurred. This damage could take many possible forms: delamination of the glass fibre layers within the PCB, failure of the epoxy to fibre bond, or - most likely - local yielding of the PCB around the fixing that resulted in lower bolt tension. Although the exact cause of failure can not be determined it is enough to know that at high responses such variations can occur and should be measured if possible, if measurement is not possible then appropriate safety factors should be included. An in-depth analysis into the exact cause of variation is not performed as this is only a case study to highlight this issue, and that manufacturers should measure specific values for their type of equipment. Also, it should be noted that the damage did not affect any of the electrical connections on the PCB in this case study, but for multi-layer PCBs the possibility of damage to electrical connections could possibly be significant.

6.4 Discussion

Say the response of a piece of equipment is known, to what extent should responses of other identical pieces of equipment expected to be the same?
First, let's consider a worst-case scenario based on the results published here. For example, if the assembly of a piece of equipment is not tightly controlled, resulting in different bolt torques and tightening patterns, the response magnitude may have a standard deviation of up to 30% (based on the highest variation seen in table 6.2). Low manufacturing tolerances may contribute up to another 22% standard deviation (based on the highest variation seen in table 6.3). As most engineering companies work to at least three sigma, the standard deviation should be considered to be 150% (double this for six sigma). Based on these values, for a worst-case scenario, the actual response may be 150% higher or lower than the measured value. Furthermore, this does not consider that the frequencies may vary by up to 18% higher or lower than the measured value, possibly placing the resonant frequencies of the structure into a region of higher input acceleration. Finally, if large accelerations are present damage may occur to the structure that could alter the response further.
Now let's consider a best-case scenario. For equipment that is assembled in a very controlled environment, the response magnitude may vary by as little as 3% (based on the lowest variation seen in table 6.2), whilst the lowest deviation observed because of manufacturing variations was 3% (based on the lowest first mode variation seen in table 6.4). At three sigma this amounts to the response being possibly 18% higher or lower than the measured response. Thus, to answer the original question of how similar responses may be is not so straightforward, as it can be seen that the variability depends on the specific case at hand. For example, the motherboards in Set-up C seemed to be more sensitive to small variations in boundary conditions, possibly because of their relatively small number of fixing points. Therefore, any estimate of variability should be based on set-ups and assembly processes as similar as possible to the equipment for which they are intended.

6.5 Conclusion

The responses for identical PCBs have been shown to vary significantly because of relatively small differences in manufacturing and assembly; this variation must be considered when calculating the FE predicted response. This work in this chapter accomplishes the primary

objective of illustrating a process to measure this variation. This process can be performed by a manufacturer on their own equipment to allow them to find their own statistics of variation. Additionally the two secondary objectives of highlighting the main sources of variability and providing initial ball-park values was also achieved, with small boundary condition, thickness and damage variations being highlighted as the main sources of response variability.

Chapter 7

Failure Criteria

7.1 Introduction

This chapter illustrates a proposed process to create a package failure databases, using several examples of real failure data to show how this is achieved.
Similar to the previous chapters, this chapter specifically focuses on the process of creating the data, not the actual data itself. This is because the failure varies depending on individual manufacturing techniques, PCB thickness and components used, all of which are manufacturer specific; therefore, giving specific values is not appropriate.
Again, similar to the previous chapters the chapter also provides some additional insight into the cause of failure, allowing future work to be carried out much more effectively. Some of this insight is very significant as it directly refutes previous research on the problem, showing the root cause of failure to be curvature and not acceleration.
Unlike the other chapters, the work presented in this chapter is a lot more exploratory and despite the large amount of progress that is made - given more time and resources - significantly more is possible. For example, the data here shows wide variation; as a result more components (in both quantity and type) need to be tested before a useable database could be created. As such, the use of the data here for ball-park figures should only be for very similar situations.
In the simplest terms, the experiments involve shaking a populated PCB on a shaker table and measuring the time it takes the components to fail. In practice the details of running such a test are much more complicated than the initial description would suggest: there needs to be a system to detect exactly when the components fail, consideration must be given to how the exact local PCB response is quantified, the PCB BCs must be carefully designed to give certain

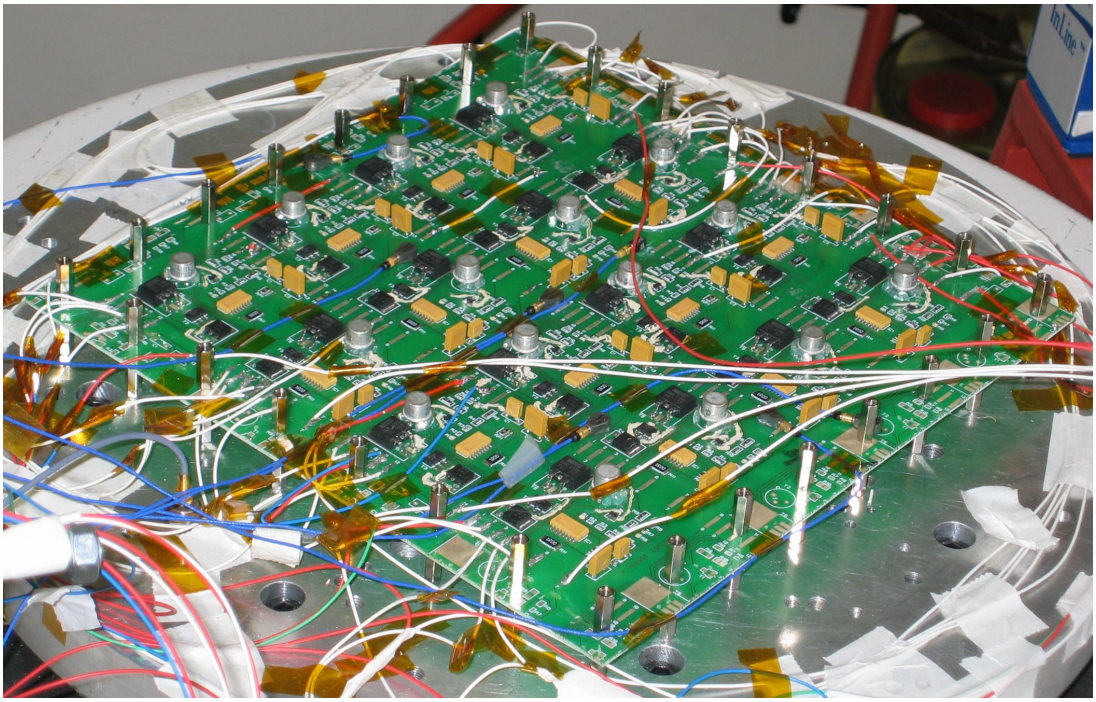

Figure 7.1: Fully supported set-up attached to the shaker head.

curvatures, and the analysis of the results requires advanced statistical methods. All of these points are now addressed in the rest of this chapter.

7.2 Test Set-up

7.2.1 Set-up Attachment

In the most basic terms the set-up involves a PCB populated with components attached to a shaker head. Two test set-ups are tested: one fully supported and one cantilever set-up. The fully supported set-up (shown in figure 7.1) is the same as in earlier experiments (as shown in figure 4.2 on page 50), except that it is now populated with components (as shown in detail in figure 7.2).

The second set-up uses a similar PCB but in a cantilever arrangement (as shown in figure 7.3). For the rest of this chapter these shall be referred to as the fully supported and cantilever set-ups respectively.

The reason for using two different setups is that they allow different strains to be examined; where the strain is considered to arise from the PCBs' local curvature (or - more precisely - bending moments). The fully supported test is to examine how bi-axial curvatures influence

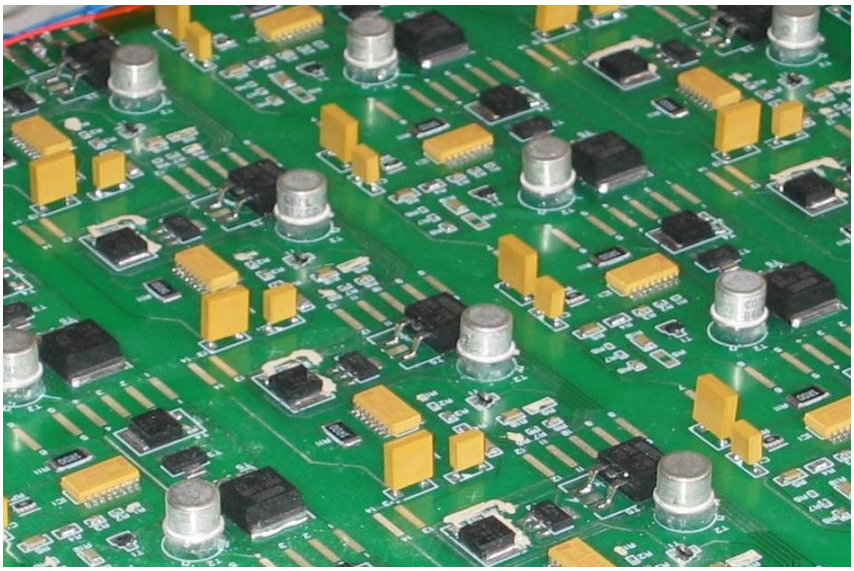

Figure 7.2: Close-up of components attached to the PCB.

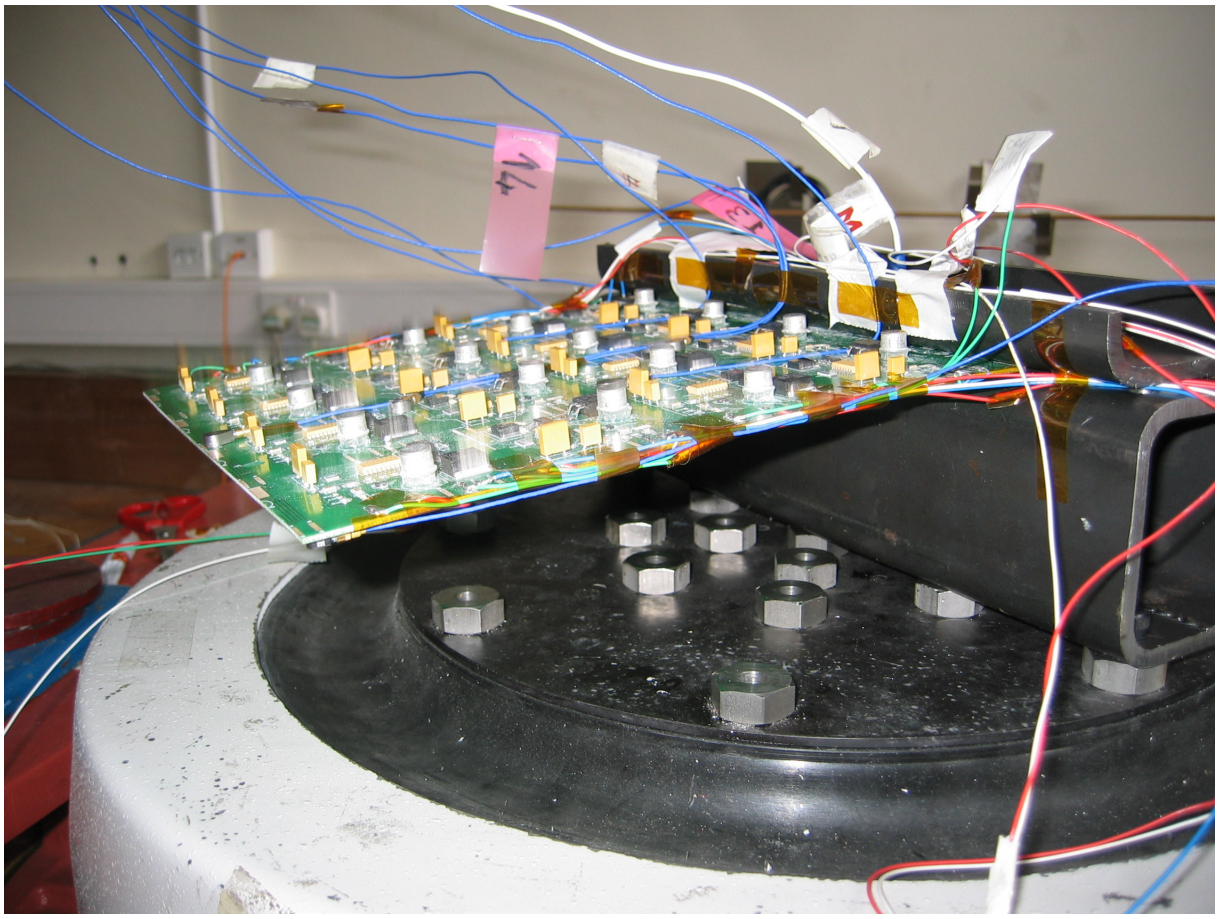

Figure 7.3: Cantilever set-up attached to the shaker head expander.

Figure 7.4: Entire experimental set-up (from left to right) shaker head with fully supported PCB attached, power supplies and detector circuits, continuity testing computer. Not shown: shaker control computer and dynamic signal acquisition computer.

the component reliability, as these types of curvatures have been identified in previous work to be more damaging to some component types. These bi-axial curvatures are shown to be highest in the corners of the set-up; therefore any bias of the failures towards the corners shall indicate that bi-axial curvature is relevant for the given components.

The cantilever test - on the other hand - is much simpler, as the curvature simply decreases along the length of the PCB. However, the cantilever test permits investigation into the relative significance of acceleration and curvature on failure rate. Previously, practically all research on component failure has focused on either acceleration or curvature as the major cause of failure (see section 2.4.2 for examples), whilst no research has investigated which of these criteria is more significant. The cantilever test simply solves this problem, as the components at the free end of the cantilever specimen experience very high accelerations and very low curvatures, whilst the exact opposite is true for the components nearer the clamped end. If more failures happen at the free end then acceleration can be assumed to be more significant, and if more failures happen at the clamped end then curvature is the principal failure driver. In a similar way to the bi-axial investigation of the fully clamped setup, these conclusions should only be considered to be true for packages that are similar to those under test.

It is important to remember that the last two issues of bi-axial curvature and the acceleration/curvature significance are secondary to the main priority of this work, which is to illustrate a process to create failure data. Only by clever experimental design can these investigations be included without affecting the creation of the primary data.

The cantilever set-up is fixed to the shaker head using the method shown in 7.3. This method is used as it gives significant support to the PCB, making the support as close to a fully fixed boundary condition as possible. Additionally, this method also gives enough clearance for the end of the PCB, as the dynamic displacements are very large at high accelerations. The design of the fixture is ensured to be stiff enough that its response is negligible when compared to the PCB response.

The response of each PCB is measured at seven locations, using a dynamic signal Acquisition Board (NI PCI-4472) and several small accelerometers attached to the boards (Piezotronics 0.6 or 0.2grams). The raw data is recorded at 2000Hz to allow full flexibility in post processing of the data, should it be required. The accelerometer placement ensured that the exact response of the PCB could be built up after the test.

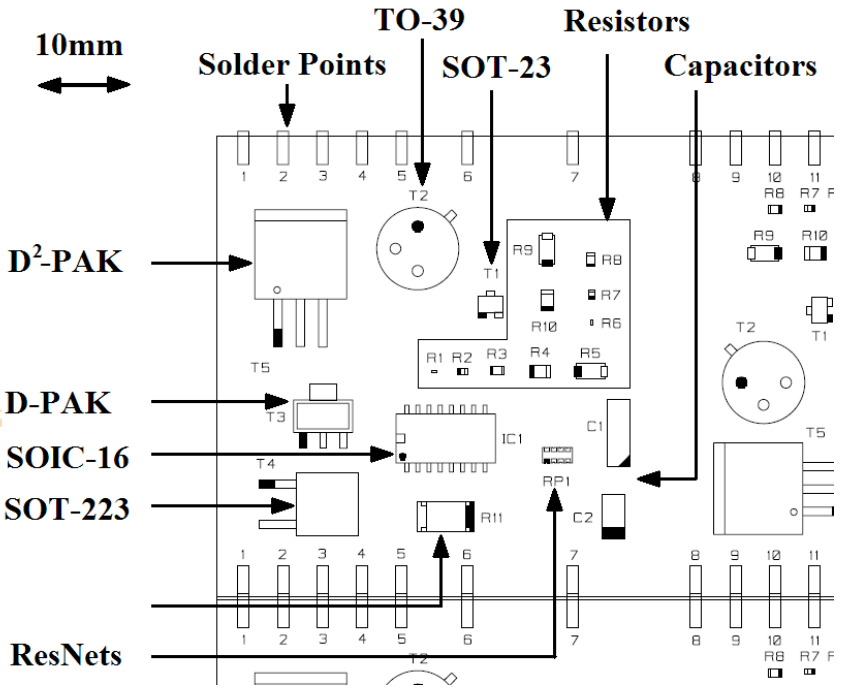

Figure 7.5: Component Location for one cell.

7.2.2 Components Tested

Each PCB is populated with several different types of components dispersed evenly over the entire area as shown in figure 7.5. The components were equally spread out over the area of the PCB, this ensured that each type of component received several different levels of curvature, thus creating more useful end failure data. The spacing of the components also ensured that they did not influence each other, either electronically or by locally increasing strain. The components used for this case study were relatively small (such as discrete resistors, capacitors and transistors), and use a combination of PTH and SMT mounting technologies. This section includes a detailed description of each of these components. It is important to note that ultimately it is the package that is being tested and not the component, i.e. whether the package contains a resistor, transistor or capacitor is irrelevant to the overall failure statistics, as long as the package can be continuity tested; however, the type of component does influence the design of the continuity test circuit.

The resistors considered in this experiment range from very small (0.3mm) discrete units through to larger resistor arrays (10.2mm) that house several different resistors (see figure 7.6), all of these resistor packages used a SMT mounting method. The SMT transistors that are

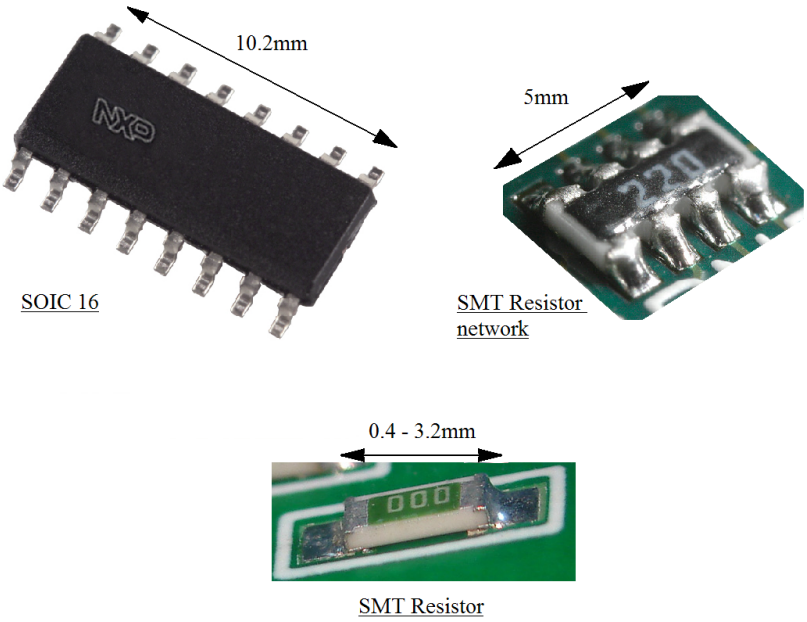

Figure 7.6: Resistor packages that are tested.

considered are shown in figure 7.7. The PTH packages that are considered are shown in figure 7.8, there is both a PTH capacitor and transistor. All the components are soldered to the PCB using the same manufacturing facility; therefore, all the results presented here are specific to this facility or other facilities that use the same manufacturing standards.

7.2.3 Continuity testing

A continuity testing system is required to determine the exact time when component failure occurs. This is achieved by connecting the components in series and passing current through them, if any of the components should then fail the circuit is broken and current can not flow, which is measured with a voltmeter across a sense resistor (see figure 7.9)[1]. The continuity is tested in real-time to determine the exact time of failure.

There are three different kinds of detector circuits for the three different types of components, these increase in complexity from the resistors, through the transistors and onto the Capacitors. These circuits are shown in figures 7.9 to 7.11.

The resistor continuity test circuit is shown in figure 7.9; for simplicity this diagram shows only

[1] note: based on the practical experience of these continuity circuits a different system would be recommended in future, this is described later in the chapter

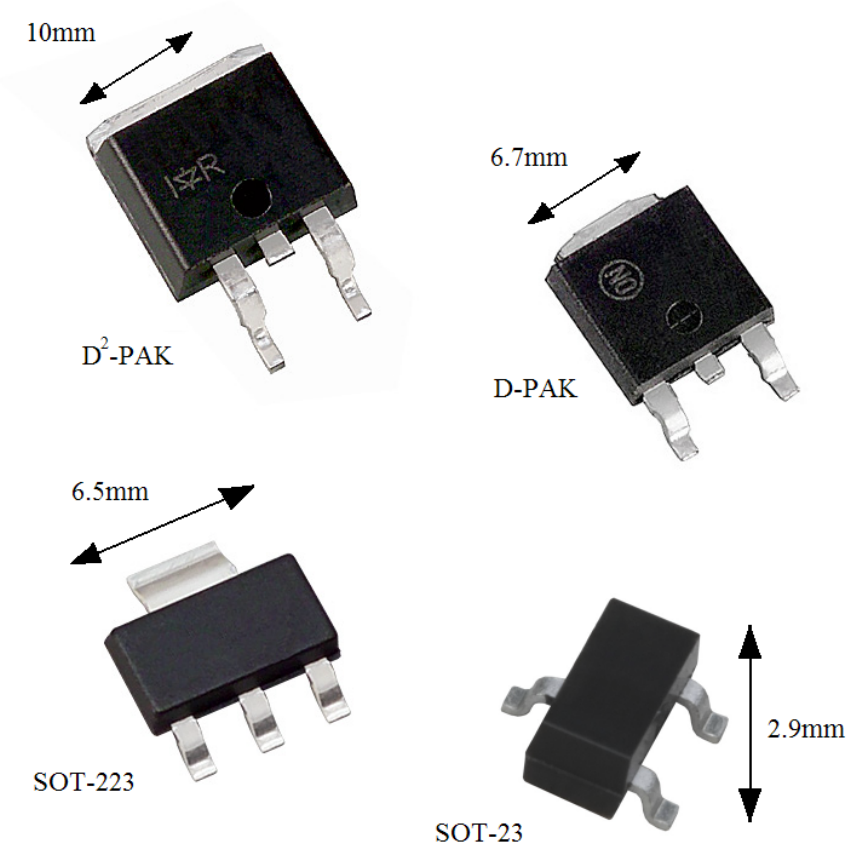

Figure 7.7: SMT transistor packages that are tested.

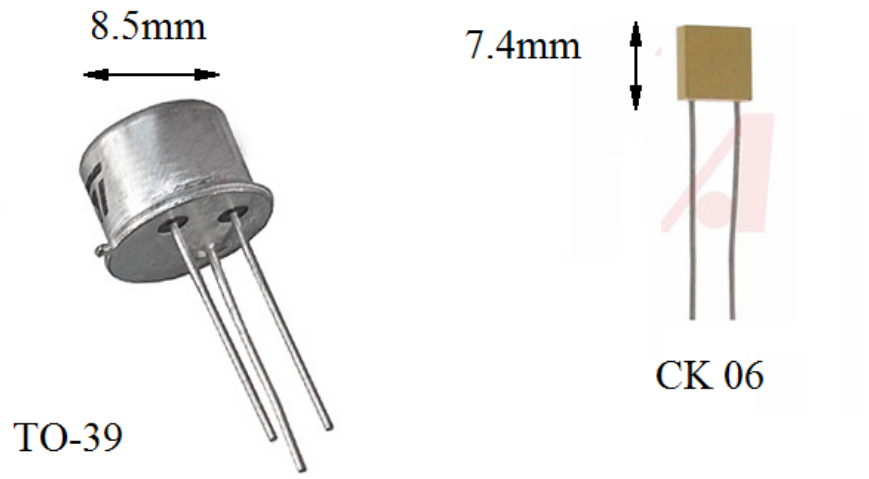

Figure 7.8: PTH packages that are tested. A CK05 capacitor was also tested that is identical to the CK06 but half the size.

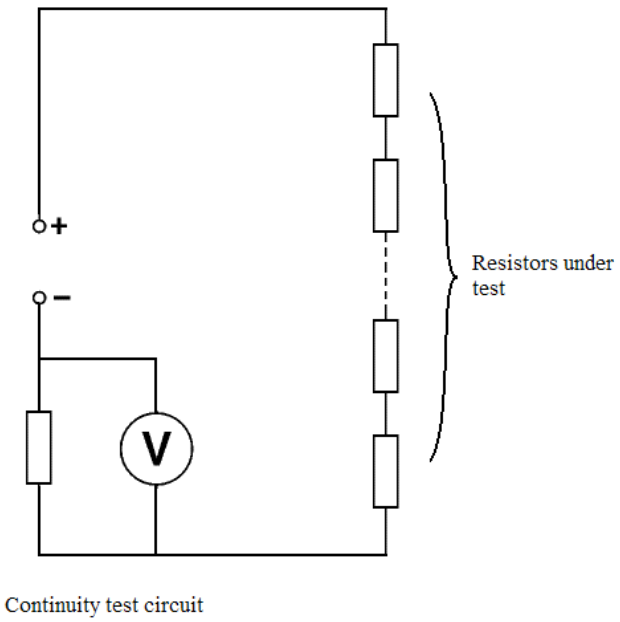

Figure 7.9: Schematic for the resistor continuity circuit.

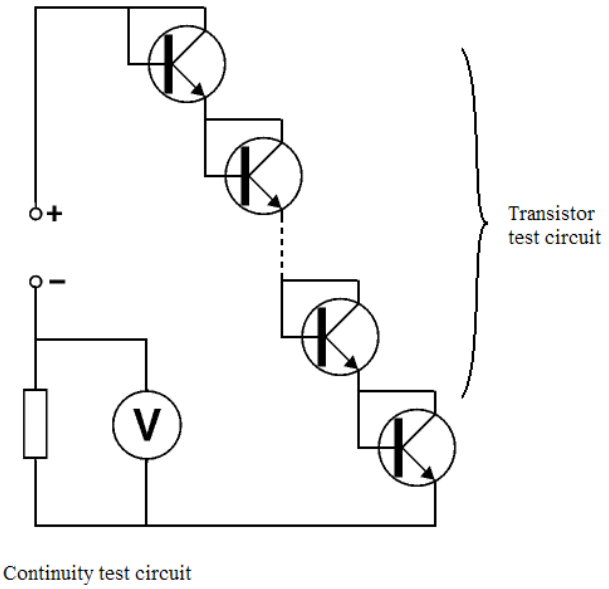

Figure 7.10: Schematic for the transistor continuity circuit.

4 resistors, although - in reality - over 160 were actually tested. A voltage is then applied across the resistors and measured using a National Instruments Ni-DAQ data acquisition system. The acquisition system samples at least ten times the frequency of the shaker test, this ensures enough resolution to pick up all intermittent failures.

The transistor test circuit is slightly more complicated, as the transistors have three leads and can not be simply daisy-chained. To overcome this problem, the base and collector of the transistor are connected together (see figure 7.10), this effectively short circuits these two parts of the transistor, causing the transistor to remain in a permanently "on" state. Then, if the base lead fails, the transistor stops conducting and the current flow stops. If the collector lead fails, the current can only flow through the base, which has a much higher resistance; therefore the current is greatly reduced. Finally, if the emitter fails, the circuit is broken and no current can flow. The transistor circuit continuity is tested in similar way to the resistor continuity test circuit.

The capacitor test circuit is the most complicated, it requires both a sinusoidal voltage source and a special current smoothing circuit (as shown in figure 7.11). The smoothing circuit takes the AC signal coming from the capacitors and changes it into a DC signal that can be easily measured by the acquisition system.

The system is verified by two methods. First, the system is left on for several hours to see if

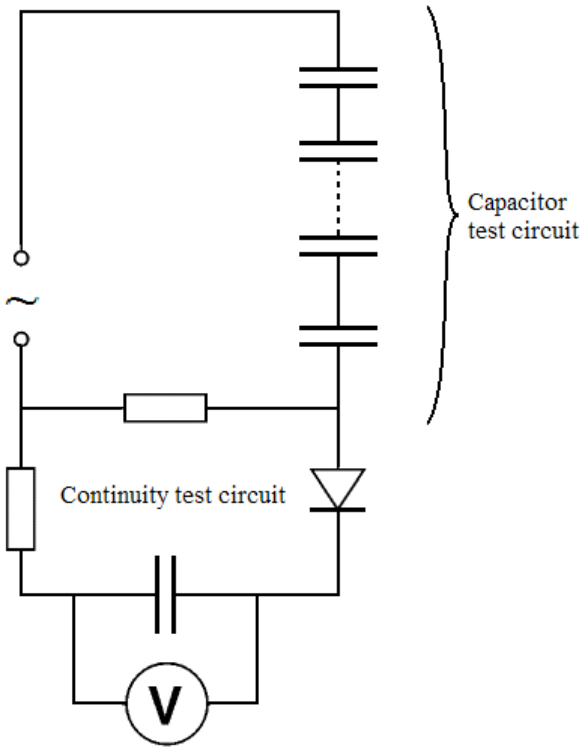

Figure 7.11: Schematic for the capacitor continuity circuit.

any false positives occur. Secondly, an intermittent failure is simulated by briefly striking an exposed part of the circuit with a grounded cable; a sudden drop in the voltage across the circuit should then be seen, testing both the circuit and the resolution of the voltage measuring system. If either of these tests fail then the circuit should be examined and the cause of the failure determined and remedied.

7.3 Test Method

The test described here is slightly different to the test that would be used in practice, the reason for this is that because this is only an initial exploratory test to determine at what rough level of vibration the components begin to fail. This is achieved by initially using very low vibration input and then increasing the input level until failures are seen to occur. The percentage increase from one level to the next is high enough to ensure that any damage occurring in one level would be insignificant in the next.

Before any failure testing occurs the boards are subjected to a pre-test, this is only to measure the frequency response of the PCB, it comprises of a sine sweep to accurately measure the

response and a random vibration test to confirm this data. This test is run at a very low level to ensure that the components sustain no damage. This data is useful later to determine whether any permanent damage has occurred to the PCB.

The initial failure test is run for ten minutes at a low level, whilst all the components are measured for continuity. The duration of ten minutes is chosen as this is how long spacecraft qualification tests take, this ensures that the results are within the same order of magnitude as is required. The input vibration is a fixed sine input at a frequency 2% under the first natural frequency of the PCB; this provides better control over the PCB response whilst still giving high responses. The test is broken into one minute intervals so that the continuity of the components could be verified every minute.

After the ten minutes of vibration the sine sweep is re-run to ascertain whether any damage has occurred to the PCB, as any damage would cause the frequency response to differ.

The failure test is then run for another ten minutes, but this time at double the input of the previous attempt. The response is doubled as this assures that any damage from the previous level is insignificant to the damage sustained in the current level. The test is repeated using exponentially higher levels of vibration, until either all the components have failed or the limits of the shaker system are reached. This exponential method is only used in this work as it is an initial exploratory analysis, future tests are expected to only need testing at one level.

The continuity of the circuits is continually monitored during the test, when the continuity fails the failed component is found and removed from the test. When a drop in continuity is observed the failed components are found by manually testing the voltage across each component using a hand-held voltmeter. In some cases it was found that the failed components could not be found using this method, in this situation it is usually enough to gently stress the PCB, this technique works because the component has an intermittent failure and a small amount of stress is required to open the failed lead. When a failed component is found it is short circuited to remove it from the test and allow the other components to be tested. This "short-circuiting" is achieved by using a conducting ink to create a by-pass circuit that allows current to pass around the failed component. This is a relatively straight forward process that seemed to work well; although many alternative means of accomplishing the same thing could easily be envisaged (this is considered in the discussion).

In addition to this electrical continuity testing, the circuit was subjected to regular visual inspections, both to the whole PCB and also with specific attention to the components that

had electrically failed. During this set of experiments no visual sign of failure could be observed with the naked eye. This suggests that the failures were either internal, too small to see with the naked eye or located on the lead but just inside the package body.
Additionally, it was found that the damping and non-linearity was enough to shift the frequencies, as a result the input frequency had to be increased slightly at higher vibration levels. Furthermore, at these higher vibration levels the response of the PCB became non-linear.

7.4 Analysis

This section details the analysis of the data, starting from the recreation of the PCB strain in an FE model, then through the different treatments of the failure data of Ceiling strain values and S-N analysis.

7.4.1 Reconstructing PCB Strain

After running the tests the exact PCB response and strain must be calculated, this was achieved using a combination of experimental data and corrected FE models. The models are the same as were detailed in chapter 4. They were further verified against the raw data that was created during each failure run, ensuring that the deflection predicted by the model is exactly the same as the experimentally measured deflection. The PCB surface strain is used to correlate with failure, as this is both the most accurate and convenient measure of the PCB response (as opposed to trying to measure local curvature, bending moment or surface stress). Additionally, it allows the bending moment or curvature to be reconstructed if required.

7.4.2 S-N Analysis

It was found that one of the packages (D^2-PAK) had enough failures to allow S-N curves to be created, these are shown in figures 7.13 and 7.14, where the X direction of curvature is defined as in figure 7.12. After removing intermittent failures and Y direction failures, the correlation of the failures is relatively high (as shown in 7.13).
In addition to the S-N analysis of the D^2-PAK packages a similar analysis is also applied to the SOT-223 packages, unfortunately the correlation is not as good, as is shown in figure 7.15. In this figure it can be seen that the failures in the X or Y direction have very little correlation; however, if the shear strain is used instead then some correlation can be observed.

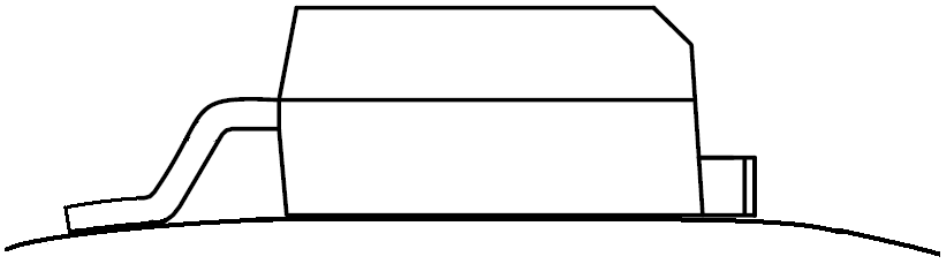

Figure 7.12: Definition of X direction bending for a D^2-PAK package.

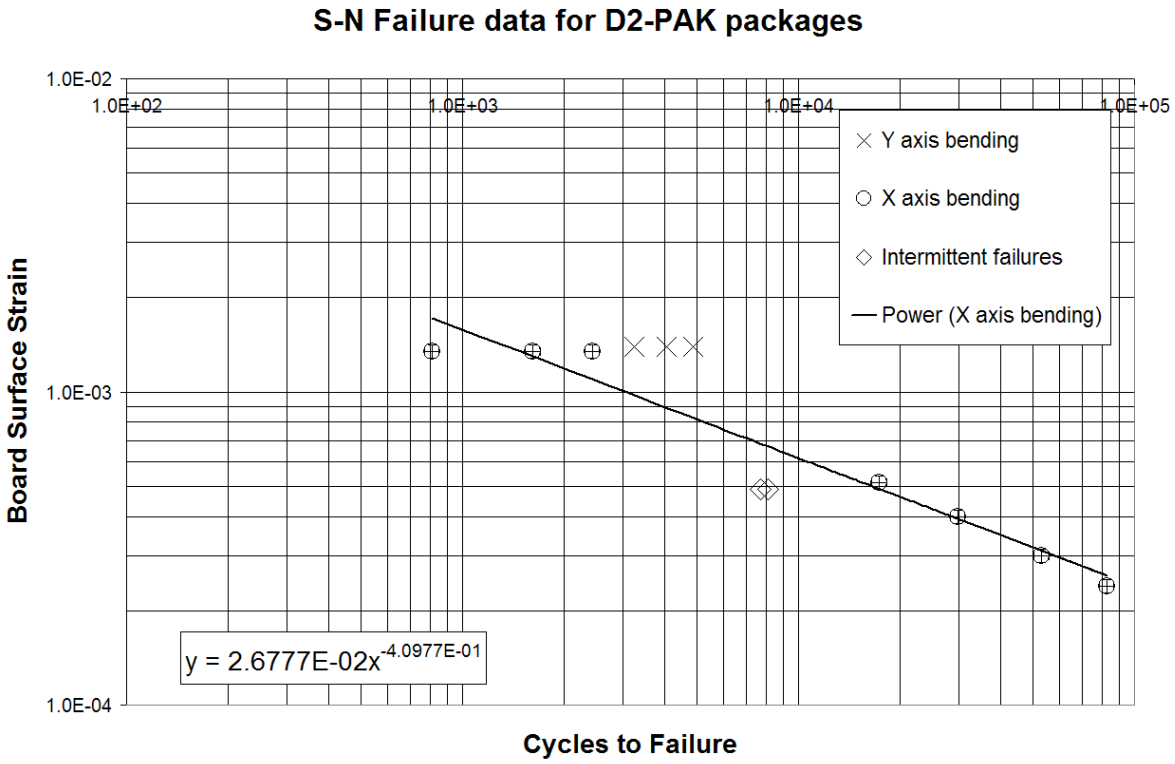

Figure 7.13: Logarithmic S-N graph for D^2-PAK failures. Failure for components that are principally strained in the Y direction are shown with crosses, failures that were intermittent in nature are shown by diamonds.

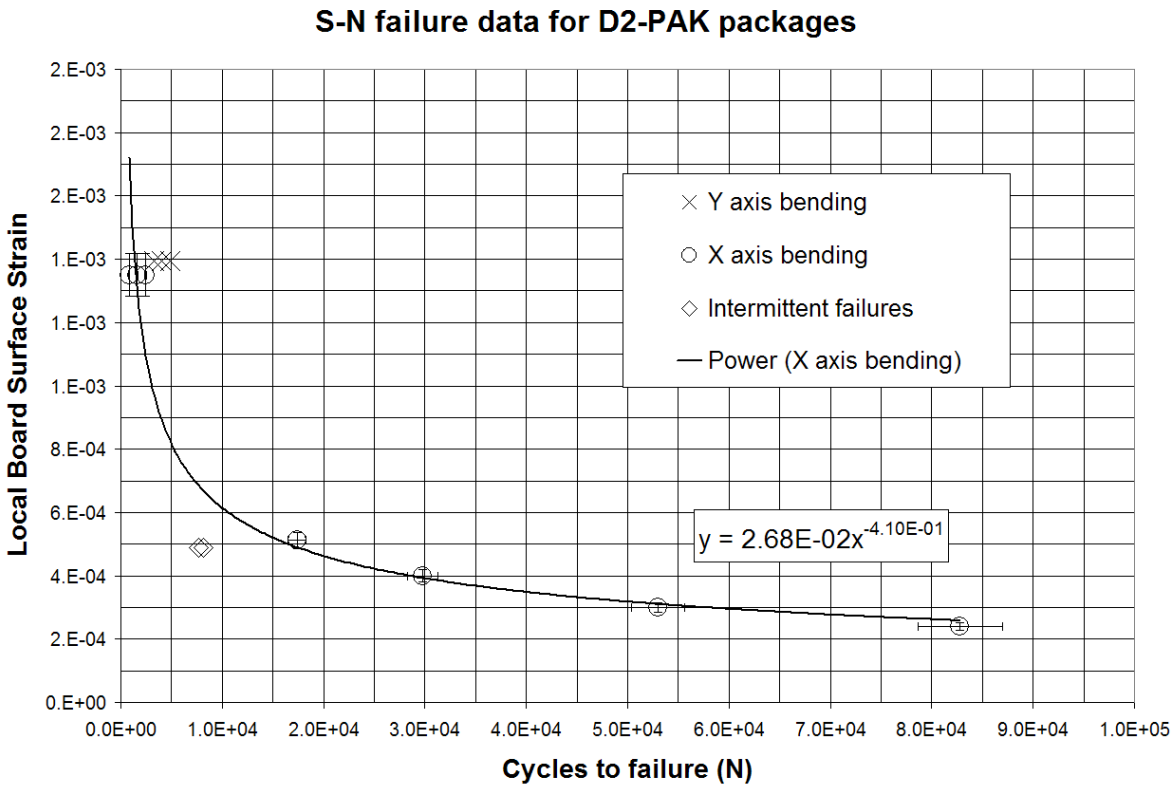

Figure 7.14: S-N graph for D^2-PAK failures. Failure for components that are principally strained in the Y direction are shown with crosses, failures that were intermittent in nature are shown by diamonds.

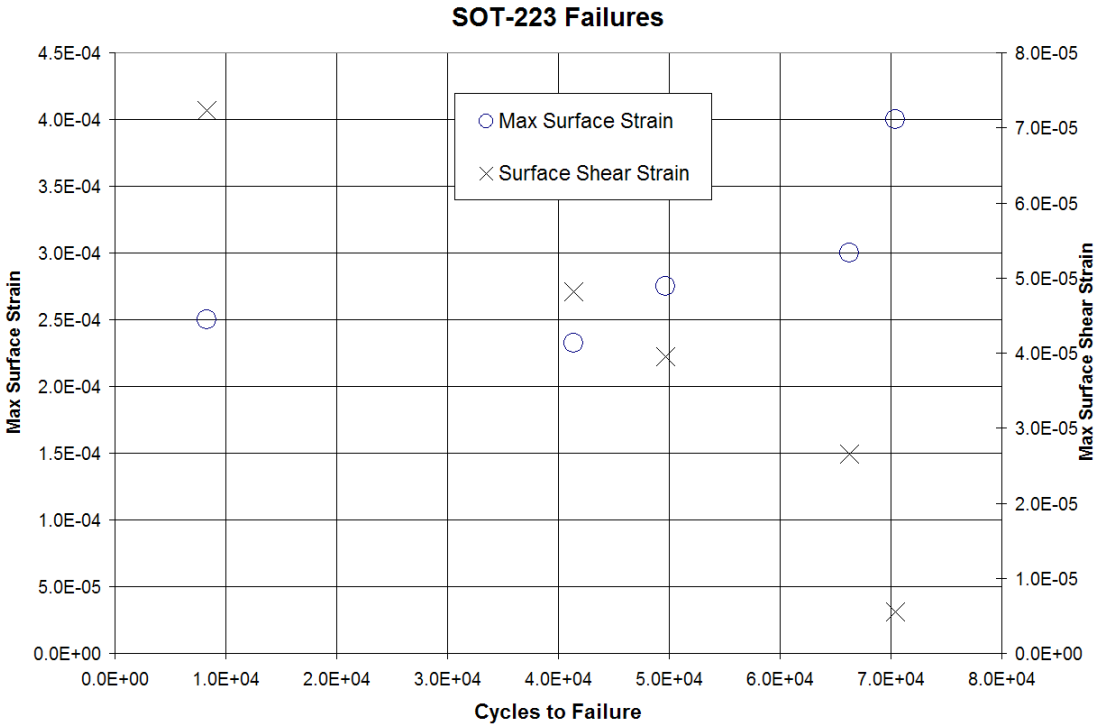

Figure 7.15: S-N graph for SOT-223 failures. Maximum strain for each failure is plotted on the left axis, where this is the maximum strain experienced in either the X or Y direction. Shear strain is plotted on the right axis for the same failures.

Unfortunately, more failures are needed to create better statistics. The stronger correlation with failure for the shear strain over the uni-axial strain lends some support to the theory that - for this component at least - shear strain is more damaging. This can be explained by the shape of the SOT-223 package in relation to the other larger packages: whilst the other large components (D^2-PAK and D-PAK) both have a large contact area and two relatively thick leads coming off, the SOT-223 has a higher aspect ratio and relatively smaller leads on both sides of the package. So whilst the first two packages can be imagined to be very stiff in terms of shear strain, effectively local stiffening the PCB, the SOT-223 can be envisaged to not have this stiffening effect and be more susceptible to shear strain by its design.
The failures of the other components did not show any correlation when plotted on an S-N diagram, either because there were too few failures or because the failures did not correlate in any direction. Fortunately all these components managed to withstand failures far higher than could ever reasonably be expected in any real situation.

Unfortunately, one of the drawbacks of the S-N method is its inability to include non-failures into the graph, as it is unknown whether the un-failed components on the board are on the verge of failure or have plenty of useful life left. In fact, it is very difficult to use the data from the components that have not failed, they are an unknown quantity.

7.4.3 Maximum Strain Values

This is the simplest data that can be provided. It is simply the highest strain that the components have experienced without any failures being observed, where this strain is experienced for ten minutes duration. The results are shown in table 7.1. A factor of two safety is included for all results.

The values do not discriminate between the causes of failure, so say a component fails because of high strain in the X direction and there is a low strain in the Y direction, then both this high X and low Y value are used in the table, even if the strain in the X direction actually caused the failure. In this way the results can be seen to be very conservative; however, they are very useful as starting values, especially in the cases where very few failures are observed. It is possible to reduce the conservativeness of the data when good S-N data exists. For example, the cause of failure of the D^2-PAK packages was previously determined to be a cause of bending in the X axis with no correlation being found between shear bending strains and failure. However, because the maximum strain method can not distinguish between the different causes of failure, the D^2-PAK packages have been incorrectly given a low shear acceptable strain. In this case - and other cases where S-N data is available - it is advisable to reconsider the maximum allowable strains. For the other case of the SOT-223 failures it is likely that the X bending strain is too low and that a value of $6 * 10^6$ is more reasonable.

7.4.4 Curvature or Acceleration as Primary Cause of Failure

An additional reason for the set-ups used in this work was to observe whether acceleration or strain is the principal driver of failure. Considering the results for the cantilever test it can obviously be seen that - for the components used here - failure is predominantly as a result of curvature. Over twelve components failed on the row closest to the clamping mechanism, whilst none failed at the free end even though they experienced by far the highest accelerations. The components closest to the clamping mechanism that experienced the highest curvatures, failed first and the failures progressed from there towards the free end.

Component	$strain_{max}$ without failure		
	X direction	Y direction	Shear
D^2-PAK	$1.25 * 10^{-4}$	$1.1 * 10^{-4}$	$1.1 * 10^{-5}$
D-PAK	$2.5 * 10^{-4}$	$4.2 * 10^{-4}$	$7.2 * 10^{-5}$
SOT-223	$1.3 * 10^{-4}$	$1.1 * 10^{-4}$	$2.8 * 10^{-6}$
SOT-23	$1.9 * 10^{-3}$	$1.5 * 10^{-3}$	$7.2 * 10^{-5}$
TO-39	$1.8 * 10^{-5}$	$1.7 * 10^{-5}$	$2.2 * 10^{-5}$
SMT Resistors	$1.9 * 10^{-3}$	$1.5 * 10^{-3}$	$7.2 * 10^{-5}$
SMT ResNets	$1.9 * 10^{-3}$	$1.5 * 10^{-3}$	$7.2 * 10^{-5}$
SOIC 16	$1.5 * 10^{-3}$	$1.5 * 10^{-3}$	$7.2 * 10^{-5}$
CK05	$1.9 * 10^{-3}$	$1.2 * 10^{-3}$	$7.2 * 10^{-5}$
CK06	$1.9 * 10^{-3}$	$1.5 * 10^{-3}$	$7.2 * 10^{-5}$

Table 7.1: Table of maximum failures strains survived for each component without any failures occurring within ten minutes. Surface strain in X, Y and shear are considered.

7.5 Discussion of Results

As mentioned at the start this chapter has two functions first to illustrate the process, but also to investigate what is the main failure driver and what ball-park estimates of failure parameters. Before discussing individual failures it is useful to consider some overall observation. First, the failure is - for the components tested at least - primarily as a result of curvature. This is very useful as it means that acceleration can be ruled out as a failure cause, reducing the amount of work required in future investigations and also meaning that future set-ups do not have to be designed with acceleration in mind. However; this is only true for the components tested here, but even if heavier components were to be tested, the cantilever set-up shown in this chapter illustrates a good method to find the relative significance of curvature and acceleration on failure rates.

A second overall observation is that failure is not simple, different package types have different types of failure. Some package types do not fail at any reasonably achievable strain level; for example, the small resistor packages. Some package types only showed a single failure with no apparent trend or pattern, for example, the single capacitor failure, though this could be a result of a manufacturing defect. Whilst other package types had some failures that loosely

Component	$strain_{max}$ without failure		
	X direction	Y direction	Shear
D^2-PAK	$1.25 * 10^{-4}$	$1.1 * 10^{-4}$	$1.1 * 10^{-5}$†
D-PAK	$2.5 * 10^{-4}$	$4.2 * 10^{-4}$	$7.2 * 10^{-5}$
SOT-223	$4.0 * 10^{-4}$*	$1.1 * 10^{-4}$†	$2.4 * 10^{-5}$*
SOT-23	$1.9 * 10^{-3}$	$1.5 * 10^{-3}$	$7.2 * 10^{-5}$
TO-39	$1.8 * 10^{-5}$	$1.7 * 10^{-5}$	$2.2 * 10^{-5}$
SMT Resistors	$1.9 * 10^{-3}$	$1.5 * 10^{-3}$	$7.2 * 10^{-5}$
SMT ResNets	$1.9 * 10^{-3}$	$1.5 * 10^{-3}$	$7.2 * 10^{-5}$
SOIC 16	$1.5 * 10^{-3}$	$1.5 * 10^{-3}$	$7.2 * 10^{-5}$
CK05	$1.9 * 10^{-3}$	$1.2 * 10^{-3}$	$7.2 * 10^{-5}$
CK06	$1.9 * 10^{-3}$	$1.5 * 10^{-3}$	$7.2 * 10^{-5}$

Table 7.2: Modified table of maximum allowable failure strains. * indicates values that have had accuracy improved by considering failure trend data. †indicates values that are probably very conservative (as the failures were a result of strain in another direction).

correlated with input curvature and one package type that had strongly correlated failures. Ultimately what this observation highlights is the need for more failure data, which is not financially possible for this research. Regardless of this fact, the overall trends can be expected to be the same, albeit a little less well defined. With this in mind it is possible to loosely place the different package types into broad "robustness" categories: (1) tough packages, that are not expected to fail (SMT resistors, SOT-23, ResNets); (2) medium packages (SOICs); and (3) weak packages, that are expected to be the first to fail (SOT-223, D^2-PAK and TO-39), where these categories the based on the minimum strains experienced without a single failure occurring for ten minutes (as shown in table 7.1). The reason for using the minimum strain table for the D^2-PAK package - even when it can be defined well by S-N tables - is that they are more convenient to use than S-N data during the design process. If the S-N data is to be used at all it should only be to increase the confidence in the minimum strain tables' values[2]. As a result of this discussion an improved set of results is proposed in table 7.2.

A final point to make concerning the failures examined here is that only out-of-plane vibrations

[2]Although it may also be possible to use the S-N data if a more in-depth analysis by the MCAD department, but the discussion here is primarily focused on the use of the PRDB and the ESM

are considered. It is possible that if very strong lateral vibrations are present then some of the taller components - specifically the capacitors and the TO-39 - may fail. However, this effect has been already been examined in previous research by other authors Steinberg (2000); Suhir (2000) and formulas given for predicting when this failure may occur.

During the testing it was found that the continuity testing method is very time consuming, the reasons for this are considered here and alternatives suggested. The testing method is time consuming because of the time it takes to set-up and the time it takes to find a failed component. The set-up is slow because of the large number of wires that must be soldered to the board, the difficulty in keeping track of all these different wires, the large amount of pre-testing that must take place to ensure that each new wire does not interfere with a previous one. This could be solved, in theory at least, by testing fewer components at a time, as the smaller number of wires would be much easier to keep track of. Testing fewer components at a time would also be of benefit during the testing stage, as there would be less components to probe when trying to find a failure. Additionally, to solve the problem of the soldering, push fit connections could be used instead of soldered connections, provided they are able to resist the bending strains imposed upon them and do not alter the PCB response (the original reason for using wires) and depending the financial constraints of the test.

The second major time consuming task during testing is the location of failed components, especially when probing individual components with a volt meter. This could be solved by using less components per circuit (as already discussed), as this means there would be less components to probe; however, this means either having a greater number of volt probes (the system used in this test was limited to 8 circuits) or testing less components. The problem could also be alleviated by moving away from using complicated circuits with transistors or capacitors, and instead using the much simpler resistor circuits. These simpler circuits are much easier to find faults in. It is possible to create such circuits by using “dummy” components, where these components use standard package dimensions but internally only consist of pass-through circuits (effectively a zero ohm resistor). The perfect solution would be to have one continuity test system for each component, as this would allow very simple testing; if this is financially viable then it would be strongly recommended.

7.6 Summary

The primary aim of this chapter is to illustrate a process to create useful failure statistics; this has been achieved for an initial exploratory case. Two different possible techniques for analysing the failure data have been given, maximum survivable strain and S-N analysis. The simple maximum survivable strain analysis is most convenient for later use in the PRDB, whilst the S-N analysis is useful (when enough failure data exists) to assess the confidence in the maximum survivable strain analysis.

The additional observation of the relative insignificance of local acceleration on package failure rates is also very useful, as it allows future failure experiments to be made more efficiently.

Chapter 8

Example Application

8.1 Introduction

This chapter brings together all the work from the previous four chapters and shows how it could be used in a real situation. For this purpose, a case study is given based on the SSTL Microtray form factor (as shown in figure 4.1 on page 49), which is to be hypothetically populated with the components tested in the previous chapter. At the end of the chapter there is discussion on the overall effectiveness of this method.
The case study is made in the following order: (1) the data required to create the ESMs (Environment Severity Maps) is defined and an example of some of these ESMs are created, (2) a basic form of a PRDB (Package Robustness DataBase) is created from the failure data in the previous chapter; and (3) the ESMs and the PRDB are then considered together to show how they can be used to provide safer component placement.

8.2 Environment Sensitivity Map Creation

For this case study the first task is to create the ESMs based on various input parameters, these can be considered to be either fixed (i.e. constant across all the ESMs) or variable (i.e. several different values are given so that several different ESMs can be created), this requires the following parameters:

8.2.1 Fixed Input Parameters

These are the parameters that do not alter at all between any of the ESMs.

Form Factor: For this case study the SSTL MicroTray form factor is used. This is the same as in Set-up A in chapter 4 (see figure 4.1 on page 49).

Damping: The value of damping is the same as measured in chapter 4, this is experimentally measured from an already existing prototype and is 2.5% of critical.

Boundary Conditions: Again, the experimental values were used similar to those measured in chapter 4.

8.2.2 Variable Input Parameters

These are the parameters that may be varied between the different ESMs:

Vibration Input: The vibration input environment was a fixed value between 1 - 1000Hz, this is initially set at $0.1g^2/Hz$ as this the same as the highest value of the Acceleration Spectral Density curves normally required for qualification testing. Using a constant value is a conservative assumption as usually a curve is specified, but using a constant value is easier as it avoids the need to specify individual curves and decreases the number of ESMs that must be created. This vibration input can then be multiplied by a factor to account for any amplification that occurs through the spacecraft structure, for this study a value of $1g^2/Hz$ is used (ten times magnification factor) to reflect a relatively harsh base excitation for the equipment. This multiplication method is considered the most convenient to use as it means that complex input spectrums do not have to be considered, resulting in less ESMs to create and choose from. It is relatively simple to create several ESMs at different levels of input vibration, for example, $0.1 - 1g^2/Hz$ in $0.1g^2/Hz$ steps. Additionally, it is assumed that the approximate magnification factors of most spacecraft can be calculated prior to design, based on the general overall spacecraft structural mass and layout.

PCB Mass Ratio: This is the ratio of the mass of the underlying PCB to the total mass of the PCB and components. Similar to the vibration input, ESMs with several different levels of mass ratios could be easily created. Then, when it comes to choosing the correct ESM for the case at hand, it is a simple matter of choosing the ESM with the matching mass ratio. For this study ESMs are created with mass ratios of 1-2 in steps 0.1.

Thickness: For this case study only values of 1.6 and 2mm are considered, other equipment

manufacturers may use different thicknesses and, if so, should adjust their calculations accordingly.

8.2.3 Safety Factors

After the different ESMs are created it is then necessary to apply the safety factors based on the analysis in chapters 4-6. These can be considered in terms of the "overall" safety factors that can be applied to all equipment and the "specific" safety factors that vary depending on the specific application where they are applied.

Overall Safety Factors

These are applied to all ESMs and are the same for each one.

Manufacturing Variability: In this case study the manufacturing variability is considered to be an overall safety factor; however, in other situations this might be inappropriate if the ESMs were to be applied to equipment from different manufacturing houses, with different form factors or some other factor that alters the expected variability. For this case study the overall safety factor is a value of 1.2 based on the analysis in chapter 6.

Modelling Accuracy: To account for any possible variation as a result of modelling inaccuracy (this is different to simplification accuracy which is considered shortly); however, it was found that during the modelling that the FE model would slightly over-predict the strains for this specific case study, as such this factor is disregarded.

Altered Board Response After High Acceleration: A final safety factor that may be applied is to account for the possibility of any local micro-damage that occurs around the PCB fixing. This is considered at the end of chapter 6. Fortunately, it is found that - in this case - the damage only served to reduce the response; therefore, this safety factor may be disregarded.

Specific Safety Factors

These are the values that are considered in the work in chapter 5. They are calculated by simply taking the reciprocal of the expected error values provided in that chapter (see table 8.1). These values can then be used to factor the strains predicted by the FE model, making them safe to use.

Simpl'n id.	Simplified properties			Equipment type			
	Mass	Stiffness	Torsional stiffness	1	2	3	4
1	E	E	E	*1*	*1*	*1*	*1*
2	A	E	E	*1.29*	*1.24*	*1.06*	*1.08*
3	E	A	A	*1.1*	*1.07*	*1.05*	*1.05*
4	A	A	A	*1.27*	*1.25*	*1.08*	*1.24*
5	E	A	N	*1*	*1*	*1*	*1*
6	E	N	N	*1*	*1*	*1*	*1*
7	A	N	N	*1.14*	*1.13*	*1*	*1.01*
8	N	N	N	*2.45*	*2.84*	*1.2*	*1.21*

Table 8.1: Factors of safety (in italics) for a 1.6mm thick PCB, divided into different equipment types and simplification methods. The first four columns define the simplification method used (as defined in table 5.5) by which properties have been simplified, where E, A and N denote Exact, Averaged and Neglected respectively. The results are then further sub-divided into different equipment types (as defined in table 5.4).

8.2.4 RMS Strain Correction

The final factor to include is required to correct the RMS strain so that it reflects the sinusoidal strain experienced in the failure tests. This is simply achieved using Steinbergs equivalent strain approach, which assumes that the stresses occur within the following probabilities (assuming a Gaussian distribution):

- 68.3% of the time at 2*RMS
- 27.1% of the time at 4*RMS
- 4.3% of the time at 6*RMS

this leads to the following formula:

$$S_{equivalent} = (0.683 * (2 * RMS)^m + 0.271 * (4 * RMS)^m + 0.043 * (6 * RMS)^m)^{(1/m)} \quad (8.1)$$

where $m = -1/b$ and b is the power factor of the fatigue curve. For the rest of this case study a value of m of -0.4 is used, where this comes from the slope of the S-N curve for the D^2-PAK failures.

8.3 Environment Sensitivity Map Example

Using the above data the following ESMs have been created (see figures 8.1 to 8.3). These maps are based on a worst case scenario of $1g^2/Hz$ input vibration, x2 mass factor and 1.6mm thickness. For this case study the specific safety factor of 1.14 is used, as a worst case scenario of heavy components is taken (Equipment type 1 in table 8.1), whilst the simplification method used is type 7 which is smeared mass and ignored stiffness.
It is easy to imagine that many more ESMs could be created by using different combinations of input parameters, resulting in a large database of different maps that can be chosen from.

8.4 Package Robustness Data Base

A simple package robustness database is created based on the maximum allowable strain data in the previous chapter (see table 7.1 on page 111; although, some values in this table are slightly altered as per the discussion in section 7.4.3 on page 110, to make the values more realistic.

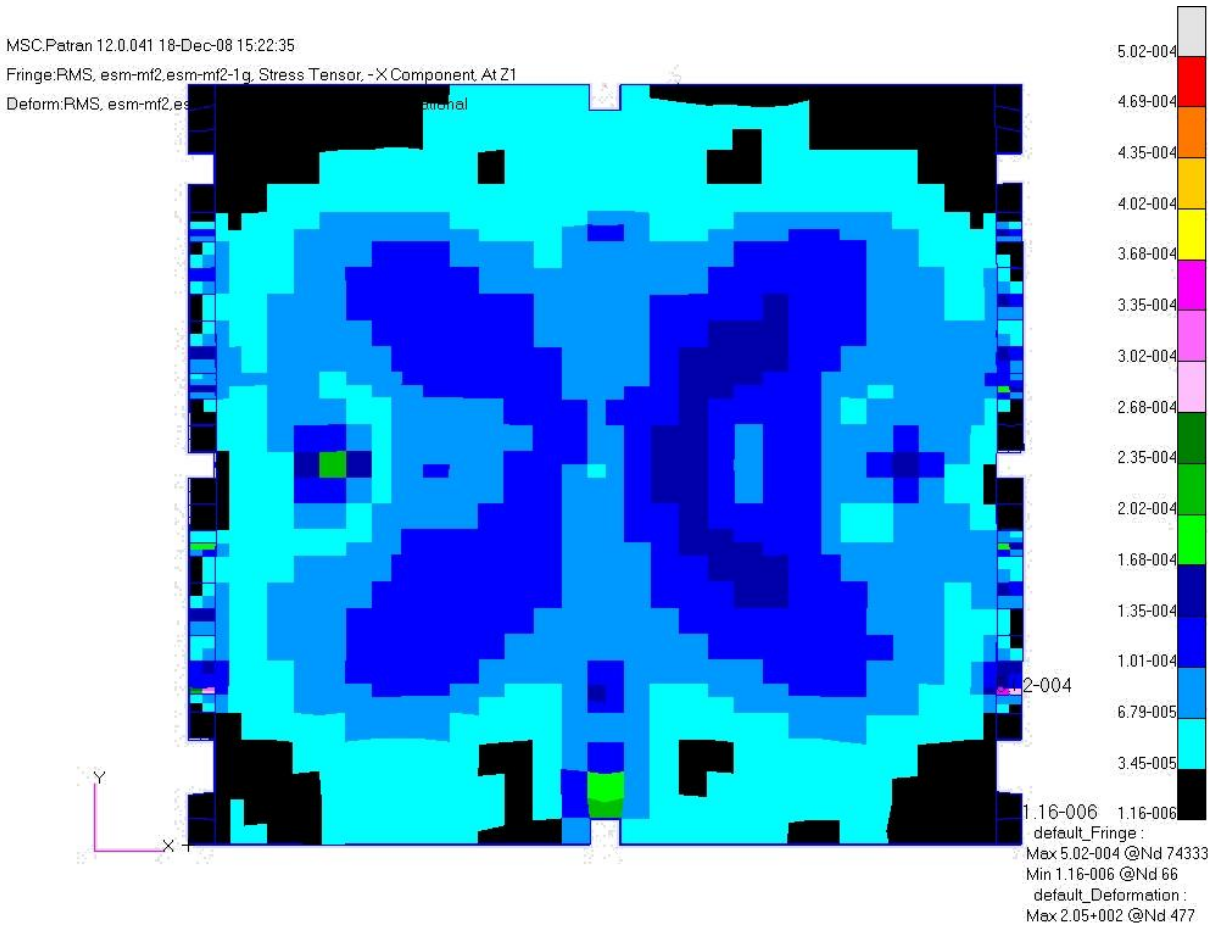

Figure 8.1: ESM for x direction bending strain. $1g^2/Hz$, x2 mass factor, 1.6mm thickness. With safety factors included. RMS results were factored using equation 8.1 to account for sinusoidal failure data.

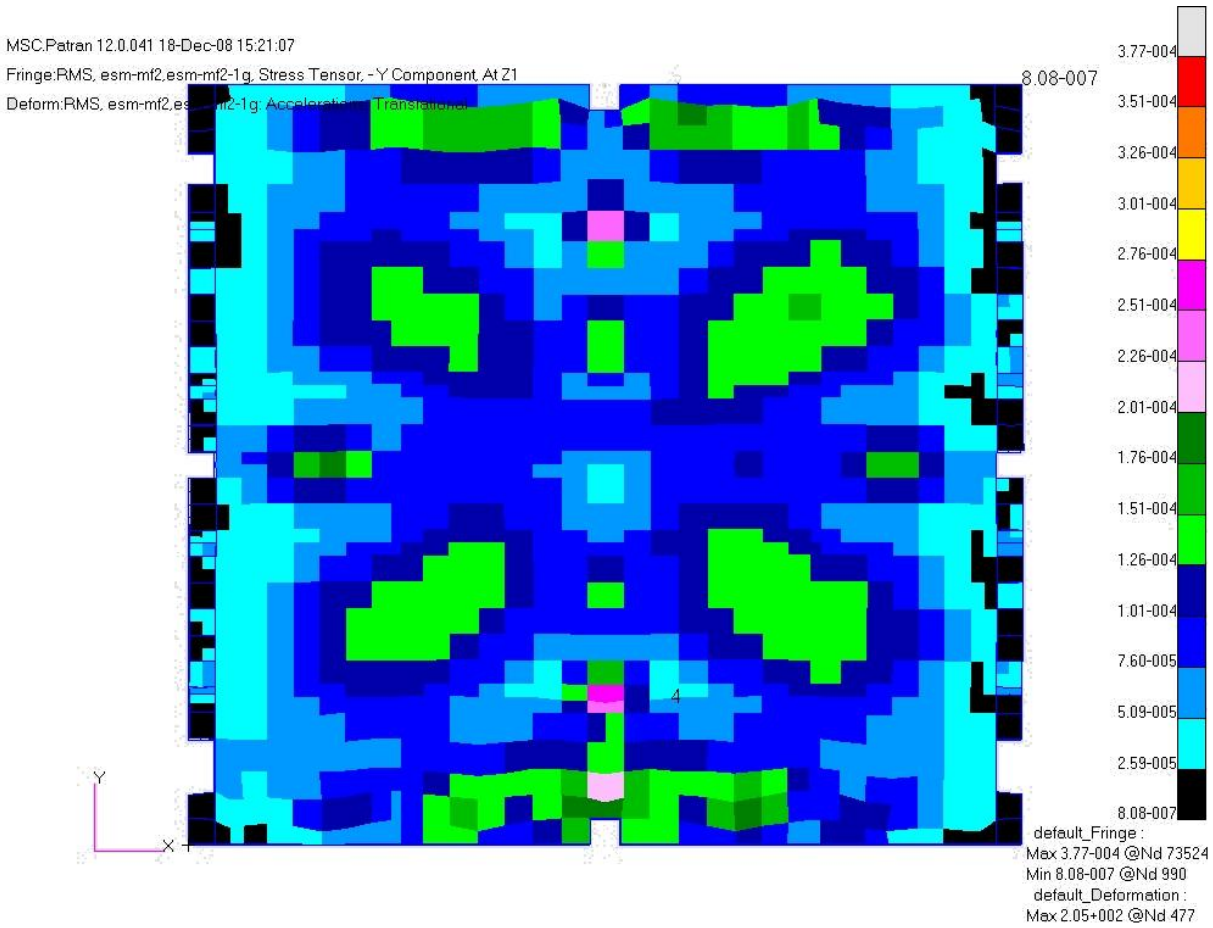

Figure 8.2: ESM for y direction bending strain. $1g^2/Hz$, x2 mass factor, 1.6mm thickness. With safety factors included. RMS results were factored using equation 8.1 to account for sinusoidal failure data.

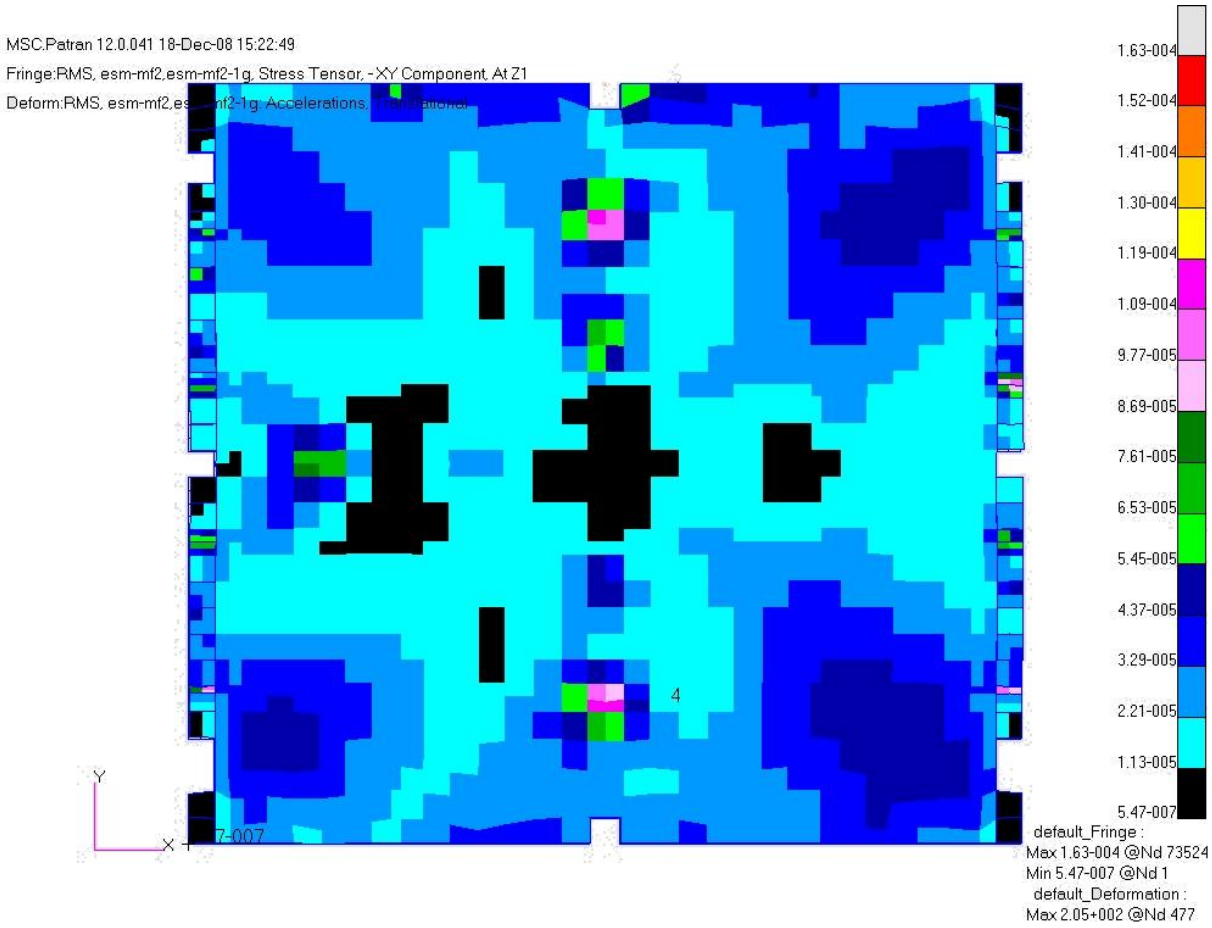

Figure 8.3: ESM for shear strain. $1g^2/Hz$, x2 mass factor, 1.6mm thickness. With safety factors included. RMS results were factored using equation 8.1 to account for sinusoidal failure data.

Component	$strain_{max}$ without failure		
	X direction	Y direction	Shear
D^2-PAK	$1.25 * 10^{-4}$	$1.1 * 10^{-4}$	$1.1 * 10^{-5}$†
D-PAK	$2.5 * 10^{-4}$	$4.2 * 10^{-4}$	$7.2 * 10^{-5}$
SOT-223	$4.0 * 10^{-4}$*	$1.1 * 10^{-4}$†	$2.4 * 10^{-5}$*
SOT-23	$1.9 * 10^{-3}$	$1.5 * 10^{-3}$	$7.2 * 10^{-5}$
TO-39	$1.8 * 10^{-5}$	$1.7 * 10^{-5}$	$2.2 * 10^{-5}$
SMT Resistors	$1.9 * 10^{-3}$	$1.5 * 10^{-3}$	$7.2 * 10^{-5}$
SMT ResNets	$1.9 * 10^{-3}$	$1.5 * 10^{-3}$	$7.2 * 10^{-5}$
SOIC 16	$1.5 * 10^{-3}$	$1.5 * 10^{-3}$	$7.2 * 10^{-5}$
CK05	$1.9 * 10^{-3}$	$1.2 * 10^{-3}$	$7.2 * 10^{-5}$
CK06	$1.9 * 10^{-3}$	$1.5 * 10^{-3}$	$7.2 * 10^{-5}$

Table 8.2: Table of maximum failures strains survived for each component without any failures occurring within ten minutes. Surface strain in X, Y and shear are considered. * denotes values that have had accuracy improved by looking at failure trends. †denotes values that are probably very conservative.

8.5 Example Component Placement

The PRDB in the previous section is now considered in comparison to the ESMs created earlier. Before starting this discussion, however, it is important to note that this case study uses components that are all relatively tough and therefore their allowable strains are very high and also very closely grouped. If more failure data existed for a greater range of, larger and weaker, components then it is expected that there would be a much greater spread of results, leading to a more distinct and simpler grouping of components. It is even possible that the groupings would be so pronounced that the need for three different failure directions (x, y and shear) could be avoided. Furthermore, the larger components are much more likely to have 90◦ symmetry which further reduces the requirement for three separate failure directions. Thus, it can be seen that this case study considers quite a difficult choice of packages with only subtle differences in failure, with this in mind the short discussion on component failure can begin. The easiest packages to consider are those that have very high allowable strains, these are the resistor packages, SOT-23 and capacitors. All of these packages have allowable strain values

that are far in excess of anything predicted by the ESM; therefore, they should not fail regardless of where they are placed.
Next is the D-PAK package, based on the values given in the table this should not fail, although it would only take a slight increase in the input acceleration for the strain to reach dangerous levels. Therefore, it would be advisable to take caution when placing this package. Finally, there are the packages that have a possibility of failing, these are the D^2-PAK and the SOT-223. First, the D^2-PAK has a maximum allowable uni-axial bending strain of $1.25 * 10^{-4}$, both the x and y direction maps have areas with a greater strain than this in an x-shape around the centre of the PCB; therefore, it would be advisable to keep these packages away from this location. Additionally, for the D^2-PAK, based on the maximum allowable shear strain values provided in the table the component could fail; however, the predicted strains are probably very conservative, as discussed in section 7.4.3. Next, for the SOT-223 package, the maximum allowable shear strain is $2.41 * 10^{-5}$, shear strains greater than this are predicted in the corners of the PCB (as shown in figure 8.3); therefore, these packages should not be placed in the corners.

8.6 Overall Design Process Summary

Although this is only one example it shows clearly how simple this method is to implement, especially when compared to traditional methods that involve the time consuming creation of detailed FE models. In this method, once the initial ESMs and PRDB has been created, it is a very quick and simple task to optimise the component location to reduce the probability of failure. This process would not significantly alter the current design process, making it much more likely to be used. Furthermore, unlike previous methods that only state whether a component may fail or not, this method actually provides information on how to place the component to reduce the likelihood of failure.

Chapter 9

Summary

9.1 Summary of Main Achievements

This section briefly summarises the main contributions achieved in this work, this then leads on to a general overall discussion of these points in the following "Conclusions" section.

Literature Review

- Provides an in-depth literature review on both the cause of failure, and also the traditional methods that predict when these failures may occur. This literature review also provides a useful classifying structure within which future developments can be categorised.

Response Prediction

- Primary achievement:
  - This work illustrates that, under certain conditions, the modelling process is sufficiently accurate for what is required (Chapters 4-6).
- Additional insight that can be useful for future response predictions:
  - The relative importance of correctly specifying the following inputs (in general order of importance): boundary conditions, damping, PCB mechanical properties, manufacturing variability and *attached component* effects. Where in the first three inputs the importance of accurately measurement is shown, in the fourth input (manufacturing variability) the importance of measuring the expected variability is

shown, whilst for the last input (component effects) a method to account for many different scenarios is illustrated.

  - The work provides two example modelling situations, that other engineers may follow in future as an example of a correct modelling process.
  - It is shown that certain types of simplified PCB models can result in a large amount of modelling error, an issue that has not been accurately quantified in past research (chap 5).
  - A tuning method is given to measure the rotational edge stiffness of the boundary conditions.
  - It is highlighted that damping may vary significantly between different modes of vibration on the same PCB.
  - The importance of accurately measuring and specifying the stiffness in both x and y directions is shown (as well as being sceptical of mechanical properties claimed by the manufacturer).

- Provides some ball-park data for the degree of accuracy that can be expected in future work.

Failure Criteria

- Primary achievement:
  - A method is shown to create package failure criteria (Chapter 7).
- Additional Insight for future failure criteria generation:
  - This work shows that component failures exhibit greater correlation with local PCB curvature than with local acceleration, an important observation that is crucial for the accuracy and relevancy of future work. A test configuration is illustrated that specifically distinguishes between these two causes of failures.
  - One type of event detection system is demonstrated, this measures exactly when the packages fail. Based on the use of this system, several suggestions have been made for an improved system in future. With the insight gained from this system and more resources, alternative systems with better performance could evolve.

- Provides some ball-park data for the types of failures that can be expected in future.

Design Process

- A set of tools are given that can be used to improve the design process, and prove that these tools are viable through all the other tests in the thesis.
- The Pareto and the DSM analysis are given as a suggested justification for the effectiveness of these tools in improving the design process, this is primarily based on a pseudo-optimisation that achieves considerable design optimisation for very little effort. The proposed design process is further justified by the fact that should a design still fail the qualification test, the resultant corrective modifications can then focus on other options (ruggedisation, boundary condition modification, damping modifications, thickness increase) rather than the costly process of redesigning the whole PCB.

9.2 Conclusion

The work in this thesis satisfies the original requirements that are stated in the introduction. A set of simple but effective design tools (PRDB and ESM) are proposed. These tools provide a modest level of design optimisation for very little effort. The tools ease-of-use ensures that they are more likely to be implemented in a working environment, whilst the optimisation is sufficient to prevent the majority of failures. An additional benefit of these tools is that in the case of a design still failing the qualification test (even though this is now less likely), then the initial optimisation negates the need to re-iterate the whole design process; instead, other simpler options (ruggedisation, boundary condition modification, damping modifications, thickness increase) may be considered that are less costly and time-consuming than having to reconsider the component choice and layout.

The majority of the work in this thesis is not concerned with proving these tools, as they are relatively straightforward; instead, the work has been focused on proving the validity and accuracy of the processes required to create these tools. These can be broken down into two distinct fields: response prediction and failure criteria. In terms of the response prediction processes, a great deal of progress has been made, this is primarily in terms of achieving good modelling accuracy and also in examining the principal factors that influence this accuracy. Therefore, not only does this work prove that the proposed design tools are viable and have

sufficient levels of accuracy, but this work also shows the relative significance (and insignificance) of the various model input parameters allowing future models to be developed with more efficient use of resources. In terms of the second main field - failure criteria - the same is also true. However, for this second field some additional observations also have been made; specifically, determining local board curvature as the primary cause of failure, and not local acceleration. If this observation is understood and implemented in future failure experiments, then it will significantly improve the relevancy of future failure data.

9.3 Possible Future Work

In this section some ideas are put forward to progress the existing work.

9.3.1 Response Prediction

Some software (either stand alone or a plug-in for current FE software) that automatically creates ESMs, with this proposed software a user could specify the input parameters and their distributions (similar to the start of this chapter) and create ESMs with minimum user effort. This would both speed up the creation of the initial ESMs, but also reduce the time required to create a new ESM should a non-standard situation arise.
An investigation could be performed to look at typical rotational stiffness rates for different mounting types, local chassis conditions, bushings, PCB thickness etc. In this way a body of data could be created to allow the PCB boundary conditions to be predicted without requiring a pre-existing prototype. This would greatly speed up the time required to create models. A similar idea could be applied to damping values, performing an experiment to find what variables most closely correlate with damping, allowing future models to be created from this information instead of experimental data.

9.3.2 Failure Data

As stated at the end of chapter 7, more failure data would be useful to obtain a better understanding of the overall failure trends and ballpark values[1]. Specifically, the following components need to be tested, BGA, QFP and larger PTH components. In addition to this, an

[1]However, this would not make a better failure database, as the databases are specific to each manufacturer. This proposal is only to better understand the problem

investigation should be performed into the effect of PCB thickness on failure rate, as this is likely to be an important factor.

It might be possible - if the exact point of failure can be identified - to use the failure data to create and correct a detailed FE model of a component. If this model can be shown to be consistent with a statistically significant number of real experimental failures, then perhaps this model can be used to predict future failures in similar situations. This would reduce the experimental burden and allow small variations in component design to be investigated, provided these small variations do not alter the component so much that it is not similar enough to the model anymore.

In addition to the S-N and minimum acceptable strain analyses provided in the previous chapter, it could also be insightful to perform a Weibull analysis. The best way to achieve this would be in a manner similar to previous researchLau et al. (1988, 1990); Li and Poglitsch (2001b), where the methods that specifically investigate two input parameters Li and Poglitsch (2001b) are most useful for the type of failure being investigated here. An example of this two parameter Weibull method is not included in this work as there is not enough data points to make such an analysis possible.

9.3.3 Overall Design Process

A feedback administration layer is suggested, the idea of this is to allow failures and non-failures experienced during real qualification tests to be used to improve the quality of the data. If the exact mechanical life of the electrical equipment is known, then any failure (or non-failure) data can be fed back into the database by some system. This system would need to know the exact vibration life experienced by the equipment, including the local PCB response (so either an FE model or good accelerometer data is required) and then compare this with the already existing data, either increasing the confidence when the two sources agree or highlighting problem areas when they do not. This feedback idea would also hold for improving the quality of boundary condition or damping data.

An administrative system to measure the average time spent on each equipment design, the amount of vibration failures experienced, number of design iterations would also be useful, as this could shed light on how well the proposed process is working.

It would also be useful to have a system that could show when it is useful to redesign a piece of electronic equipment or when it is best to use a bolt-on ruggedization device as detailed in

Appendix E, as in some situations this may be a much quicker, cheaper and more reliable method of fixing an unreliable PCB. This would require an in-depth look at the performance of these different devices, which specifically should examine how they perform at extremes of temperature.

Appendix A

Thermal Considerations

The majority of publications that are available on the subject of electronics reliability are concerned with failures from thermal cycling, which agrees with the findings in Steinberg (2000) that thermally induced fatigue is the major cause of failure in electronic equipment, this would initially suggest that any work on electronic equipment reliability must consider thermal cycling as the predominant if not the sole cause of failure. This does not strictly apply to spacecraft applications as they generally have higher levels of vibrations than other applications, while the thermal environment is less severe than those considered in past research. In fact, if the life of the spacecraft is considered in terms of manufacture, transportation, storage, launch and post-launch, then it is possible to define the expected temperature excursions a spacecraft component would experience during its lifetime:

Manufacturing Stage The manufacturing stage is the stage that is expected to produce the most thermal damage, as the temperature required to produce a certain solder joint may damage other joints that have already been formed.

Transportation and Storage Thermal damage during the transportation and storage stages can be simply avoided by ensuring that the spacecraft is in a stable temperature environment (room temperature is satisfactory), the expected cost of achieving this requirement is a very good investment when the increased reliability is considered.

Launch Stage The launch can only produce a maximum of one thermal cycle, so is not expected to produce much damage.

Mission Stage Unless there is a pointing system failure during the mission phase; the

temperature of the components are expected to be well within safe working limits. Standard practice requires the temperature to be maintained in the range of -20^0 to 50^0 during the mission(Peter Fortescue and Swinerd, 2003).

Thus the justification for not considering thermal failures in terms of thermal cycling, is that the spacecraft is not expected to experience severe temperature variations, where the definition of severe temperature is considered to be any temperatures above -50^0 or below 115^0(Steinberg, 2000). In addition the temperature variations experienced during the mission (-15^0 to 50^0) are not deemed to be a major contributor to failure, as the life of a typical component in these temperature ranges is found to be at least thirty years(Estes et al., 2003). However it has been noted that thermal damage may occur during the manufacturing stages which could reduce the vibration fatigue life of the component, unfortunately control of the manufacturing process is outside the scope of this research, it is also noted that the manufacturing process has been extensively developed and is very well controlled in the case of spacecraft electronics, so may not allow much scope for further development.

Appendix B

Shock

A survey of launches from the early 1960's to 1977 showed that out of 85 in-flight failures 41 could be directly attributed to shock, with a further 19 possible failures, this is 14 times higher than the number of failures from vibration(Moening, 1984). The results of this survey suggest that shock induced failures should be the primary area of research, however the number of failures from shock have decreased for the following reasons:

- The ability of shock to induce failures was seriously unappreciated, consequently a considerable amount of research was carried out on this topic(Steinberg, 2000), as such shock failures are much less predominant.
- The use of pyrotechnic devices is less widespread, most separation devices now use Shape Memory Alloys (SMA), which drastically reduce the intensity of the shock spectrum.
- Qualification tests now usually incorporate a shock test, which means that potential shock failures are usually identified before the launch.

The combination of the three reasons above means that shock can be disregarded for this research; however, to reduce the chance of shock failures, it is important that the following conditions are met when specifying electronic equipment.

There are more than three joints between the shock source and enclosure A rule of thumb states that every mechanical joint reduces the peak intensity of the shock spectrum by 0.6, up to a total of three joints, or 0.22 of the original shock spectrum(Sarafin, 1995).

The Enclosure should not be very close to the shock source Experience has shown that shock rapidly attenuates and loses its high frequency component with increasing

distance along the load path, for example a reduction of approximately 30% within 30 cm or 50% by 50 cm(Sarafin, 1995).

Pyrotechnic release mechanisms should not be used Pyrotechnic devices typically exhibit much higher shock responses, SMA actuators are preferred.

B.1 Shock Related Literature

The majority of past research has principally focused on random vibration as the PCB load; however the following research specifically looks at shock related failures. The methods are not fully discussed here as they fall under the classification of PoF methods, therefore they are discussed fully in sections 2.4.1 and 2.4.2.

Hin et al. (2003) created a test board to characterise the reliability of BGA solder joints to shock. Lau et al. (1990) looked at the reliability of PLCC, PQFP and QFP components to in-plane and out-of-plane shocks. Pitarresi et al. (2002, 2004) look at the failure of PC motherboards to shock loads and provides a good review of shock related literature of electronic equipment. Steinberg (2000) provides a complete chapter on the design and analysis of electronic equipment subjected to shock, looking at both how to predict the shock environment and also providing some practical advice on how to avoid shock failure. Suhir (1992b,a) looked at errors in linear calculations of the response of a PCB to a shock load applied at their supports. Handbook and field data methods may consider shock related failures, but not explicitly.

Appendix C

Additional Operable Causes of failure

This section describes the two additional operable failure causes that are not included in section 2.2.4 as they are outside the scope of the discussion there.

C.1 Inaccurate or Incomplete Specification of the Environment

This classification includes any failures because of incorrect specification of the vibration environment expected to act on the chassis (i.e. it does not consider the response of the PCB to the vibration environment, only the accuracy of the input environment itself). For example, failures as a result of incorrect specification of the launch envelope or from ignoring the contributions of transportation, shock and thermal effects. Quite simply, a higher than expected vibration environment causes higher than expected PCB responses, increasing stresses on the components and increasing likelihood of failure.

In terms of the time to failure, poorly defined environments can contribute to all failure types except infant mortalities.

To prevent such failures it is simply a case of better predicting the environment. In terms of the launch environment, this may be achieved by either better FE models of the spacecraft structure that supports the electronics or by measuring the vibration environment experienced in previous launches. A significant proportion of vibrations experienced outside the launch environment occur during the transportation stage, which can - in some cases - use a significant proportion of the fatigue life(Sarafin, 1995). This can be simply remedied by better packing methods or measuring and including the expected transit vibrations and including them in any preliminary analysis.

C.2 Manufacturing and Assembly Process

This cause comprises failures because of defects in the solder joints, residual manufacturing stresses and poor installation, where these factors cause either reduced strength or altered PCB response. This classification mainly contributes to infant mortalities. QFP and BGA are most at risk because of the large number of joints. Medium sized components are more susceptible to manufacturing defects, purely because of the large number of leads.

Small variations in dimensions or mechanical properties of the PCB and components alter the frequency response and strength of the structure. Specifically, poor installation (specifically variations in the tightening torques of the PCB fixing bolts) is most likely to cause the response of the PCB to be significantly different to what is expected. If the distributions of variability are not taken into account during the design stage by either a worst case scenario, Monte Carlo analysis or some other technique, then an accurate prediction of the stress is not possible, which may result in an increase in probability of the infant mortality or wear-out failures.

To prevent manufacturing process failures is simply a case of reducing the variability and increasing the quality, this is most usually achieved by better training of staff, better materials and better equipment. Additionally, most manufacturing failures are highlighted during the qualification test stage.

Finally, recent advances in the manufacturing process have made manufacturing defects less likely for two reasons. First, automated manufacturing methods mean that similar components from the same manufacturer usually show very little variation. Secondly, spacecraft electronics are generally subjected to a detailed visual inspection before under-going qualification testing, this highlights poorly soldered joints and allows them to be reworked.

Appendix D

Handbook, Test Data and Field Data Methods

D.1 Handbook Methods

Of all the handbook methods available the only two that consider vibration failure are Mil-Hdbk-217 and CNET (Bowles, 1992), Mil-Hdbk-217 being accepted as a bench-mark by the majority of manufacturers. Like all handbook methods these are empirical approaches that aim to predict the reliability of a component from field or laboratory data. Handbook methods are relatively simple to implement, in that they do not require complex mathematical modelling, only part types, part counts, application environments and other readily available parameters, these parameters are then input into a model to calculate the MTBF. Despite its advantages Mil-Hdbk-217 is increasingly falling out of favour (Pecht and Nash, 1994; Foucher et al., 2002; Luthra, 1990; Pecht and Kang, 1988; Cushing et al., 1993), a non-exhaustive list of the limitations are:

- The data is becoming increasingly obsolete as it was last updated in 1995 and is not relevant for new components, there is no chance of a revised model as the Defense Standards Improvement Council decided to let the method "die a natural death" (IEEE, 2003).
- The method does not give information on the mode of failure; therefore the PCB layout can not be improved or optimised.
- The models assume that the failure is independent of design, ignoring the components

location on the PCB; however the component layout is known to have a large effect on performance (Pecht and Kang, 1988).

- The empirical data collected contains many inaccuracies, data from first-generation components with un-naturally high failure rates, defective records of operating times, repair blunders, etc, which has resulted in low confidence in the results (Pecht and Nash, 1994).

All these disadvantages would suggest that the handbook methods should be avoided; however the limits of this method should be realised and the method only be used it when appropriate, i.e. during early design trade-off stages (Morris and Reilly, 1993). Unfortunately even this use should be approached with some caution as the method has not been revised since 1995. In summary, handbook methods are inherently poor at predicting mechanical reliability and should be used with caution.

D.2 Test Data Methods

Test data methods are the simplest of the reliability prediction methods available. A prototype of a proposed PCB design is subjected to a laboratory simulation of the vibration environment, analysis of the failure parameters (MTTF, shock spectrum) is then used to create a reliability metric (IEEE, 2003). The test data method should be used with respect to its advantages and disadvantages. The main advantage of test data methods is the high accuracy and confidence in the results, thus for high risk equipment the final step of the design process should always include a qualification vibration test. The disadvantage is the long time to manufacture, set-up and stress a test specimen, making the method unsuitable for guiding design improvements for equipment with high failure probability, for this type of iterative design process a quicker method should be considered. The test time can be reduced by using accelerated tests, where models are available to subsequently calculate the actual service life (Zhao et al., 2004; Zhao and Elsayed, 2005). These accelerated testing methods are more suited to thermal failures than vibration failures, because of the very long time for thermal failures and relatively short time for vibration. The additional complexity and error would mean these methods would generally not be applied for vibration failures, unless there are extenuating circumstances, for example, very low stresses leading to very long time to failure.

Examples of test data methods can be seen by Hart (1988); Hin et al. (2003); Li (2001); Lau

et al. (1990); Shetty et al. (2001); Liguore and Followell (1995); Estes et al. (2003); Wang et al. (2004); Jih and Jung (1998) and a good overall synopsis of the method is available from the IEEE (2003).

D.3 Field Data Methods

As the field data method is based on failure data from previous PCBs which have experienced a particular environment; the method is only correct for PCBs which experience the same dynamic environment. The field data method has two main aspects, building the failure database and implementing the method on a proposed design. To build the database for the field data method there must be appropriate failure data that has been collected from similar designs; this means that failure data from similar equipment must exist. The failed equipment must also have been analysed and collected properly, it is insufficient to state that a given PCB design failed after a certain number of hours, the location, failure mode and failure cause must be determined; therefore unless all previous failure data have been collected thoroughly there is a long period of data collection required before the field data method can be used. A possible work-around for this limitation is to implement Highly Accelerated Life Testing (HALT) for the purposes of quickly building a failure rate database, although accurately determining the exact environment is difficult but vital. Johnson and Gullo (2000) describes the second stage of implementing the field data method, using an example this paper shows how to predict the MTTF for a proposed design, where this design is modified from existing equipment for which detailed failure data exists. Other reviews of field data methods exist by Condra et al. (1999); Foucher et al. (2002); Gullo (1999); IEEE (2003).

Appendix E

Equipment Ruggedization

This section discusses bolt-on post-design modifications that reduce the vibration response of the PCB, these are within the class of reliability improvement methods.
These fall into two distinct categories, those that modify the PCB boundary conditions and those that increase the damping.
The primary aim of the first category of boundary condition modifications is to reduce the PCB dynamic deflection; this can be achieved by stiffening ribs, additional supports or reducing the vibration input environment.
Stiffening ribs can be useful as they raise the natural frequencies thereby reducing the dynamic deflection (Steinberg, 2000), the same applies to adding additional supports (Aglietti and Schwingshackl, 2004), although support location can also be optimised as shown by J.H.Ong and Lim (2000). Unfortunately ribs and supports would usually require a redesign of the circuit layout, therefore these methods are best considered early in the design cycle, normally when designing the form factor. Additionally, care should be taken to ensure that the modifications do not alter the natural frequencies to coincide with natural frequencies of the supporting structure, as this would be counter-productive.
Isolation achieves higher reliability by reducing the dynamic environment transmitted through the boundary conditions and into the equipment, and can be achieved either passively or actively.
Passive methods are usually simple and cheaper to implement, examples include, cable isolators (Veprik, 2003) and recent approaches that exploit the pseudoelastic properties of Shape Memory Alloys (SMA) (Khan et al., 2004), although poorly designed isolators can sometimes increase response.

Active methods provide better performance over a wider range of frequencies usually at the expense of simplicity and mass, thus they are generally reserved for increasing the accuracy of very sensitive precision instruments as opposed to preventing damage.

Examples of active vibration isolation include electromagnetic (Spanos et al., 1995) and piezoelectric approaches (Garcia-Bonito et al., 1998; Marouze and Cheng, 2002), though these methods have not been applied to PCBs.

In contrast to the first category of boundary condition modification methods, the second category - damping modifications - aims to reduce the peak resonant response of electronic equipment, with negligible effect on the actual natural frequencies. As with vibration isolation damping this may take the passive and active approach, with similar properties of simplicity in the former approach and higher complexity and performance in the latter. Passive approaches include very simple methods such as bonding material that exhibit high damping properties to the PCB (Steinberg, 2000) through to more recent approaches such as particulate damping (Xu et al., 2004) and wideband dynamic absorbers (Ho et al., 2003). Active vibration control is usually achieved through the use of piezoceramic elements bonded to the PCB surface (Aglietti, 1999; Moheimani, 2003).

The use of ruggedization methods depends on the specific case at hand, and should be considered carefully with relation to other methods. Applying these techniques to equipment that is not known to have reliability issues would un-necessarily increase cost and weight. However, if a design is showing failures it may be much quicker and simpler to apply a ruggedization technique than to re-design the equipment.

Appendix F

Standard PCB Modelling Process

The whole FEA process can be broken into three main parts: (1) modelling (including estimating input parameters, creating a mesh and incorporating measured parameters in the model), (2) analysis (type of solution, linear or non-linear, etc) and (3) post-processing (looking at appropriate response parameters, such as: acceleration, curvature or deflection) Each of these three parts are considered in turn. It should be noted that the majority of published literature normally use a simplified version of this process either to save time or because it is not possible to obtain certain data. These assumptions are usually made in the following cumulative order (in increasing probability): do not specifically measure damping, instead use estimated values; do not measure the boundary condition stiffness and instead use either simply supported or fully fixed conditions; do not measure torsion modulus, instead use a FE material property that does not require this value; assume the Young's modulus is isotropic; assume the material properties provided by the manufacturer are correct and use them; and - finally - assume that the effect of components can be ignored during modelling.

F.1 Creating FE Models of Electronic Equipment

In creating any FE model of a PCB it is convenient to break the model down into five separate areas: PCB properties, Component effects, Chassis, damping and boundary conditions.

F.1.1 PCB Properties

The main difficulty in creating a model of a PCB is not in creating the mesh but in specifying the properties: stiffness moduli, Poisson ratio, density and thickness. These properties may be

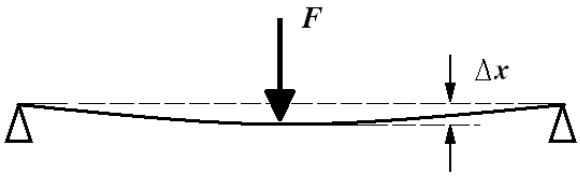

Figure F.1: Diagram of experimental set-up of two point bend test.

provided by the PCB manufacturer but those that are not should be measured.
The Young's modulus is most simply calculated using a static bend test(Pitarresi and Primavera, 1991) as shown in figure F.1 and using:

$$E = \frac{K_b l^3}{48I} \tag{F.1}$$

where K_b is the slope of the load displacement curve, l is the specimen length and I is the second moment of area of the specimen across its width. It is important to note that as most PCBs are laminates their properties may vary depending on the direction of loading, this necessitates that the Young's modulus be measured in both the x and y axis of the PCB.
The shear modulus of a PCB may most conveniently be determined through use of a static four point bend test(Pitarresi and Primavera, 1991) as shown in Figure F.2, allowing the shear modulus to be calculated using:

$$G_{xy} = \frac{3K_t ab}{4t^3} \tag{F.2}$$

where K_t is the slope of the load displacement curve, a and b are the specimen edge lengths and t is the specimen thickness.
The density of a PCB can be simply found using:

$$\rho = \frac{M}{lwt} \tag{F.3}$$

where M is sample mass, l, w and t are sample length, width and thickness respectively, where there is the implicit assumption that the thickness is constant over the PCB.

F.1.2 Components

When components are soldered to a PCB they locally increase the mass and stiffness of the PCB. For good accuracy, especially when large numbers of components are present, the FE model should include this added mass and stiffness effect. Theoretically, this could be achieved

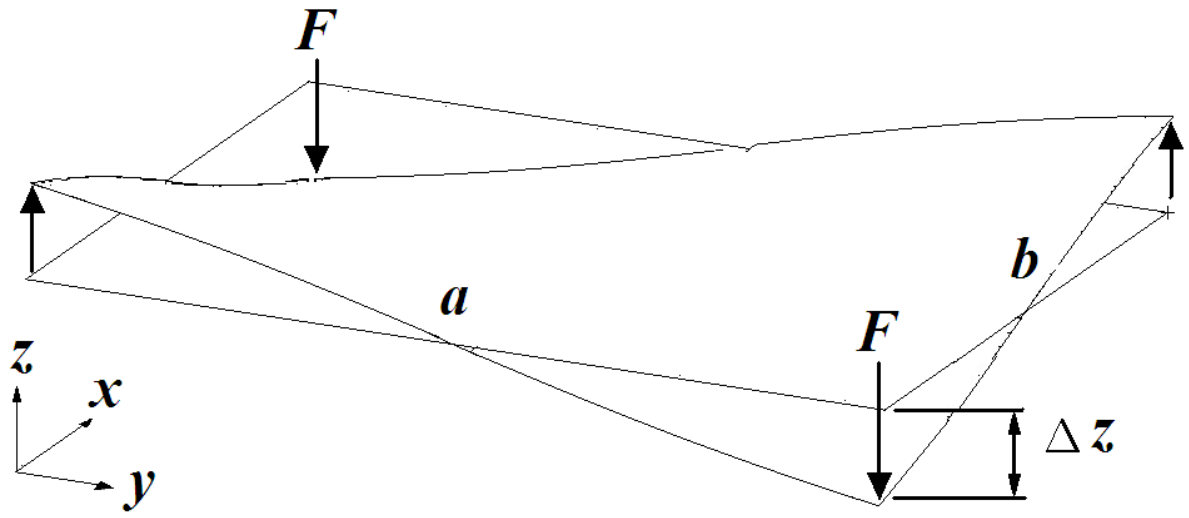

Figure F.2: Diagram of experimental set-up of torsion test. Loads are placed on the four corners of the specimen and the corner deflection is measured. Total load = 2F.

by including each individual component in the model. Several good examples of such detailed models exist(Dehbi et al., 2005; Gu et al., 2007; Chen et al., 2008; en Luan et al., 2006b). The high level of detail in these models is justified as these works look at stresses within the component. However, if only the PCB response is required then detailed models require too much time and effort then can normally be justified. One solution that avoids excessively complicated models is to assume that the additional mass and stiffness of the component can be included by artificially increasing the PCB Young's modulus and density(Pitarresi et al., 1991; Pitarresi and Primavera, 1991). This increase may be simplified by averaging (or "smearing") the additional mass and stiffness over the entire area of the board. The accuracy of the method depends on the level of simplification used and the mass and stiffness of the components present(Amy et al., 2007).
Additionally, it has been calculated that slight errors in placement of components can drastically affect the accuracy of the prediction and that it is much more important to accurately include the effect of added mass than added stiffness(Cifuentes, 1994).

F.1.3 Chassis

A general rule of thumb for the FE modelling of any piece of equipment is to always model the next level up from the object of interest(Sarafin, 1995). In the case of electronic equipment that means the chassis (sometimes referred to as enclosure) should also be modelled. Failure to

include the chassis response in the model may severely affect the accuracy, unless the chassis is extremely rigid relative to the PCB. Generally, modelling a chassis is fairly simple as they are relatively straightforward structures, although it is always highly recommended to validate the FE model predicted response of the bare chassis with experimentally measured values.

F.1.4 PCB boundary conditions

Once the FE models of the PCB and chassis have been created, the next step is to combine the two together so that the overall response can be calculated. To achieve this, rigid and/or spring FE elements are used to connect the two models, where these elements are intended to represent the effect of the PCB-chassis fixing method (e.g. bolts or card-lok systems).
In terms of translational displacement, most fixings are stiff enough that they effectively rigidly constrain the PCB translational displacement to that of the chassis; this means that simple rigid FE elements are sufficient to constrain the x, y and z displacement of the PCB to the chassis. However, in terms of rotational displacement all fixing methods display some flexibility, therefore rotational spring elements are required to tie the two models together. The main difficulty in incorporating these rotational spring elements into the FE model is in specifying the value of the spring constant. There are two possible approaches to this based on whether a prototype of the PCB exists or not: First, if a prototype of the PCB and chassis does not exist then the users options are very limited and the only way to obtain spring constants is to either estimate the value based on subjective experience of previous fixings or to create a detailed FE model of the joint (which would probably be too time consuming to be practical). Secondly, if a real example of the PCB and chassis does exist then the accuracy may be improved, as experiments may be performed on this combined structure to calculate the rotational stiffness of that fixing (Barker and Chen, 1993).
This second approach requires an experimental set-up incorporating the fixing method of interest attached to a PCB to be created. This set-up should hold the PCB in such a way that can be modelled by classical analytical methods if the supports can be assumed to simply support the structure (e.g. either supporting structure at opposite edges or all edges). It is then possible to use a trial and error ("tuning") approach on an FE model of this structure, where the spring rotational stiffness tuned until the predicted frequencies match those measured experimentally. When the two frequencies match, assuming everything else in the model is correct, the stiffness used in the model is assumed the same as the real stiffness. This

method has been illustrated in works by various authors(Barker and Chen, 1993; Lim et al., 1999), and also extended to allow calculation of a non-dimensional parameter for the rotational stiffness(Barker and Chen, 1993). It is also pertinent to mention that previous studies have attempted to calculate the boundary rotational stiffness based on the static deflection of an experimental set-up, but the process was deemed impracticable(Barker and Chen, 1993).
The method described in this previous work was originally intended for use with card-lok style fixing mechanisms, which provide clamping force along the entire edge of a PCB, not just in discrete location as happens with bolted PCBs. Thus, the method should be used with caution if it is applied to bolted-down PCBs, as it may not be a correct application of the method. If a large number of bolts are present on the edge of the PCB then the situation may be considered similar to that of a card-lok fastened PCB, whereas if the PCB is fixed in only a few locations such an assumption could prove unrealistic. This method also refutes a previous method from Steinberg(Steinberg, 1988) that states the rigidity of card-lok fasteners depends on the natural frequency of the PCB, as it shows the fixidity of the card-lok to be approximately constant and independent of the PCB natural frequency.
Other works relevant to boundary conditions also exist. The effects of very small variations in screw tightness on shock response have been examined en Luan et al. (2006a), showing that even half an M3 screw pitch of variation can alter the PCB response. The same work also showed that the number and location of fixings dramatically alters the response, similar results have also been shown in other workWang et al. (2004).

F.1.5 Damping

Although there are several techniques to experimentally measure the damping, this work focuses on the three most convenient methods: the logarithmic decrement method, the magnification factor method and the bandwidth method(de Silva, 1999). First, let's consider the logarithmic decrement method, which is a time domain method based on the free decay of oscillations of the PCB. To perform this method the PCB should be excited, either with a shaker or with an impact hammer, and once the excitation force has ceased the response of the PCB should be measured (see figure F.3). It is then possible to use equations F.4 and F.5 to calculate the damping (ζ_{ld} logarithmic decrement).

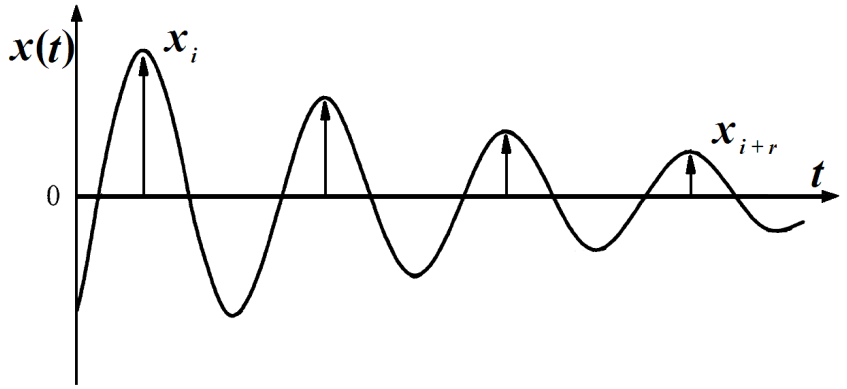

Figure F.3: Measurement of damping using the logarithmic decrement method

$$\sigma = \frac{1}{r} \ln \left(\frac{x_n}{x_{n+r}} \right) = \frac{2\pi\zeta_{ld}}{\sqrt{1-\zeta_{ld}^2}} \tag{F.4}$$

$$\zeta_{ld} = \frac{1}{\sqrt{1+(2\pi/\sigma)^2}} \tag{F.5}$$

Where σ is the logarithmic decrement per unit cycle, and r is the number of cycles apart in the time history.

The second method of damping measurement, the bandwidth method, is a frequency domain method and requires that the frequency response of the PCB is known. Once the frequency response has been obtained, the response at the half power points is measured (see figure F.4) and the damping (ζ_b bandwidth) calculated using equation F.6.

$$\zeta_b = \frac{1}{2} \frac{\Delta\omega}{\omega_r} \tag{F.6}$$

Where $\Delta\omega$ is the width of the frequency response curve at the half power level, and ω_r is the resonant frequency.

The Magnification-factor method is also a frequency domain method where the damping (ζ_{mf} magnification factor) is calculated from the peak transmissibility at resonance as shown in figure F.5.

$$Q = \frac{1}{2\zeta_{mf}\sqrt{1-\zeta_{mf}^2}} \tag{F.7}$$

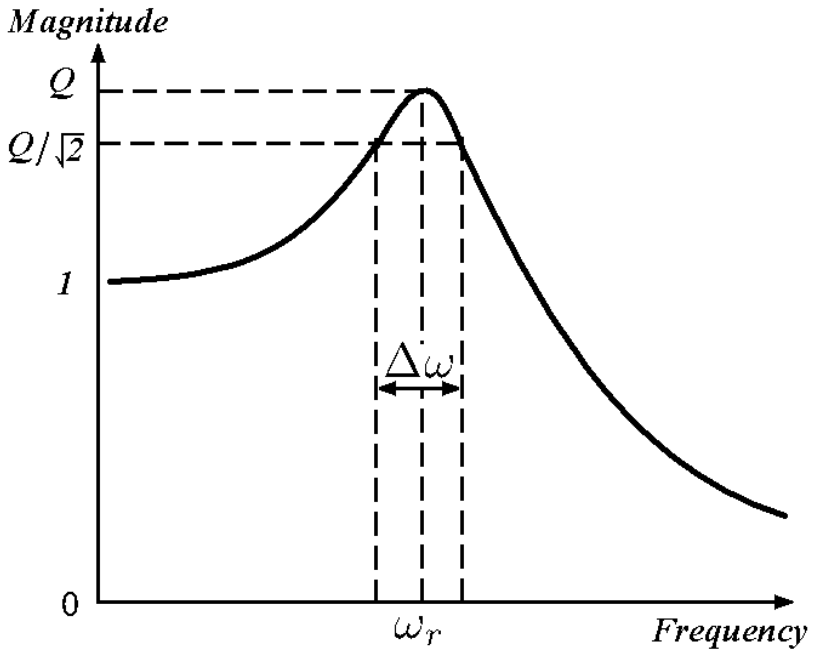

Figure F.4: Measurement of damping using the bandwidth method

or for low damping ($\zeta < 0.1$) this simplifies to

$$Q = \frac{1}{2\zeta_{mf}} \tag{F.8}$$

which is simply re-arranged to

$$\zeta_{mf} = \frac{1}{2Q} \tag{F.9}$$

To use this method the frequency response curve should be normalised so that the response at zero frequency is unity.

When choosing which of the previous three methods to use the following points should be considered(de Silva, 1999). The frequency domain methods are poor for low damping ($< 1\%$) as the curves are difficult to measure accurately because of the high rate of change of the frequency response curve. When such low damping is present then the time domain methods are preferred. Another point to consider is that the damping may increase with increasing deflection in the structure, necessitating the damping to be measured at more than one level of input vibration. Finally, all the methods here assume that only one mode is being excited, if other modes exist close to the one of interest then more detailed analysis is required outside the scope of this work (see de Silva (1999) for more information).

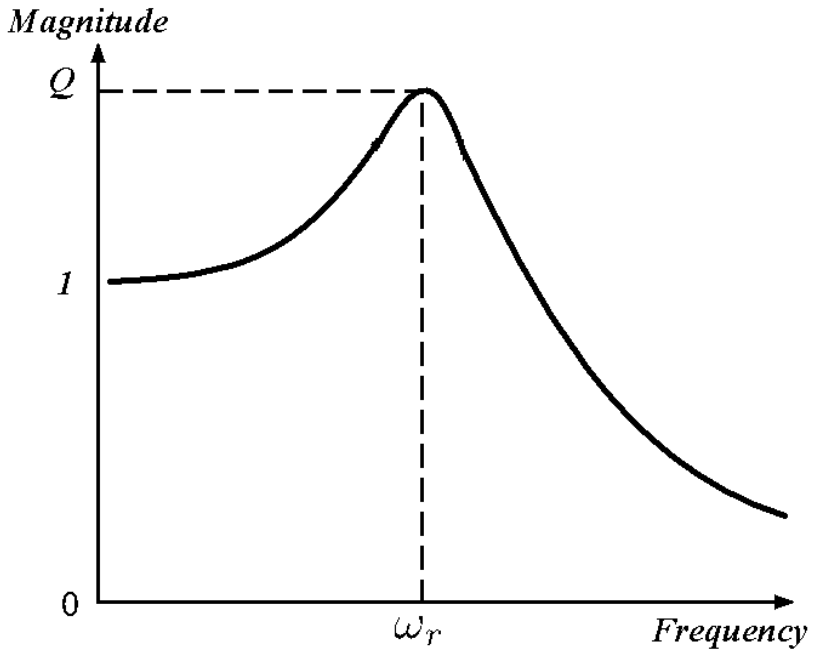

Figure F.5: Measurement of damping using the Magnification-factor method.

Analytical methods of finding the damping value of a structure also exist. Steinberg(Steinberg, 2000) states that the transmissibility at resonance of an electronic sub-assembly is equal to two times the square root of the resonant frequency:

$$Q_{peak} = a\sqrt{\omega_r} \tag{F.10}$$

Where a is a fitting factor based on ω_r and Q_{peak} is the transmissibility at resonance. The factor a equals 0.5 if ($\omega_r \leq 100$), 0.75 if ($100 < \omega_r \leq 200$), 1 if ($200 < \omega_r \leq 400$) and 2 if ($400 < \omega_r$). Subsequently the damping can be calculated from the transmissibility by equation F.9, provided that the level of damping is low($\zeta < 0.1$). Unfortunately the data on which Steinbergs method is based are unavailable and therefore the method is unverifiable.

F.2 Analysis Stage

Typically, the dynamic response of the board is calculated using a mode superposition method. To avoid large errors when solving for the dynamic response of a PCB, two points should be considered(Cifuentes, 1994): First, the solution of the model should consider enough modes so that a significant fraction (roughly at least 90%) of the total mass of the structure is excited.

In addition, when the board deflections are comparable to that of the board thickness a nonlinear analysis is preferred(Cifuentes, 1994).

F.3 Post-processing Stage

The final stage of the FE process is to decide what values to take from the FE solution; this depends on the purpose of the analysis. Most users are expected to want to compare the results with some pre-defined failure criteria; for example, relating the acceleration experienced by a component to probable time for it to fail. These failure criteria may take the form of local acceleration experienced by a component(Liguore and Followell, 1995), local bending moments(Sidharth and Barker, 1996), local board surface strain(Shetty et al., 2001; Shetty and Reinikainen, 2003) or board deflection(Steinberg, 2000).

Appendix G

Deciding Input Variables for Sensitivity Analysis

This section details the process to decide the input variables used in the sensitivity analysis in chapter 5. The sensitivity analysis in this chapter uses the variables of component type and PCB thickness to decompose the results into more convenient values: How and why are these values used instead of other, equally valid, variables? Furthermore, In addition to these values there are a range of other input variables that are also randomly varied between each simulation: Why are these values used? And why are they not used in place of the previous values to decompose the results? The answer to these questions is that prior to the proper sensitivity analysis that was detailed in chapter 5, there was a preliminary analysis that used a much larger set of random input variables. After considering the results of this preliminary analysis the aforementioned variables were chosen as the ones with the greatest influence on variability. This preliminary analysis is detailed in the rest of this chapter [1].

G.1 Input Variables Considered During Preliminary Analysis

In the preliminary study the input variables that were considered could be broken into two distinct groups, those that could be directly controlled and those that could only be indirectly controlled. For example, thickness could be directly controlled by altering the parameters of the random distribution that defined it, whereas the effective mass ratio (ratio of stiffness of underlying PCB and stiffness of PCB component system) was dependant on the PCB thickness

[1] The work in this section is partly based on a conference paper by the same author(Amy et al., 2006a)

distribution, component type distribution and component areal density; therefore, the mass ratio could only be indirectly controlled by altering these other parameters. The main direct and indirect input parameters are as follows:

Direct

- PCB thickness;
- Component Areal Density: area of the PCB covered by components;
- Component type
- Longest Edge Length
- Edge Length Ratio: aspect ratio of the PCB;
- Rotational Edge Stiffness

Indirect

- Component mass;
- Mass Ratio, ratio of mass of unpopulated PCB to populated PCB;
- Simplified Mass Ration, the ratio of the mass of the original PCB to the simplified PCB;
- Stiffness Ratio, ratio of stiffness of unpopulated PCB to populated PCB;

Many more variations on these variables were tested than it is relevant to list here, totalling around 30 direct and indirect input variables. Many of these were found to have no significant correlation with modelling error, so were disregarded.

G.2 Output Variables Considered During Preliminary Analysis

The output variables obtained from the preliminary sensitivity analysis fall into two main categories: those that look at the difference in curvature over the PCB and those that look at the variation in frequency. The first are of primary importance whilst the second are more for interest. The more important curvature output variables included a large number of different statistical measures of variation (e.g mean, median, range, inter-quartile range, max, min, standard deviation).

G.3 Presentation of Results

After the preliminary sensitivity analysis was run it was then necessary to compare the correlation between all the input and output variables. This was simply achieved using the Matlab correlation function "corrcoef" which gave a measure of correlation between two columns of data. In total, there were over a hundred different input and output variables, this complicated the task of comparing the correlation coefficients. To solve this problem it was found that that the correlation coefficients could be plotted on a correlation matrix as shown in figure G.1. In this figure each square represents the correlation of one variable with another, the darker the shade of the square the higher the correlation. The diagonal of the matrix shows the correlation of each variable with itself, by definition these values are perfectly correlated; therefore the square is black. It can be seen that there exists some high correlation between some of the input variables, this is expected as it shows where indirect variables are being strongly influenced by the direct variables: as would be expected.

G.3.1 Analysis of Preliminary Test Results

Using the correlation matrix and observing the different correlation over different smearing the input variables that most closely correlated with failure can be found, this resulted in the variables that were used in the current sensitivity analysis in chapter 5. Although some indirect variable showed a strong correlation with modelling error it was decided not to use them, as not only would this have made the analysis difficult but these values would also have been difficult to use in an engineering situation. For example, it was found that the stiffness ratio (the ratio of stiffness of a populated to unpopulated PCB) showed very strong correlation, but this ratio is very difficult to measure or estimate without having either a detailed FE model or PCB prototype, defeating the whole purpose of this method. Thus it can be seen that the variables used in the case study are a compromise between accuracy and usability.
Some of the indirect variables were also found to have a strong correlation with failure, as shown in figure G.3. In this figure each point represents the error between a model of a hypothetical PCB and a simplified model of the same PCB, in this example stiffness smearing is used. The horizontal axis plots the stiffness ratio between the effective stiffness of the populated model and the stiffness of the underlying unpopulated PCB. In this way it can be seen that the PCBs that have the greatest amount of stiffening from components are the ones

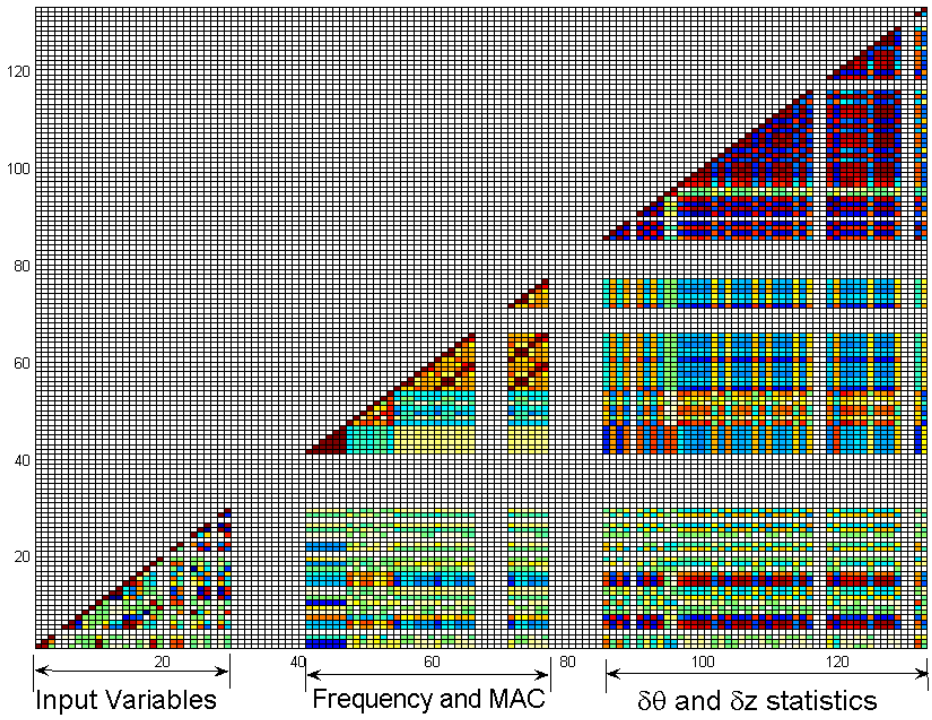

Figure G.1: Cross-correlation of variables for the stiffness smeared case, each number is an index that relates to a specific variable, with x and y axis plotting the same variables. Note that the diagonal of the matrix shows perfect correlation, this is a result of the variables being correlated against themselves. See fig. G.2 for further clarification

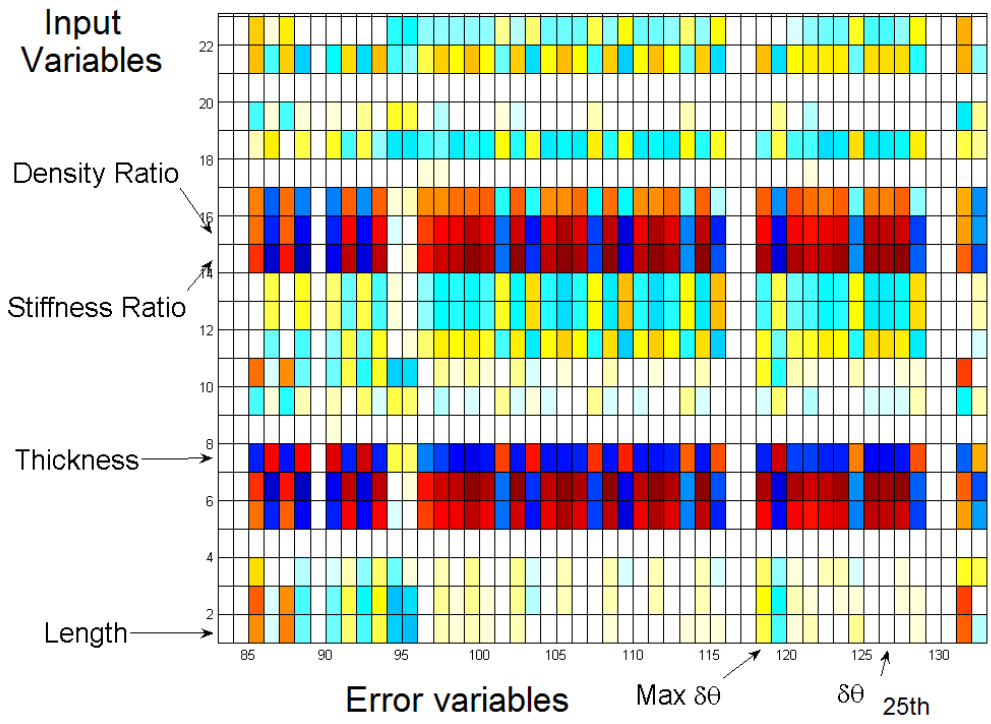

Figure G.2: Magnification of lower right corner of fig. G.1, several variables have been referenced, the shade of each square represents the correlation between two variables, with darker shades indicating higher correlation.

that suffer the most when the additional components stiffness is ignored during modelling. Unfortunately it is too difficult to use these indirect variables in either the sensitivity analysis or a real engineering situation; therefore, the sensitivity analysis used the more convenient variables of thickness and component type.

G.4 Additional Observations on Boundary Condition Effects

In addition to looking at the effect of simplifying the mass and stiffness properties, another simulation was run that looked at the effect of simplifying the boundary conditions. This simulation considered the effect of simplifying the edge rotational stiffness to 0% fixidity, again looking at the error in the curvatures between a simplified and non-simplified case. In agreement with past research (Lim et al., 1999; Barker and Chen, 1993) the results were very sensitive to error in specifying the edge rotational stiffness. The cases where the edge rotational stiffness was originally low (close to 0% fixidity) showed fairly good accuracy, whilst the cases

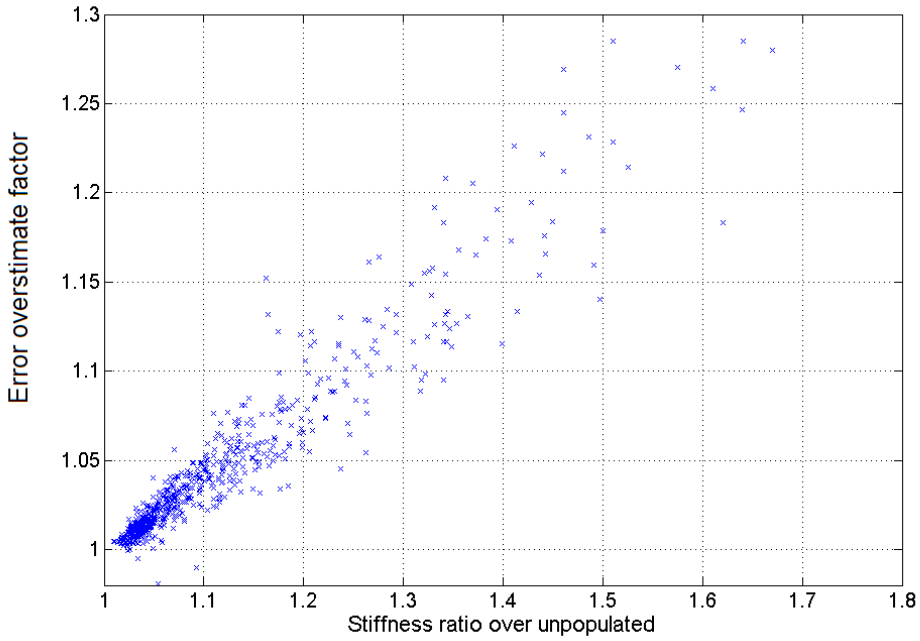

Figure G.3: Stiffness ratio plotted against curvature delta for the stiffness smearing case.

where the edge rotational stiffness was high (up to 60% fixidity) showed poor accuracy (see figure G.4). In effect the cases with high percentage fixidity had much more to lose from the simplification process, therefore they showed greater error. It was noted that assuming the PCB to be simply supported is conservative as it only overestimated the results, although in extreme cases this overestimate can approach a factor of three times the actual results. Figure G.4 illustrates the effect of a large amount of boundary simplification on the curvature overestimate, with the cases that originally had high boundary stiffness showing the largest error. It is interesting to see that the spread of results stays fairly constant at any level of boundary simplification.

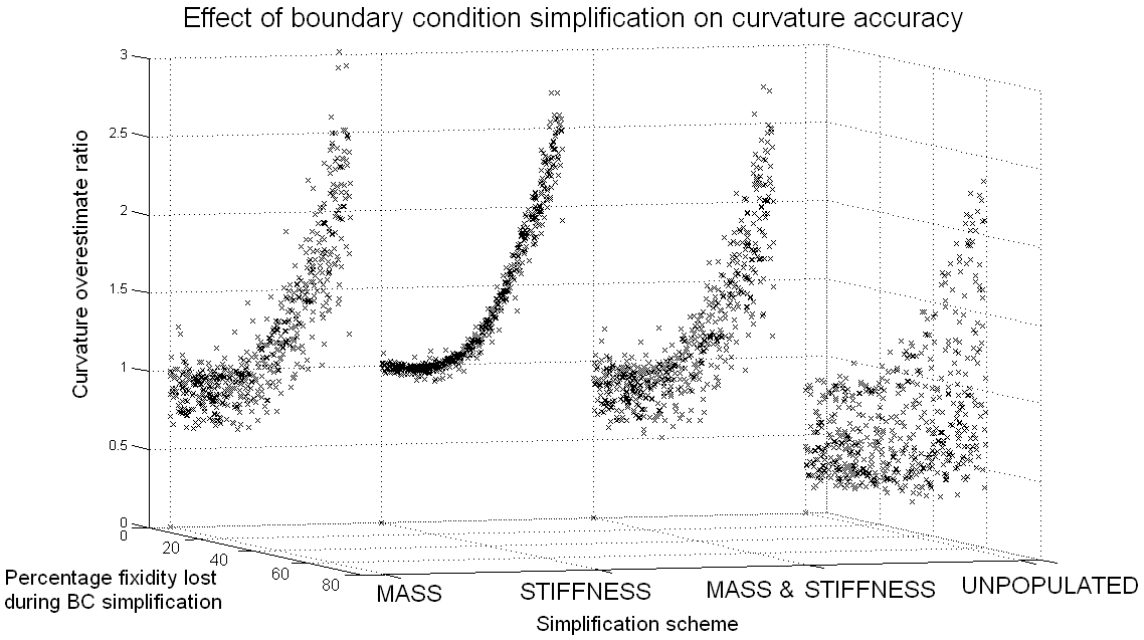

[t]

Figure G.4: Graph to show relationship between amount of boundary condition simplification and curvature overestimate, four different levels of property smearing are considered here.

Bibliography

Aglietti, G. S. (1999). *Active Control of Microvibrations for Equipment Loaded Spacecraft Panels*. PhD thesis, University of Southampton.

Aglietti, G. S. (2002). A Lighter Enclosure for Electronics for Space Applications. *Proceeding of Institute of Mechanical Engineers*, part G vol. 216:131–142.

Aglietti, G. S. and Schwingshackl, C. (2004). Analysis of Enclosures and Anti Vibration Devices for Electronic Equipment for Space Applications. *Proceedings of the 6th International Conference on Dynamics and Control of Systems and Structures in Space*, pages 261–270.

Amy, R. A., Aglietti, G. S., and Richardson, G. (2006a). Simplified modelling of printed circuit boards for spacecraft applications. In *International Astronautical Congress 2006*.

Amy, R. A., Aglietti, G. S., and Richardson, G. (2006b). Tools for efficiently designing electronic equipment to withstand the spacecraft launch environment. In *Proceedings of the 7th International Conference On Dynamics and Control of Systems and Structures in Space (DCSSS)*.

Amy, R. A., Aglietti, G. S., and Richardson, G. (2007). Sensitivity Analysis of Simplified PCB FE Models. In *Proceedings of the 1st CEAS European Air and Space Conference CEAS-2007-466*.

Amy, R. A., Aglietti, G. S., and Richardson, G. (2009a). Reliability Analysis of Electronic Equipment Subjected to Shock and Vibration, a review. *Shock and Vibration*, Vol. 16(1).

Amy, R. A., Aglietti, G. S., and Richardson, G. (2009b). Sensitivity analysis of simplified PCB FE models. *Microelectronics Reliability*, 49 (7):791 – 799.

Barker, D. B. and Chen, Y. (1993). Modeling the Vibration Restraints of Wedge-lock Card Guides. *ASME Journal of Electronic Packaging*, 115(2):189 – 194.

Barker, D. B., Chen, Y., and Dasgupta, A. (1993). Estimating the vibration fatigue life of quad leaded surface mount components. *ASME Journal of Electronic Packaging*, 115(2):195 – 200.

Barker, D. B., Dasgupta, A., and Pecht, M. (1991). PWB solder joint life calculations under thermal and vibrational loading. *Annual Reliability and Maintainability Symposium. 1991 Proceedings (Cat. No.91CH2966-0)*, pages 451 – 9.

Barker, D. B., Sharif, I., Dasgupta, A., and Pecht, M. (1992). Effect of SMC lead dimensional variabilities on lead compliance and solder joint fatigue life. *ASME Journal of Electronic Packaging*, 114(2):177 – 84.

Barker, D. B. and Sidharth, K. (1993). Local PWB and component bowing of an assembly subjected to a bending moment. *American Society of Mechanical Engineers (Paper)*, pages 1 – 7.

Bowles, J. (1992). A survey of reliability-prediction procedures for microelectronic devices. *IEEE Transactions on Reliability*, 41(1):2 – 12.

Chatterjee, S. and Sorensen, E. (1995). Pareto-like effect in regression? *Quality and Reliability Engineering International*, 11(5):382 – 385.

Chen, Y., Wang, C., and Yang, Y. (2008). Combining vibration test with finite element analysis for the fatigue life estimation of PBGA components. *Microelectronics Reliability*, 48(4):638 – 44.

Cifuentes, A. O. (1994). Estimating the Dynamic Behavior of Printed Circuit Boards. *IEEE Transactions on Components, Packaging, and Manufacturing Technology Part B: Advanced Packaging*, 17(1):69 – 75.

Condra, L., Bosco, C., Deppe, R., Gullo, L., Treacy, J., and Wilkinson, C. (1999). Reliability assessment of aerospace electronic equipment. *Quality and Reliability Engineering International*, 15(4):253 – 60.

Cushing, M. J., Mortin, D. E., Stadterman, T. J., and Malhotra, A. (1993). Comparison of electronics-reliability assessment approaches. *IEEE Transactions on Reliability*, 42(4):542 – 546.

Darveaux, R. and Syed, A. (2000). Reliability of area array solder joints in bending. *SMTA International Proceedings of the Technical Program*, pages 313 – 24.

de Silva, C. W. (1999). *Vibration Fundamentals and Practice*. CRC.

Dehbi, A., Ousten, Y., Danto, Y., and Wondrak, W. (2005). Vibration lifetime modelling of PCB assemblies using Steinberg model. *Microelectronics Reliability*, 45(9-11):1658 – 1661.

ECSS (1999). The manual soldering of high-reliability electrical connections (ECSS–Q–70–08A). Technical report, ESA.

en Luan, J., Tee, T. Y., Pek, E., Lim, C. T., and Zhong, Z. (2006a). Dynamic responses and solder joint reliability under board level drop test. *Microelectronics Reliability*, 47(2-3):450 – 60.

en Luan, J., Tee, T. Y., Pek, E., Lim, C. T., Zhong, Z., and Zhou, J. (2006b). Advanced numerical and experimental techniques for analysis of dynamic responses and solder joint reliability during drop impact. *IEEE Transaction on Components and Packaging Technologies*, 29(3):449 – 456.

Enke, N. F., Kilinski, T. J., Schroeder, S. A., and Lesniak, J. R. (1989). Mechanical behaviors of 60/40 tin-lead solder lap joints. *Proceedings - Electronic Components Conference*, 12:264 – 272.

Estes, T., Wong, W., McMullen, W., Berger, T., and Saito, Y. (2003). Reliability of class 2 heel fillets on gull wing leaded components. *Aerospace Conference, 2003. Proceedings*, 6:6–2517–6–2525.

FIDES (2004). *FIDES Guide 2004 issue A Reliability Methodology for Electronic Systems*. FIDES Group.

Foucher, B., Das, D., Boullie, J., and Meslet, B. (2002). A review of reliability prediction methods for electronic devices. *Microelectronics Reliability*, 42(8):1155 – 1162.

Garcia-Bonito, J., Brennan, M., Elliott, S., David, A., and Pinnington, R. (1998). A novel high-displacement piezoelectric actuator for active vibration control. *Smart Materials and Structures*, 7(1):31 – 42.

Gericke, W., Gregoris, G., Jenkins, I., Jones, J., Lavielle, D., Lecuyer, P., Lenic, J., Neugnot, C., Sarno, M., Torres, E., and Vergnault, E. (2002). A methodology to assess and select a suitable reliability prediction method for EEE components in space applications. *European Space Agency, (Special Publication) ESA SP*, (507):73 – 80.

Gu, J., Barker, D., and Pecht, M. (2007). Prognostics implementation of electronics under vibration loading. *Microelectronics Reliability*, 47(12):1849 – 1856.

Gullo, L. (1999). In-service reliability assessment and top-down approach provides alternative reliability prediction method. *Annual Reliability and Maintainability. Symposium. 1999 Proceedings (Cat. No.99CH36283)*, pages 365 – 77.

Guo, Q. and Zhao, M. (2005). Fatigue of SMT solder joint including torsional curvature and chip location optimization. *International Journal of Advanced Manufacturing Technology*, 26(7-8):887 – 895.

Guo, Q., Zhao, M., and Wang, H. (2005). SMT solder joint's semi-experimental fatigue model. *Mechanics Research Communications*, 32(3):351 – 8.

Ham, S.-J. and Lee, S.-B. (1996). Experimental study for reliability of electronic packaging under vibration. *Experimental Mechanics*, 36(4):339 – 44.

Han, W. and Pety, M. (1996). Linear vibration analysis of laminated rectangular plates using the hierarchical finite element method. I. free vibration analysis. *Computers and Structures*, 61(4):705 – 12.

Hart, D. (1988). Fatigue testing of a component lead in a plated through hole. *IEEE Proceedings of the National Aerospace and Electronics Conference*, pages 1154 – 1158.

Hin, T. Y., Beh, K. S., and Seetharamu, K. (2003). Development of a dynamic test board for FCBGA solder joint reliability assessment in shock & vibration. *Proceedings of the 5th Electronics Packaging Technology Conference (EPTC 2003)*, pages 256 – 62.

Ho, V., Veprik, A., and Babitsky, V. (2003). Ruggedizing printed circuit boards using a wideband dynamic absorber. *Shock and Vibration*, 10(3):195 – 210.

IEEE (2003). IEEE guide for selecting and using reliability predictions based on IEEE 1413. pages v+90 –.

Jackson, T., Harbater, S., Sketoe, J., and Kinney, T. (2003). Development of standard formats for space systems reliability models. *Annual Reliability and Maintainability Symposium. 2003 Proceedings (Cat. No.03CH37415)*, pages 269 – 76.

Jensen, F. (1995). *Electronic Component Reliability*. Wiley.

J.H.Ong and Lim, G. (2000). A simple technique for maximising the fundamental frequency of structures. *ASME Journal of Electronic Packaging*, 122:341–349.

Jih, E. and Jung, W. (1998). Vibrational fatigue of surface mount solder joints. *ITherm'98. Sixth Intersociety Conference on Thermal and Thermomechanical Phenomena in Electronic Systems (Cat. No.98CH36208)*, pages 246 – 50.

Johnson, B. and Gullo, L. (2000). Improvements in reliability assessment and prediction methodology. *Annual Reliability and Maintainability Symposium. 2000 Proceedings. International Symposium on Product Quality and Integrity (Cat. No.00CH37055)*, -:181 – 7.

Johnson, E. and Brockman, J. (1 Sept. 1996). Towards a model for electronic design process refinement. *Computers in Industry*, 30(1):27 – 36.

Khan, M., Lagoudas, D., Mayes, J., and Henderson, B. (2004). Pseudoelastic SMA spring elements for passive vibration isolation: part I modeling. *Journal of Intelligent Material Systems and Structures*, 15(6):415 – 41.

Kotlowitz, R. (1989). Comparative compliance of representative lead designs for surface-mounted components. *IEEE Transactions on Components, Hybrids, and Manufacturing Technology*, 12(4):431 – 48.

Kotlowitz, R. (1990). Compliance metrics for surface mount component lead design. *1990 Proceedings. 40th Electronic Components and Technology Conference (Cat. No.90CH2893-6)*, pages 1054 – 63.

Kotlowitz, R. and Taylor, L. (1991). Compliance metrics for the inclined gull-wing, spider j-bend, and spider gull-wing lead designs for surface mount components. *1991 Proceedings. 41st Electronic Components and Technology Conference (Cat. No.91CH2989-2)*, pages 299 – 312.

Lau, J., Harkins, G., Rice, D., Kral, J., and Wells, B. (1988). Experimental and statistical analyses of surface-mount technology plcc solder-joint reliability. *IEEE Transactions on Reliability*, 37(5):524 – 30.

Lau, J., Powers-Maloney, L., Baker, J., Rice, D., and Shaw, B. (1990). Solder joint reliability of fine pitch surface mount technology assemblies. *IEEE Transactions on Components, Hybrids, and Manufacturing Technology*, 13(3):534 – 44.

Li, R. (2001). A methodology for fatigue prediction of electronic components under random vibration load. *ASME Journal of Electronic Packaging*, 123(4):394 – 400.

Li, R. and Poglitsch, L. (2001a). Fatigue of plastic ball grid array and plastic quad flat packages under automotive vibration. *SMTA International. Proceedings of the Technical Program*, pages 324 – 9.

Li, R. and Poglitsch, L. (2001b). Vibration fatigue, failure mechanism and reliability of plastic ball grid array and plastic quad flat packages. *Proceedings 2001 HD International Conference on High-Density Interconnect and Systems Packaging (SPIE Vol.4428)*, pages 223 – 8.

Liguore, S. and Followell, D. (1995). Vibration Fatigue of Surface Mount Technology (SMT) Solder Joints. *Annual Reliability and Maintainability Symposium 1995 Proceedings (Cat. No.95CH35743)*, -:18 – 26.

Lim, G., Ong, J., and Penny, J. (1999). Effect of edge and internal point support of a printed circuit board under vibration. *ASME Journal of Electronic Packaging*, 121(2):122 – 6.

Luthra, P. (1990). Mil-Hdbk-217: What is wrong with it ? *IEEE Transactions on Reliability*, 39(5):518 –.

Marouze, J. and Cheng, L. (2002). A feasibility study of active vibration isolation using thunder actuators. *Smart Materials and Structures*, 11(6):854 – 862.

MIL-HDBK-217F (1995). *Reliability Prediction of Electronic Equipment.* US Department of Defense, F edition.

Moening, C. (1984). Pyrotechnic shock flight failures. *Aerospace Testing Seminar*, 8:95–109.

Moheimani, S. R. (2003). A survey of recent innovations in vibration damping and control using shunted piezoelectric transducers. *IEEE Transactions on Control Systems Technology*, 11(4):482 – 494.

Morris, S. and Reilly, J. (1993). Mil-Hdbk-217-a favorite target. *Annual Reliability and Maintainability Symposium. 1993 Proceedings (Cat. No.93CH3257-3)*, pages 503 – 9.

O'Connor, P. (1981). *Practical reliability engineering.* Wiley.

Osterman, M. and Stadterman, T. (1999). Failure assessment software for circuit card assemblies. *Annual Reliability and Maintainability. Symposium. 1999 Proceedings (Cat. No.99CH36283)*, pages 269 – 76.

Pecht, M. and Dasgupta, A. (1995). Physics-of-failure: an approach to reliable product development. *IEEE 1995 International Integrated Reliability Workshop Final Report (Cat. No.95TH8086)*, pages 1 – 4.

Pecht, M. and Kang, W.-C. (1988). A critique of Mil-Hdbk-217e reliability prediction methods. *IEEE Transactions on Reliability*, 37(5):453 – 7.

Pecht, M. G. and Nash, F. R. (1994). Predicting the reliability of electronic equipment. *Proceedings of the IEEE*, 82(7):992 – 1004.

Peter Fortescue, J. S. and Swinerd, G. (2003). *Spacecraft Systems Engineering*. John Wiley & Sons/Praxis.

Pitarresi, J., Caletka, D., Caldwell, R., and Smith, D. (1991). The "Smeared" Property Technique for the FE Vibration Analysis of Printed Circuit Cards. *ASME Journal of Electronic Packaging*, 113:250–257.

Pitarresi, J., Geng, P., Beltman, W., and Ling, Y. (2002). Dynamic modeling and measurement of personal computer motherboards. *52nd Electronic Components and Technology Conference 2002.*, (Cat. No.02CH37345)(-):597 – 603.

Pitarresi, J. and Primavera, A. (1991). Comparison of Vibration Modeling Techniques for Printed Circuit Cards. *ASME Journal of Electronic Packaging*, 114:378–383.

Pitarresi, J., Roggeman, B., Chaparala, S., and Geng, P. (2004). Mechanical shock testing and modeling of PC motherboards. *2004 Proceedings. 54th Electronic Components and Technology Conference (IEEE Cat. No.04CH37546)*, Vol.1:1047 – 54.

Sandor, B. I. (1991). *Solder Mechanics - A State of the Art Asssessment*. The Minerals, Metals and Materials Society.

Sarafin, T. P. (1995). *Spacecraft Structures and Mechanisms: From Concept to Launch*. Kluwer Academic Publishers.

Shetty, S., Lehtinen, V., Dasgupta, A., Halkola, V., and Reinikainen, T. (2001). Fatigue of chip scale package interconnects due to cyclic bending. *ASME Journal of Electronic Packaging*, 123(3):302 – 8.

Shetty, S. and Reinikainen, T. (2003). Three- and Four-point Bend Testing for Electronic Packages. *ASME Journal of Electronic Packaging*, 125(4):556 – 561.

Sidharth, K. and Barker, D. B. (1996). Vibration induced fatigue life estimation of corner leads of peripheral leaded components. *ASME Journal of Electronic Packaging*, 118(4):244 – 9.

Spanos, J., Rahman, Z., and Blackwood, G. (1995). Soft 6-axis active vibration isolator. *Proceedings of the American Control Conference*, 1:412 – 416.

Steinberg, D. (1988). *Vibration Analysis for Electronic Equipment*. John Wiley & Sons.

Steinberg, D. (1991). *Vibration Analysis for Electronic Equipment*. John Wiley & Sons.

Steinberg, D. (2000). *Vibration Analysis for Electronic Equipment*. John Wiley & Sons.

Suhir, E. (1988). Could compliant external leads reduce the strength of a surface-mounted device? *1988 Proceedings of the 38th Electronics Components Conference (88CH2600-5)*, pages 1 – 6.

Suhir, E. (1992a). Nonlinear dynamic response of a printed circuit board to shock loads applied to its support contour. *ASME Journal of Electronic Packaging*, 114(4):368 – 377.

Suhir, E. (1992b). Response of a flexible printed circuit board to periodic shock loads applied to its support contour. *American Society of Mechanical Engineers (Paper)*, 59(2):1 – 7.

Suhir, E. (2000). Predicted fundamental vibration frequency of a heavy electronic component mounted on a printed circuit board. *ASME Journal of Electronic Packaging*, 122:3–5.

Veprik, A. (2003). Vibration protection of critical components of electronic equipment in harsh environmental conditions. *Journal of Sound and Vibration*, 259(1):161 – 75.

Wang, H., Zhao, M., and Guo, Q. (2004). Vibration fatigue experiments of SMT solder joint. *Microelectronics Reliability*, 44(7):1143 – 56.

Xu, Z. W., Chan, K., and Liao, W. (2004). An empirical method for particle damping design. *Shock and Vibration*, 11(5-6):647 – 64.

Yamada, S. (1989). A fracture mechanics approach to soldered joint cracking. *IEEE Transactions on Components, Hybrids, and Manufacturing Technology*, 12(1):99 – 104.

Yeh, C.-P., Fulton, R., Umeagukwu, C., and Hughes, J. (1990). A multidisciplinary approach to PWB design. *1990 Proceedings. 40th Electronic Components and Technology Conference*, pages 1090 – 6.

Zhao, W. and Elsayed, E. (2005). Modelling accelerated life testing based on mean residual life. *International Journal of Systems Science*, 36(11):689 – 96.

Zhao, W., Mettas, A., Zhao, X., Vassiliou, P., and Elsayed, E. A. (2004). Generalized step stress accelerated life model. *Proceedings of 2004 International Conference on the Business of Electronic Product Reliability and Liability*, pages 19 – 25.